Lawrence Berkeley National Laboratory
Recent Work

Title

REVERSIBLE INTERCALATI0N OF GRAPHITE BY FLUORINE AND RELATED SYNTHETIC AND THERMODYNAMIC STUDIES

Permalink

https://escholarship.org/uc/item/4r7645kq

Author

Mallouk, T.E.

Publication Date

1983-07-01

eScholarship.org Powered by the California Digital Library
University of California

LBL-16778

Lawrence Berkeley Laboratory

UNIVERSITY OF CALIFORNIA

RECEIVED
LAWRENCE
BERKELEY LABORATORY
JAN 17 1984
LIBRARY AND
DOCUMENTS SECTION

Materials & Molecular Research Division

REVERSIBLE INTERCALATION OF GRAPHITE BY FLUORINE AND RELATED SYNTHETIC AND THERMODYNAMIC STUDIES

T.E. Mallouk
(Ph.D. Thesis)

July 1983

TWO-WEEK LOAN COPY

This is a Library Circulating Copy which may be borrowed for two weeks. For a personal retention copy, call Tech. Info. Division, Ext. 6782.

Prepared for the U.S. Department of Energy under Contract DE-AC03-76SF00098

LBL-16778

DISCLAIMER

This document was prepared as an account of work sponsored by the United States Government. While this document is believed to contain correct information, neither the United States Government nor any agency thereof, nor the Regents of the University of California, nor any of their employees, makes any warranty, express or implied, or assumes any legal responsibility for the accuracy, completeness, or usefulness of any information, apparatus, product, or process disclosed, or represents that its use would not infringe privately owned rights. Reference herein to any specific commercial product, process, or service by its trade name, trademark, manufacturer, or otherwise, does not necessarily constitute or imply its endorsement, recommendation, or favoring by the United States Government or any agency thereof, or the Regents of the University of California. The views and opinions of authors expressed herein do not necessarily state or reflect those of the United States Government or any agency thereof or the Regents of the University of California.

REVERSIBLE INTERCALATION OF GRAPHITE BY FLUORINE AND RELATED SYNTHETIC AND THERMODYNAMIC STUDIES

Thomas Edward Mallouk
(Ph.D. Thesis)

Materials and Molecular Research Division
Lawrence Berkeley Laboratory and Department of Chemistry
University of California, Berkeley, California 94720

July 1983

This work was supported by the Director, Office of Energy Research, Office of Basic Energy Sciences, Chemical Sciences Division of the US Department of Energy under Contract Number DE-AC03-76SF00098.

REVERSIBLE INTERCALATION OF GRAPHITE

BY FLUORINE AND RELATED SYNTHETIC AND THERMODYNAMIC STUDIES

Table of Contents

	Page
List of Tables	vi
List of Figures	viii
Abstract	x
I. GENERAL INTRODUCTION AND EXPERIMENTAL PROCEDURES	1
A. General Introduction	1
B. Apparatus and handling of materials	1
1. Vacuum lines	2
2. Reaction and storage vessels	3
3. Glove boxes	3
C. Characterization of materials	3
1. X-ray powder photography	3
2. X-ray powder diffraction	4
3. Raman spectroscopy	4
4. Infrared spectroscopy	5
5. Single crystal x-ray diffraction	5
6. Chemical analysis	5
References	7
II. SYNTHESIS, STRUCTURE, AND VIBRATIONAL ANALYSIS OF PENTAFLUOROGERMANATE SALTS	8
A. Introduction	8
B. Experimental	10
1. Reagents	10
2. ONF/GeF_4	11
3. SF_4/GeF_4	12
4. NO_2F/GeF_4	13
5. XeF_6/GeF_4	13
6. XeF_5GeF_5 crystal structure	13
7. ClO_2F/GeF_4	15
8. ClO_2GeF_5 crystal structure	15
9. IF_7/GeF_4	15
10. ClF_3/GeF_4	16
11. $(n\text{-}C_4H_9)_4NGeF_5$	16
C. Results and discussion	16
1. XeF_5GeF_5 structure	16
2. ClO_2GeF_5 structure	17
3. Vibrational analysis of salts containing the GeF_5^- ion	18
i) $XeF5_{GeF5}$	18

ii) ClO_2GeF_5. 20
iii) $NOGeF_5$. 21
iv) NO_2GeF_5, SF_3GeF_5. 21
v) $(n\text{-}C_4H_9)_4NGeF_5$. 21
vi) Comparison of the cis and trans bridging structures. 22

Summary. 24
References 25
Tables 28
Figures. 43

III. THE FLUORIDE ION AFFINITIES OF GeF_4 AND BF_3 AS CALCULATED FROM BORN-HABER CYCLES. 51

A. Introduction. 51

B. Experimental. 52
1. $(SF_3)_2GeF_6$. 52
2. Dissociation pressure measurements for ClO_2GeF_5 and $(SF_3)_2GeF_6$. 53

C. Lattice Energy Calculations 54
1. Electrostatic Terms 54
2. London energy terms 55
3. The zero point vibrational energy and associated terms 55
4. The repulsion energy term 56
5. Derivation of parameters and calculations 56
6. An empirical lattice energy determination for ClO_2GeF_5 61

D. Results and discussion. 62
1. $(SF_3)_2GeF_6$ structure. 62
2. Fluoride ion and electron affinities. 63
i) Boron trifluoride 63
ii) Uranium hexafluoride. 63
iii) Sulfur tetrafluoride. 64
iv) Germanium tetrafluoride 64

Summary. 64
References 66
Tables 68
Figures. 76

IV. CALCULATION OF THE THERMODYNAMIC STABILITY OF SOME FLUORO-CATIONS AND ANIONS 80

A. Introduction. 80

B. Estimation of entropy changes 81
1. Correlation of $\Delta S°_{298}$ with molecular volume 81
2. The Debye model for $S°_{298}$ 81

C. Estimation of electron and fluoride ion affinities. . . . 84

1. Transition metal hexafluorides. 84
i) PtF_6. 85
ii) RuF_6, RhF_6. 85
iii) IrF_6. 85
iv) OsF_6. 86
v) ReF_6. 86
2. Fluoride ion donors 86
i) XeF_6. 86
ii) ClF_3. 87
iii) IF_7 87
3. Arsenic pentafluoride 88

Summary. 90
References 91
Tables 93
Figures. 95

V. SOME NEW METAL FLUORIDE AND HYDROFLUORIDE INTERCALATION COMPOUNDS OF GRAPHITE 97

A. Introduction. 97
B. Reactions of graphite with MF_x Lewis acids and fluorine . 98
1. Graphite/SiF_4/F_2. 98
2. Graphite/AlF_3/F_2. 99
3. Graphite/SnF_4/F_2. 100
C. Intercalation compounds of graphite with HF and F_2. . . . 101
1. Graphite bifluorides. 102
i) Preparation 102
ii) Crystal structure 102
iii) ^{19}F - nmr of graphite bifluoride. 103
iv) Electrical conductivity of C_xHF_2. 105
2. First stage graphite hydrofluorides 106
i) Preparation 106
ii) Powder patterns and structure of $C_xF_{1-\delta}(HF)_\delta$. . 106
iii) Physical properties 107
iv) XPS spectrum of $C_{2.5}F_{1-\delta}(HF)_\delta$ 108
v) ^{19}F and ^1H nmr spectra of $C_{2.15}F_{0.83}(HF)_{0.17}$. . 109
vi) ^{13}C nmr of $C_xF_{1-\delta}(HF)_\delta$. 110
vii) Vibrational spectra of $C_xF_{1-\delta}(HF)_\delta$. 112
viii) Bonding and electronic structure in $C_xF_{1-\delta}(HF)_\delta$ 114
3. HF - deficient second-stage compounds 115
4. Chemical and electrochemical reactions of graphite hydrofluorides. 116
i) Intercalation reactions 116
ii) Electrochemical reversibility 117

Summary. 119
References 120
Tables 123
Figures. 134

Appendix 146

Acknowledgements 152

List of Tables

		Page
II-1.	Vibrational assignments for $(NO^+)_2GeF_6^{2-}$	28
II-2.	X-ray powder data for $NO^+GeF_5^-$ prepared in SO_2 solution	29
II-3.	X-ray powder data for $SF_3^+GeF_5^-$	30
II-4.	X-ray powder data for $NO_2^+GeF_5^-$	31
II-5.	Crystallographic data for $XeF_5^+GeF_5^-$ and $ClO_2^+GeF_5^-$	32
II-6.	Observed and calculated structure factors for XeF_5GeF_5	33
II-7.	Positional and thermal parameters for XeF_5GeF_5	34
II-8.	Observed and calculated structure factors for ClO_2GeF_5	35
II-9.	Positional and thermal parameters for ClO_2GeF_5	36
II-10.	Selected internuclear distances and angles for XeF_5GeF_5	37
II-11.	Selected internuclear distances and angles for ClO_2GeF_5	38
II-12.	Vibrational assignments for XeF_5GeF_5	39
II-13.	Vibrational assignments for ClO_2GeF_5 and $NOGeF_5$	40
II-14.	Vibrational assignments for NO_2GeF_5 and SF_3GeF_5	41
II-15.	Vibrational assignments for GeF_5^- in $(n\text{-}Bu)_4N^+GeF_5^-$	42
III-1.	Crystallographic data for $(SF_3^+)_2GeF_6^{2-}$	68
III-2.	Observed and calculated structure factors for $(SF_3)_2GeF_6$	69
III-3.	Positional and thermal parameters for $(SF_3^+)_2GeF_6^{2-}$	70
III-4.	ℓnK_p vs. 1/T data for ClO_2GeF_5 and $(SF_3)_2GeF_6$	71
III-5.	Lattice energy calculations for SiF_4, UF_6, and OsO_4	72
III-6.	Lattice enthalpies and basic radii	73
III-7.	Selected internuclear distances and angles for $(SF_3)_2GeF_6$	75
IV-1.	Calculated reaction entropies	93
IV-2.	Calculated lattice enthalpies	94
V-1.	X-ray powder data for third stage graphite fluorosilicate	123

		Page
V-2.	X-ray powder data for second stage graphite fluorostannate	124
V-3.	Observed and calculated 00ℓ diffraction intensities for graphite bifluoride.	125
V-4.	Powder diffraction data for $C_{11.2}HF_2$	126
V-5.	a-b plane electrical conductivity of graphite bifluorides.	127
V-6.	X-ray powder diffraction patterns for first stage $C_xF_{1-\delta}(HF)_\delta$.	128
V-7.	Some physical properties of $C_xF_{1-\delta}(HF)_\delta$.	129
V-8.	XPS binding energies of $C_{2.5}F_{1-\delta}(HF)_\delta$ and comparison materials.	130
V-9.	Observed and calculated ^{13}C n.m.r. intensities for $C_{2.05}F_{0.82}(HF)_{0.18}$	131
V-10.	X-ray powder diffraction data for $C_{8.8}F_{0.60}(HF)_{0.40}$.	132
V-11.	Characteristics of some electrochemical cells with $C_{2.7}F_{1-\delta}(HF)_\delta$ cathodes	133

List of Figures

		Page
II-1.	Raman and infrared spectra of $(NO^+)_2GeF_6^{2-}$	43
II-2.	Vibrational spectra of $NO^+GeF_5^-$.	44
II-3.	Raman spectra of GeF_5^- salts	45
II-4.	Infrared spectra of GeF_5^- salts.	46
II-5.	The $XeF_5^+GeF_5^-$ crystal structure	47
II-6.	The $ClO_2^+GeF_5^-$ crystal structure	48
II-7.	Chlorine coordination environments in $ClO_2^+GeF_5^-$	49
II-8.	Vibrational spectra of $(n\text{-}C_4H_9)_4N^+GeF_5^-$.	50
III-1.	The pressure transmitter gauge	76
III-2.	Correlation of lattice energies with molecular volumes . .	77
III-3a.	Sulfur coordination environment in the $(SF_3^+)_2GeF_6^{2-}$ structure.	78
III-3b.	Germanium coordination environment in the $(SF_3^+)_2GeF_6^{2-}$ structure.	79
IV-1.	Correlation of $S°_{298}$ with the molecular volumes of solids.	95
IV-2.	Correlation of $S°_{298}$ with repulsion energy	96
V-1.	X-ray diffractometer tracings for graphite hydrofluorides.	134
V-2.	The crystal structure of $C_{12}^+HF_2^-$.	135
V-3.	^{19}F nmr spectra of graphite hydrofluorides	136
V-4.	Proton nmr spectrum of $C_{2.15}F_{0.83}(HF)_{0.17}$.	137
V-5.	^{13}C nmr spectrum of $C_{2.05}F_{1-\delta}(HF)_\delta$	138
V-6.	Variable contact time $^{19}F \rightarrow {}^{13}C$ cross-polarization nmr spectra of $C_{2.05}F_{1-\delta}(HF)_\delta$.	139
V-7.	Infrared spectrum of $C_{2.5}F_{1-\delta}(HF)_\delta$	140
V-8.	Raman spectra of first stage graphite hydrofluorides . . .	141
V-9.	(a) A possible structure for a single sheet of C_2F, and (b) the same structure showing localized double bonds .	142

Page

V-10. Another possible structure for C_2F 143

V-11. A possible structure for C_8F in the hk0 projection 144

V-12. X-ray powder patterns of graphite hydrofluorides and their reduction products 145

REVERSIBLE INTERCALATION OF GRAPHITE BY FLUORINE AND RELATED SYNTHETIC AND THERMODYNAMIC STUDIES

Thomas Edward Mallouk

Materials and Molecular Research Division
Lawrence Berkeley Laboratory
and
Department of Chemistry
University of California
Berkeley, California 94720

ABSTRACT

The pentafluorogermanate salts of a variety of cations (ClO_2^+, NO^+, SF_3^+, NO_2^+, and XeF_5^+) were synthesized and characterized by x-ray crystallographic and vibrational methods. The pentafluorogermanate ion was found to exist in one monomeric and at least three polymeric modifications in its salts. Lattice energy calculations and vapor pressure/temperature measurements established the following gas phase fluoride ion affinities: GeF_4, 100(6); BF_3, 92(6); AsF_5, 115(7); XeF_5^+, 202(7); ClF_2^+, 223(7); SF_3^+, 211(7); IF_6^+, 211(7) kcal $mole^{-1}$. The electron affinities of the third row transition metal hexafluorides were likewise re-evaluated.

The new graphite bifluorides, $C_{12}^+HF_2^-$ and $C_{18}^+HF_2^-$, were prepared; their crystal structures establish that they are correctly formulated as graphite salts. Fluorination of graphite in the presence of HF produced these salts and the first-stage hydrofluorides $C_xF_{1-\delta}(HF)_\delta$ ($5 > x > 2$, $x/\delta \simeq 12$), which were studied by XPS, n.m.r., vibrational spectroscopy, and crystallographic methods. In these compounds, fluorine forms weak,

semi-ionic bonds to the carbon atoms, which are disposed in virtually undistorted, planar sheets. For the range of composition in which $C_xF_{1-\delta}(HF)_\delta$ is an electrical conductor ($x \geq 2.3$), the fluorination was found to be electrochemically reversible.

CHAPTER I

GENERAL INTRODUCTION AND EXPERIMENTAL PROCEDURES

A. General Introduction

This thesis is divided into four main chapters, the first three dealing with topics relating to molecular chemistry, and the last devoted to graphite chemistry. The unifying theme (hopefully one may be apparent to the reader) concerns the correlation of the fluoride ion and electron affinities of molecules with their ability to intercalate graphite, and the techniques which are used to evaluate those affinities. Chapter II discusses the synthesis and properties of pentafluorogermanate salts; it was found that quite a variety of cations can stabilize the GeF_5^- ion in polymeric forms, while only large cations were found to favor the monomeric (D_{3h}) form. The first and second fluoride affinities of GeF_4 were of interest, since it has been found that both GeF_5^- and GeF_6^{2-} salts of graphite can be prepared[1]. Chapter III discusses the method used to determine these quantities. In Chapter IV this method is elaborated and applied to the determination of the gas phase fluoride ion and electron affinities of a number of molecular and ionic species. Some new graphite intercalation reactions are described in Chapter V; these involve molecules (namely, SiF_4 and HF) whose fluoride ion affinities put them close to the thermodynamic threshold for graphite intercalation. This chapter also describes the compounds $C_xF_{1-\delta}(HF)_\delta$ ($2 < x < 5$), which were prepared in an investigation of the graphite/HF/F_2 system. The chemical and electrochemical reversibility of graphite fluorination are discussed.

B. Apparatus and handling of materials

Since most of the compounds described in this thesis are hydrolytically and oxidatively unstable in moist air, and in many cases can also react with glass, they were manipulated almost exclusively on a metal vacuum line or in a nitrogen atmosphere dry-box. A description of the general techniques used in handling air-sensitive materials has been given by Shriver[2].

1. Vacuum lines

The vacuum line used for synthetic work consisted of two parts: a low pressure part constructed from 1/4" O.D. Monel tubing, connected via stainless steel ferrules and Swagelok fittings to 1/4" stainless steel, Kel-F tipped Whitey (IKS4) valves, and a high pressure part consisting of Autoclave Engineering 30VM6071 Monel valves and their companion connectors. The low pressure part, on which most of the work was done, had four outlet ports and was wrapped in heating tape so that it could be heated resistively to ca. 80°C. This facilitated the rapid removal of such compounds as HF, AsF_3, and BrF_3. The pressure was monitored with an Acco Helicoid gauge (0 - 1500 torr) and a Hastings thermocouple gauge (0 - 500 microns Hg). The high pressure part of the vacuum line was attached to the low pressure part near the vacuum end and was also connected to a fluorine cylinder. It had two outlet ports and was fitted with a 0 - 500 psia Crosby pressure gauge.

A good mechanical pump was connected to the vacuum line through a Pyrex cold trap. The line could be pumped out directly or through a soda-lime tower, to dispose of F_2 and other corrosive materials. Pressures of 10 to 30 microns were readily attained. Passivation of the vacuum line and reaction vessels was accomplished by exposing them to 1 - 2 atm ClF_3 or F_2 pressure for several hours.

2. Reaction and storage vessels

Reaction vessels generally consisted of 3/8" O.D. teflon FEP or fused silica tubes sealed at one end and attached with Swagelok compression fittings to a stainless steel Whitey valve. The use of teflon ferrules provided a vacuum-tight seal. For reactions which required pressures in excess of two atmospheres a miniature pressure bomb was made by drilling out a 3 inch length of 3/8" stainless steel rod; in this case metal ferrules were substituted. Larger stainless steel or Monel bombs were used for large-scale preparations. Well passivated Monel and stainless steel bulbs and cans were used for the storage of gaseous reagents such as F_2, GeF_4, ClO_2F, NO_2F, SF_4, and ONF. Those with lower vapor pressures (IF_5, XeF_6, HF, BrF_3, and the like) were stored in Kel-F tubes fitted with Whitey valves. Reaction vessels were checked for leaks with a CEC24-120B helium mass spectrometer leak detector (Consolidated Electrodynamics, Monrovia, Ca.).

3. Glove boxes

Involatile solids and liquids were handled in the nitrogen atmosphere of a Vacuum Atmospheres Corp. Dri-Lab (North Hollywood, Ca.). The atmosphere therein was kept dry and free of oxygen by circulation through drying trains which were regenerated frequently.

C. Characterization of materials

1. X-ray powder photography

Debye-Scherrer photographs were taken with a General Electric Precision powder camera (45 cm. circumference), using Ni-filtered Cu radiation, and occasionally Zr-filtered Mo radiation. Thin walled, 0.5 mm. diameter quartz capillaries (Charles Supper Co., Natick, Mass.) were typically loaded with powdered samples inside the Dri-Lab, plugged with

Kel-F grease, and then sealed off outside the Dri-Lab with a microtorch. Some solids were too unstable to permit such handling, and were prepared directly in quartz x-ray capillaries which had been blown onto quartz tubing and so fitted to the vacuum line. For powder patterns which were to be taken in the presence of liquid HF, quartz capillaries were not suitable, and teflon-FEP capillary tubing was made by drawing down a 3/8" tube and sealing at the narrow end. Such a capillary produced a background diffraction pattern (from the hexagonal, two dimensional unit cell of oriented teflon-FEP), but the capillary wall was thin enough to allow diffraction from the enclosed powder when either Mo or Cu radiation was used. X-ray films were measured on a Norelco device. A Dobson-type microdensitometer[3] was used with some samples to determine the relative intensity of the diffraction lines.

2. X-ray powder diffraction

X-ray diffractometer tracings of oriented samples and powders were obtained from a Phillips-Norelco powder diffractometer, using monochromatized CuK_α radiation. The holder for diffractometer samples has been described elsewhere[4]; it consists of a 3/8" diameter circular Monel holder covered with a thin (.025 mm) Kapton sheet, which is transparent to CuK_α radiation. The holder is made air-tight with a metal ferrule which presses the Kapton against Viton O-rings. The samples (usually freshly cleaved, intercalated HOPG chips) were mounted in the holder between the Kapton film and a 1mm. thick teflon disk, which prevented diffaction from the sample holder.

3. Raman spectroscopy

Raman spectra were recorded from a J-Y Ramanor HG.2S spectrometer with a double holographic grating monochrometer, using a krypton (647.1

nm) or argon ion (514.5 or 488.0 nm) laser as the excitation source. The samples were generally held in quartz x-ray capillaries or in 1/4" diameter teflon FEP tubing. For low temperature studies, the sample could be held in a stream of cold nitrogen, jacketed by warm nitrogen (to prevent ice condensation), and maintained at a temperature of 0 to -140°C. For colored or extremely volatile solids this measure prevented the sample from decomposing or subliming out of the beam.

4. Infrared spectroscopy

Infrared spectra were recorded on a Perkin Elmer 597 Grating Spectrophotometer. For gases, a Monel cell (8 cm path length) fitted with AgCl windows (Harshaw Chemical Co., Solon Ohio) was used; for solids, a Kel-F cell, which pressed the powdered solid between two AgCl disks, was used. The edges of the disks were smeared with Kel-F grease to provide a temporary seal against atmospheric moisture.

5. Single crystal x-ray diffraction

X-ray precession photographs were routinely taken on an Enraf-Nonius (Delft, Holland) camera, using Zr filtered Mo radiation and a Polaroid XR-7 film cassette. Intensity data collection for single crystals was carried out on an Enraf-Nonius CAD-4 four-circle automatic diffractometer, which used monochromatized MoK_{α} radiation and was interfaced through a PDP 8/a minicomputer to a DEC PDP 11/60. The solution of the structures was carried out at the U.C. Berkeley CHEXRAY facility using locally modified software (Structure Determination Package, B.A. Frenz and Associates, Inc., College Station, Texas, and Enraf-Nonius, Delft, Holland).

6. Chemical analysis

Carbon analyses were carried out by the Microanalytical Laboratory,

College of Chemistry, U.C. Berkeley. Analyses for carbon, fluorine, nitrogen, germanium, tin, and oxygen were done by Galbraith Analytical Labs (Knoxville, Tenn.). Hydrogen analysis for graphite fluoride and hydrofluoride salts was accomplished by pyrolyzing an appropriate quantity of the compound (usually ~100 mg) for one hour in a stainless steel vessel at 950 - 1000°C. The off-gases from the pyrolysis (carbon fluorides and HF) were passed through a cold trap containing a known amount of 0.1F standard KOH solution. The solution was allowed to warm up to room temperature and was back-titrated with standard (.025F) HCl solution, the end-point being determined potentiometrically. Duplicate analyses were in agreement within about 10%, the error probably arising from incomplete trapping of the HF or from "background" hydrogen (as water or HF) in the apparatus.

References

1. E.M. McCarron, Y.J. Grannec, and N. Bartlett, J. Chem. Soc. Chem. Comm., 890 (1980).

2. D.F. Shriver, "The Manipulation of Air-Sensitive Compounds", McGraw-Hill, New York, 1969.

3. A. Taylor, J. Sci. Instr., 250 (1951).

4. R.N. Biagioni, Ph.D. thesis, University of California, Berkeley (1980).

/

CHAPTER II

SYNTHESIS, STRUCTURE, AND VIBRATIONAL ANALYSIS OF PENTAFLUOROGERMANATE SALTS

A. Introduction

The GeF_5^- ion is stabilized by a wide variety of cations, including some of high electron affinity[1-4]. While the first pentafluorogermanate salt was reported[1] in 1967, to date no structural data on these compounds have appeared in the literature. Vibrational analyses[1,3,4] have indicated that the GeF_5^- ion may be either monomeric or polymeric in form.

The GeF_5^- ion is of interest for a number of reasons. First, it has been reported[5] that the hexafluorogermanate salt of graphite loses fluorine via the equilibruim:

$$C_{12}GeF_6 = C_{12}GeF_5 + \tfrac{1}{2}F_2$$

This equilibrium represents a delicate balance between the first and second fluoride ion affinities of GeF_4, the work function of the intercalated graphite, and the lattice energies of the graphite salts; hence a prime concern was the determination of the GeF_4 fluoride ion affinities (see Chapter III). Second, the apparent polymorphism of GeF_5^-, and its instability with respect to GeF_4 and GeF_6^{2-} in most simple salts, suggested that it might undergo the equilibrium:

$$GeF_5^- + F^- = GeF_6^{2-}$$

in its salts and hence conduct F^- in the solid state. Although no evidence for F^- conduction was found, the polymorphism of the GeF_5^- ion in the solid state was established.

When considering which salts of GeF_5^- will be stable with respect

to GeF_4 and the corresponding GeF_6^{2-} salts, it is helpful to think in terms of a simple Born-Haber cycle for the disproportionation:

$$\begin{array}{ccc} 2A^+GeF_5^-(s) & \rightarrow & A^+_2GeF_6^{2-}(s) + GeF_4(g) \\ \downarrow 2U_L(1) & & \uparrow U_L(2) \\ 2A^+(g) + 2GeF_5^-(g) & \xrightarrow{FA(2)-FA(1)} & 2A^+(g) + GeF_6^{2-}(g) + GeF_4(g) \end{array}$$

Here A^+ is a cation, such as K^+, NO^+, SF_3^+, etc., which forms an $(A^+)_2GeF_6^{2-}$ salt, FA(2)-FA(1) is the difference between the second and first fluoride ion affinities of GeF_4, and $U_L(1)$ and $U_L(2)$ are the lattice energies of the 1:1 and 2:1 salts. The FA(2)-FA(1) term will vary slightly since GeF_5^- has several isomers in the solid state, but the driving force for the reaction will come mainly from the difference between the two lattice energies. A rough estimate of these energies based on Kapustinskii's formula[6] gives approximately 130 kcal $mole^{-1}$ for $U_L(1)$ and 390 kcal $mole^{-1}$ for $U_L(2)$, for A^+ and GeF_x^{n-} thermochemical radii of 1.6 and 2.4 Å, respectively. These lattice energies will tend to increase in the same proportion as the radius of A^+ is decreased, and hence it is clear that smaller cations will tend to favor the disproportionation. Large cations, however, will not form stable GeF_5^- salts if $U_L(1)$ is not sufficiently great or if too much energy is required for the step:

$$AF(\text{standard state}) = A^+(g) + F^-(g)$$

The molecular fluorides NO_2F, SF_4, ClF_3, ClO_2F, IF_7, and ONF seemed to be excellent candidates for the production of GeF_5^- salts, by virture of both their size and their fluoride ion donor ability. All of these compounds have been reported to form salts (or at least solid adducts)

with BF_3 and AsF_5; the fluoride ion acceptor strengths of AsF_5 and BF_3 are close (see Chapter IV) to that of GeF_4.

B. Experimental

1. Reagents

GeF_4 was prepared by reacting either Ge metal powder (Alfa Inorganics, 325 mesh, 99.999%) or GeO_2 (Alfa, 99.995%) with excess fluorine in a Monel bomb at 250°C for 16 hours. The use of germanium dioxide was preferred since the interaction of fluorine with finely divided metal powders can present a safety hazard.

XeF_6 was made by heating a F_2/Xe mixture (10/1 mole ratio) at 300°C in a well-passivated Monel bomb for 24 hours. The small quantities of XeF_4 and $XeOF_4$ also produced were removed by condensing the crude product onto an excess of dry NaF in a fluorinated Monel can, thereby forming NaF/XeF_6 complexes[7]. This mixture was heated in a dynamic vacuum at 50°C to remove the impurities, and XeF_6 was liberated by heating the remaining salt, Na_2XeF_8, to 100-150°C.

ClO_2F was prepared[8] by condensing ClF_3 onto a twofold excess of $KClO_3$ in a Monel can. The reaction went to completion in one day, and ClO_2F, the only volatile product, was purified by trap-to-trap distillation.

SF_4 was obtained from Matheson gas products. Since this commercial product contains a substantial SOF_2 impurity it was purified by reaction[9] with BF_3 to form the salt $SF_3^+BF_4^-$. The SOF_2 and excess BF_3 were pumped away at 0°C, and the salt was sublimed onto CH_3CN (which had been distilled from P_2O_5). Gentle warming of the CH_3CN/SF_3BF_4 mixture produced SF_4, free of infrared-active impurities.

NO_2F was prepared by reacting $NaNO_2$ and F_2 in a Monel can at room

temperature[10], and separated from the N_2O_4 produced in the reaction by trap-to-trap distillation.

$\underline{IF_7}$ was made from KI and excess F_2 in a passivated Monel bomb at 200°C. It was found that the product could be prepared free of IOF_5 if the KI was dried in vacuo at 300°C, and if the bomb had been previously passivated with a crude IF_7/IOF_5 mixture at 200°C.

$\underline{ONF}$ was prepared by literature methods[11]. $\underline{IF_5}$, $\underline{SO_2}$, and $\underline{ClF_3}$ were supplied by Matheson gas products and used without further purification. $\underline{HF}$, supplied by Matheson, was stored over K_2NiF_6 to remove traces of water.

2. $\underline{ONF/GeF_4}$

Interaction of ONF with GeF_4 at room temperature produces the poorly crystalline salt $(NO^+)_2GeF_6^{2-}$, which is identified by its vibrational spectra[4] (figure II-1). The observed frequencies and Raman-i.r. selection rules are quite close to those previously observed for the GeF_6^{2-} ion, although the $\nu_2(E_g)$ mode is broadened in the Raman, indicating a slight departure from octahedral symmetry. The assignments for the vibrations of $(NO^+)_2GeF_6^{2-}$ are given in Table II-1.

The 1/1 salt $NO^+GeF_5^-$ has been reported[13], but attempts to prepare it by the literature method (from Ge metal, anhydrous HF, and NO_2) yielded only $(NO^+)_2GeF_6^{2-}$. When $(NO^+)_2GeF_6^{2-}$ was sublimed (at 220°C) in the presence of excess GeF_4, a white, involatile solid was produced which was found from vibrational spectra to be $NO^+GeF_5^-$. This salt was obtained, although the vibrational spectra were slightly different, when $(NO^+)_2GeF_6^{2-}$ was allowed to interact with excess GeF_4 in the presence of liquid IF_5, HF, or SO_2. The use of SO_2 at -20°C gave the cleanest product, which was also nicely microcrystalline. Figure II-2 shows the

Raman and infrared spectra of $NO^+GeF_5^-$, (a) prepared by subliming $(NO)_2GeF_6$ in the presence of GeF_4, and (b) prepared in SO_2 solution. A Debye-Scherrer photograph of the $NO^+GeF_5^-$ powder was taken and the low angle lines were tentatively indexed to an orthorhombic unit cell, a = 10.82(1), b = 9.77(1), c = 8.89(1) Å, V = 940(2) $Å^3$, Z = 8. The observed and calculated $1/d^2$ values for $NO^+GeF_5^-$ are given in Table II-2.

3. SF_4/GeF_4

Interaction of SF_4 and GeF_4 in any proportions invariably produced the 2:1 salt $(SF_3^+)_2GeF_6^{2-}$. It was found, however, that GeF_4 would displace BF_3 from $SF_3^+BF_4^-$ to yield the 1:1 compound $SF_3^+GeF_5^-$. The latter is unstable with respect to disproportionation to $(SF_3)_2GeF_6$ and GeF_4 at room temperature, except under liquid (i.e., several atmospheres of) GeF_4, when $SF_3^+GeF_5^-$ can be stabilized. In a typical preparation, .35 mmol SF_3BF_4 was prepared[9] by interaction of equimolar quantities of SF_4 and BF_3 in FEP tubes. The compound was transferred by sublimation into a short 1/4" O.D. quartz tube, the lower end of which had been sealed onto a 0.7mm dia. quartz x-ray capillary. GeF_4 (.50 mmol) was condensed into the reactor and after one minute at 10°C the BF_3 liberated was pumped off at -126°C (methylcyclohexane slush). After two such treatments with GeF_4, the powder was tapped down into the capillary, excess GeF_4 condensed upon it, and the capillary sealed off. The x-ray powder pattern of this material (Table II-3) was indexed to an orthorhombic cell, a = 11.66(2), b = 7.69(1), c = 6.36Å, V = 569(1) $Å^3$, Z = 4 (consistent with Zachariasen's criterion[14] of 18 $Å^3$ per fluorine atom). The Raman spectrum of this material (figure II-3) confirmed its formulation as $SF_3^+GeF_5^-$.

4. NO_2F/GeF_4

NO_2F reacted with an equimolar amount of GeF_4 at room temperature to produce a colorless, involatile solid which was identified as $NO_2^+GeF_5^-$ from its Raman (figure II-3) and infrared (figure II-4) spectra. The powder pattern of this compound was recorded, but not indexed, and the $1/d^2$ values and relative intensities are listed in Table II-4.

5. XeF_6/GeF_4

The XeF_6 - GeF_4 system has been investigated by Pullen and Cady[1], who reported the compounds $4XeF_6 \cdot GeF_4$, $2XeF_6 \cdot GeF_4$, and $XeF_6 \cdot GeF_4$. It seemed that likely formulations for these compounds were, respectively, $(Xe_2F_{11}^+)_2GeF_6^{2-}$, $(XeF_5^+)_2GeF_6^{2-}$ (or $Xe_2F_{11}^+GeF_5^-$), and $XeF_5^+GeF_5^-$, and it was hoped that the latter compound would yield crystals of suitable quality for an x-ray structure.

XeF_6 (.653 mmol) was combined with GeF_4 (.878 mmol) at 50°C for 20 minutes in a FEP U-tube which was then pumped out briefly at room temperature. The residual weight indicated the 1:1 compound $XeF_6 \cdot GeF_4$ (.636 mmol). A Debye-Scherrer photograph obtained provided d-spacings in agreement with those previously reported[1]. The Raman and infrared spectra of this material, which could be formulated as the salt $XeF_5^+GeF_5^-$, were recorded from the powder and are shown in figures II-3 and II-4, respectively.

6. $XeF_5^+GeF_5^-$ crystal structure

Colorless crystals of $XeF_5^+GeF_5^-$ were formed upon sublimation of the microcrystalline solid at 40 - 50°C in 0.7 mm dia. quartz x-ray capillaries. These had been sealed under an atmosphere of nitrogen. Precession photographs indicated a primitive orthorhombic cell, space

group Pnma or $Pna2_1$.

A crystal was mounted on an Enraf-Nonius CAD-4 four circle diffractometer, and accurate cell dimensions were obtained by a least-squares fit to three sets of eight symmetry-equivalent reflections with 2θ between 25 and 29°. The cell dimensions and data collection parameters are summarized in Table II-5.

The structure was solved by heavy-atom methods[15] at the U.C. Berkeley CHEXRAY facility using full-matrix least-squares refinement procedures detailed elsewhere[17]. Systematically absent reflections were eliminated from the data set and those remaining were corrected for absorption by means of the calculated absorption coefficient. A three dimensional Patterson synthesis gave peaks which were consistent with Xe atoms in Wyckoff position 4c and Ge atoms in 4a in space group Pnmb (see Pnma, no. 62). Three cycles of least-squares refinement for Xe and Ge with isotropic thermal parameters followed by a difference-Fourier synthesis gave the locations of the fluorine atoms (four in 4c, three in 8d). Three more cycles of isotropic least-squares refinement resulted an an R-factor of 0.110, indicating that the centric space group was probably the correct choice. Symmetry-equivalent reflections were averaged and the refinement continued with the inclusion of anisotropic thermal parameters and an extinction coefficient[18]. This led to final convergence with a weighted R factor of 0.018, unweighted R = 0.021, standard deviation of an observation of unit weight = 0.725 for 65 parameters and 437 independent data. A final difference Fourier showed no peaks with intensity greater than 0.33 $e/Å^3$. The observed and calculated structure factors for the XeF_5GeF_5 structure are listed in Table II-6.

The positional and thermal parameters for atoms in the XeF_5GeF_5 structure are listed in Table II-7.

7. ClO_2F/GeF_4

ClO_2F and GeF_4 condensed in equimolar proportions in a FEP tube produced a pale-yellow solid, which had a vapor pressure of approximately 130 torr at room temperature and so was readily sublimable. The Raman (figure II-3) and infrared spectra (figure II-4) of the sublimed powder identified it as the salt $ClO_2^+GeF_5^-$.

8. ClO_2GeF_5 crystal structure

Yellow crystals were obtained by sublimation at 30-35° in closed 0.5 mm diameter quartz capillaries under an atmosphere of nitrogen. The ready sublimation of these crystals required that the collection of data be at low temperature; an apparatus was constructed for the CAD-4 which provided a stream of dry nitrogen to maintain the crystal at -105 ± 10° in all orientations. Apart from this modification the structure solution proceeded as for XeF_5GeF_5, except that loss of the crystal immediately after the data collection made it impossible to correct the data for absorption.

Refinement of intensity data for ClO_2GeF_5 in space group $C222_1$ led to convergence with a weighted R factor = 0.068, unweighted R = 0.059, std. dev. obs. unit wt. = 3.938. The largest peak on a final difference Fourier map was .285 e/Å^3. Observed and calculated structure factors for ClO_2GeF_5 are listed in Table II-8, and positional and thermal parameters in table II-9.

9. IF_7/GeF_4

The interaction of equimolar quantities of IF_7 and GeF_4 in quartz tubing at 20°C gave no solid product. If the temperature was lowered to

10°, the solution became turbid and a few colorless crystals were precipitated; these quickly evaporated if the GeF_4/IF_7 solution was pumped away.

10. ClF_3/GeF_4

No solid product was formed from ClF_3 and GeF_4, which were condensed together into a FEP tube and allowed to warm up to 0°C.

11. $(n\text{-}C_4H_9)_4N^+GeF_5^-$

This compound was prepared according to the literature method[2]; its Raman and infrared spectra are shown in figure II-5.

C. Results and discussion

1. $XeF_5^+GeF_5^-$ structure

A stereo view of the $XeF_5^+GeF_5^-$ structure is shown in figure II-5. The structure consists of infinite chains of GeF_6 octahedra which share trans vertices, each XeF_5^+ cation having close contacts (2.75 - 2.76 Å) to four fluorine atoms of two neighboring F-bridged GeF_6 groups in the chain. The coordination of the xenon atom is nearly a capped square antiprism of C_{4v} symmetry. The bridging (and probably least negatively charged) fluorine atoms in the chain are apparently screened from interaction with the xenon atom by the non-bonding valence-electron pair of the latter, and so are bent away from the xenon atom. The coordination around each Ge atom is essentially an elongated octahedron of fluorine atoms, with cis F-Ge-F angles within the non-bridging fluorine GeF_4 set being 87.9° and 92.1°. The angle between this approximately square set and the bridging fluorine atoms is a right angle within one standard deviation. All Ge-F distances within the square plane are equal at 1.745(2) Å, and the Ge-bridging F distance is 1.890(1). This difference in length of bridging and non-bridging M-F

bonds of 0.15 Å is similar to that observed in the transition and post-transition element pentafluorides, which, with the exception of PF_5 and AsF_5, also adopt fluorine-bridging structures. If we consider that 1.75 Å represents a Ge-F single bond and use Pauling's[19] formula for fractional bond order:

$$D(n) - D(1) = -0.60 \log(n)$$

we find that the bond order for the Ge-F bridging bonds is 0.57; they are in effect half bonds. This is easily seen from a simple molecular orbital picture for the Ge-F-Ge fragment, which is a three-center, two electron system, like the B-H-B fragment in diborane.

Interactions between the infinite chains are limited to F-F van der Waals' contacts ranging from 2.99 Å (F1-F4) to 3.26 Å (F2-F4). Table II-10 gives selected bond lengths and angles for XeF_5GeF_5.

2. $ClO_2^+GeF_5^-$ structure

Figure II-6 shows a stereo view of the ClO_2GeF_5 structure. Here the infinite chains are formed from approximately octahedral GeF_6 units which share cis vertices; the chain is actually an extended helix with all the germanium atoms of a given chain nearly coplanar. The shortest Ge-F bonds (1.73 - 1.74 Å) are cis to the bridging fluorine atoms but those trans are only slightly longer (1.77 -1.78 Å). The Ge-bridging F distances are the same within one standard deviation (1.887(1)). The anion chains are linked together by close contacts (2.54 and 2.63 Å) of the chlorine atoms to the fluorine atoms trans to the Ge-F-Ge bridges. There are two crystallographically distinguishable chlorine atoms in the structure, but each lies on a twofold rotation axis. The coordination of each is shown in figure II-7. The closest cation-to-anion contacts (Cl1-F1 and Cl2-F4) are made on the faces of the triangle defined by the

two oxygen atoms and the chlorine atom. Presumably the non-bonding electron pair is in the plane of the triangle and exo to it at the Cl apex. The screening of the cation charge by the Cl non-bonding electron pair is the probable cause of the long Cl to F contacts in the plane of the ClO_2 triangle compared with the Cl to F contacts along axes roughly perpendicular to that plane. One may compare the behavior of the ClF_2^+ ion; as Lynton and Passmore point out in their discussion of the $ClF_2^+AsF_6^-$ structure[20] (and this view is supported by ab-initio calculations[21] for the free ClF_2^+ ion), the ClF_2^+ ion is a slightly distorted ClF_2E_2 tetrahedron. In the $ClF_2^+AsF_6^-$ and $ClF_2^+SbF_6^-$ structures[22] the closest anion-to-chlorine contacts are made on the FE_2 faces of the tetrahedron, giving a distorted square planar arrangement of fluorine around the chlorine atom.

A summary of internuclear distances and angles for $ClO_2^+GeF_5^-$ is given in Table II-11.

3. Vibrational analysis of salts containing the GeF_5^- ion

The Raman and infrared spectra of $NOGeF_5$ are shown in figure II-2. Those of XeF_5GeF_5, ClO_2GeF_5, NO_2GeF_5, and SF_3GeF_5 appear in figures II-3 and II-4.

i) $XeF_5^+GeF_5^-$

Assignments for the normal modes of vibration of the XeF_5^+ ion in $XeF_5^+GeF_5^-$ are given in Table II-12. In polarized Raman spectra recorded from a single crystal, the cation stretching bands which transform as A_g in the point group of the crystal (D_{2h}) are most intense for the I_{vv} polarization. The correlation $D_{2h} \rightarrow C_s \rightarrow C_{4v}$ shows that these are the A_1, B_2, and E modes of the approximately C_{4v} XeF_5^+ ion; hence the bands at 669, 622, and 602 cm^{-1} are attributed to the $\nu_1(A_1)$,

$\nu_4(B_2)$, and $\nu_2(A_1)$ modes, respectively. The other Raman and infrared bands are assigned by analogy to published spectra of XeF_5^+ salts[23]. The assignments are made according to the approximate C_{4v} symmetry of the ion, but since its crystallographic symmetry is C_s, we expect that the degeneracy of the E modes will be lifted.

Since the germanium atoms in XeF_5GeF_5 lie on crystallographic inversion centers, the Raman and infrared spectra are mutually exclusive for the $(GeF_5)_n^{n-}$ ion. To simplify the vibrational analysis of this ion, its normal modes of vibration are decomposed into those of two sets of atoms with transform separately in the point group of the crystal (D_{2h}); that is, the square plane of germanium and terminal fluorine atoms is considered separately from the chain of germanium and bridging fluorine atoms. The GeF_4 square plane has approximately D_{4h} symmetry, and so has seven normal modes, of which three are stretching vibrations: $\nu_1(A_{1g})$, $\nu_4(B_{2g})$, and $\nu_7(E_u)$. The ν_1 vibration should be the most intense, but since a Ge-F bond is less easily polarized than an Xe-F bond, its intensity in the Raman will be rather low. Thus ν_1 is assigned to the band at 654 cm^{-1}. The ν_4 stretch is not as easily assigned, but by comparison with the same type of vibration[12] in GeF_6^{2-}, it is probably seen in the weak band at 463 cm^{-1}, and for the same reason the doublet at 339, 331 cm^{-1} is attributed to the deformational modes of the square plane. The ν_7 stretch, observable only in the infrared, is found at 700 cm^{-1}. The other vibrations of the square plane, also infrared-active, are of a frequency too low (< 300 cm^{-1}) to be observed.

The remaining bands must arise, therefore, from vibrations of the infinite chains. In the 500-600 cm^{-1} region, the observed infrared (600

and 500 cm^{-1}) and Raman (518 and 526 cm^{-1}) bands are attributed to chain stretching modes. Chain-square plane deformational (381 cm^{-1}) and torsional-rotational modes (184, 124 cm^{-1}) are also seen in the Raman.

ii) $\underline{ClO_2^+GeF_5^-}$

The cation and anion bands for $ClO_2^+GeF_5^-$ are shown in Table II-13. The frequencies observed for ClO_2^+ correspond quite well to those which have previously appeared in the literature[24].

Because the anion in $ClO_2^+GeF_5^-$ consists of infinite chains of octahedra which share cis-vertices, its symmetry is lower than that of the trans-bridged anion found in $XeF_5^+GeF_5^-$, and the i.r. - Raman selection rules are not very restrictive. If one considers the group formed by the germanium and four non-bridging fluorine atoms, it approaches C_{2v} symmetry with four stretching modes which transform as $2A_1 + B_1 + B_2$, all active in both infrared and Raman. Those of type A_1 are primarily observable in the Raman, while those of types B_1 and B_2 will be most intense in the infrared. Therefore the i.r. bands at 695 and 650 cm^{-1} are assigned to the B_1 and B_2 vibrations, and the most intense Raman band (657 cm^{-1}) to the in-phase symmetric stretch (A_1) of the GeF_4 group. The bands between 500 and 600 cm^{-1} may then be attributed to the stretching modes of the chain. By analogy to the vibrational frequencies of the trans-bridged $(GeF_5)_n^{n-}$ ion in $XeF_5^+GeF_5^-$, the 395, 339 cm^{-1} band is assigned to a deformation of the angle between the GeF_4 group and the bridging fluorines; the bands between 290 and 337 cm^{-1} are attributed to deformations of the GeF_4 group, and the lower frequency bands (133 to 232 cm^{-1}) to torsional and rotational motions of the infinite chains.

The published spectra[4] of $O_2^+GeF_5^-$ show a great deal of similarity

to those of $ClO_2^+GeF_5^-$, and it is therefore probable that the anion has nearly the same structure in both compounds.

iii) $\underline{NO^+GeF_5^-}$

The vibrational assignments for $NO^+GeF_5^-$ are also given in Table II-13. The striking similarity of the Raman spectrum of $O_2^+GeF_5^-$ with that of $NO^+GeF_5^-$ prepared thermally from $(NO)_2GeF_6$ and GeF_4 indicates that the structure of the anion is very nearly the same in both, and that the two compounds may in fact be isostructural. Unfortunately, no x-ray powder data has been reported for $O_2^+GeF_5^-$.

iv) $\underline{NO_2^+GeF_5^-,\ SF_3^+GeF_5^-}$

The vibrational spectra and assignments for these two salts are given in Table II-14. Both compounds show Raman bands in the chain stretching region (507, 583 cm^{-1} in $SF_3^+GeF_5^-$ and 501, 606 cm^{-1} in $NO_2^+GeF_5^-$), indicating polymeric, <u>cis</u>-bridged $(GeF_5)_n^{n-}$ ions. The Raman spectra are quite similar to each other -- both compounds have a vibration of medium intensity near 500 cm^{-1} and a particularly simple bending region with only one strong band at 355 cm^{-1}. It seems safe to conclude, therefore, that the anions are structurally similar, and yet different from $(GeF_5)_n^{n-}$ in $ClO_2^+GeF_5^-$, wherein the infinite chains of bridged octahedra form an extended helix with the Ge atoms nearly coplanar. The anion in $NF_4^+GeF_5^-$, because its vibrational spectra[3] are very like those of $NO_2^+GeF_5^-$, is probably of the same structural type.

v.) $\underline{(n\text{-}C_4H_9)_4N^+GeF_5^-}$

The Raman and infrared spectra of the tetrabutylammonium salt, first prepared by Wharf and Onyszchuk[2], are shown in figure II-8. The vibrations of the anion may be readily assigned on the basis of D_{3h} symmetry, from selection rules and by comparison to other MX_5 species.

The ν_7 band (i.r. and Raman active) which we expect to find near 100 cm^{-1}, is obscured by a band of the tetrabutylammonium ion at 117 cm^{-1}. In measuring the intensity of this band relative to the tetrabutylammonium band at 260 cm^{-1} in this compound and in $(n\text{-}Bu)_4N^+Br^-$, we find that its intensity is enhanced in the GeF_5^- salt. It seems therefore that the ν_7 vibration of GeF_5^- should be located near 117 cm^{-1}. The vibrational assignments for GeF_5^- in $(n\text{-}Bu)_4N^+GeF_5^-$ are shown in Table II-15, and the assignments for other MX_5^- species are tabulated for comparison.

vi) Comparison of the cis and trans bridging structures

Evidently the choice of cis versus trans bridging for polymerized GeF_5^- is one of energetic subtlety. Jolly et al[25], in their analysis of the structure of liquid SbF_5, argue that the cis form may be favored on electronic grounds because there one has three orthogonal sets of short bonds. This effect seems to be important when d-orbitals are involved in the bonding since most of the known tetrameric or polymeric transition metal pentafluorides associate via cis bridges. The trans form, nevertheless, can be stabilized by steric factors: each fluorine atoms in the square plane has only two close-neighbor fluorine atoms. For main group elements, the difference in energy between the cis and trans forms appears to be smaller, and indeed both bridging modes have been found in the same compound[26] (in $SrAlF_5$). The favored coordination geometry of the cation appears to be the deciding factor for the GeF_5^- salts: the ClO_2^+ ion could not coordinate effectively to the non-bridging fluorines of a trans-bridged chain, since it prefers a coordination angle (F-Cl-F) near 180°. Such an arrangement would bring the chlorine atom nearer to the bridging (most positively charged)

fluorine atoms than to the non-bridging fluorine atoms. Larger, more non-symmetric (in their coordination geometries) cations, such as XeF_5^+, coordinate more effectively to the trans-bridged chain. When the cation is extremely large (e.g, tetra n-butylammonium, which has a radius of approximately 4.1 Å), it cannot pack effectively around an oligomeric or polymeric anion, and so the monomeric (D_{3h}) form is favored; probably only two large cations can fit around a single anion chain, and the maximum extension of the F-Ge-F-Ge-F unit in the trans- bridging chain is 7.6 Å.

The bridging angle (Ge-F-Ge) is 141° in XeF_5GeF_5 and 143 to 148° in ClO_2GeF_5. For transition metal MF_5 species the bridging angle is apparently determined by both the size and by the nuclear charge of the metal atom. The pentafluorides[27,28,29] of Nb, Ta, Mo, and W form cis-bridged tetramers in the solid state in wich the M-F-M bridging angle is 180° and the fluorine atoms form a distorted cubic close-packed array. While covalent M-F bonding would favor a more acute bridging angle, the linear bridges may be stabilized by overlap of the fluorine $2p_{x,y}$ orbitals with the empty metal d_{xz},d_{yz} set. As the nuclear charge of the metal atom is increased the d-orbitals are contracted and the linear M-F-M geometry is destabilized relative to one which is bent slightly (ca. 150° in TcF_5[30] and ReF_5[31]) to preserve some metal d - fluorine p overlap. In the pentafluorides[30,32,33] of Ru, Rh, Os, Ir, and Pt the contracted d-orbitals are no longer effective in this mode of bonding and the bridging angle decreases to ca. 135°; the fluorine atom array is then only slightly distorted away from hexagonal close packing[32]. The acuteness of the bridging angle is limited to about 130° by the steric repulsion of the non-bridging fluorine atoms of the vertex-sharing

octahedra.

In the case of post-transition metal pentafluorides and pentafluorometallate salts, the M-F-M bridging angle is likely to be determined by the most efficient packing arrangement, and so may range from about 130° to 180°; and both of these extremes are nearly attained in the case of the SbF_5 structure[34].

Summary

GeF_5^- salts of several cations (O_2^+, NF_4^+, ClO_2^+, NO_2^+, SF_3^+, NO^+) are found to adopt structures in which the anions polymerize in the form of cis-vertex sharing octahedra. The trans-bridging form is found only in $XeF_5^+GeF_5^-$. Monomeric GeF_5^- is found in salts of very large cations, such as tetra n-alkylammonium. These structural forms are readily distinguished by their vibrational spectra.

References

1. K. Pullen and G. Cady, Inorg. Chem., 6, 1300 (1967).

2. I. Wharf and M. Onyszchuk, Can. J. Chem., 48, 2250 (1970).

3. K.O. Christe, C.J. Schack, and R.D. Wilson, Inorg. Chem., 15, 1275 (1976).

4. K.O. Christe, R.D. Wilson, and I.B. Goldberg, Inorg. Chem., 15, 1271 (1976).

5. E.M. McCarron, Y.J. Grannec, and N. Bartlett, J. Chem. Soc. Chem. Comm., 890 (1980).

6. A.F. Kapustinskii, Zh. Fiz. Khim., 5, 59 (1934).

7. I. Sheft, T.M. Spitler, and F.H. Martin, Science, 145, 701 (1964).

8. D.F. Smith, G.M. Begun, and W.H. Fletcher, Spectrochim. Acta, 20, 1763 (1964).

9. N. Bartlett and P.L. Robinson, J.Chem. Soc., 3417 (1961).

10. E. Aynsley, G. Hetherington, and P.L. Robinson, J. Chem. Soc., 1119 (1954).

11. C.T. Ratcliffe and J.M. Shreeve, Inorg. Synth., 11, 194 (1968).

12. G.M. Begun and A.C. Rutenberg, Inorg. Chem., 6, 2212 (1967).

13. S. Kigoshi, Thermochim. Acta, 29, 147 (1979).

14. W.H. Zachariasen, J. Am. Chem. Soc., 70, 2147 (1948).

15. The quantity minimized in least-squares refinement was $\sum w(|F_o| - |F_c|)^2$, where $w = 4F_o^2/(\sigma(F_o^2) + (pF_o^2)^2)$, $\sigma(F_o)$ being the standard deviation of F_o and p being a "pivot factor" (taken as .03) used to downweight intense reflections. Scattering factors for neutral atoms corrected for anomalous scattering were used[16]. The residuals were of standard form (see ref. 17).

16. "International Tables for X-ray Crystallography", Kynoch Press,

Birmingham, England, vol. IV. (1974).

17. J. Bleecke, R. Burch, C. Coulman, and B. Schardt, Inorg. Chem., 20, 1316 (1981).

18. The form of the correction for secondary extinction is $|F_{corr}| = |F_o|(1 + gI_c)$, where g is the extinction coefficient.

19. L. Pauling, J. Am. Chem. Soc., 69, 542 (1947).

20. H. Lynton and J. Passmore, Can. J. Chem., 49, 2539 (1971).

21. S.R. Ungemach and H.F. Schaefer III, J. Am. Chem. Soc., 98, 1658 (1976).

22. A.J. Edwards and R.J.C. Sills, J. Chem. Soc. A, 2697 (1970).

23. C.J. Adams and N. Bartlett, Israel J. Chem.,

24. K.O. Christe, C.J. Shack, D. Pilipovich, and W. Sawodny, Inorg. Chem., 8, 2489 (1969).

25. J. Hoffman, B. Holder, and W.L. Jolly, J. Phys. Chem., 62, 364 (1958).

26. R. Van der Muehll, S. Andersson, and J. Galy, Acta Crys. B, 27, 2345 (1971).

27. A.J. Edwards, J. Chem. Soc., 3714 (1964).

28. A.J. Edwards, R.D. Peacock, and R.W.H. Small, J. Chem. Soc., 4486 (1962).

29. A.J. Edwards, J. Chem. Soc. A, 909 (1969).

30. J.H. Holloway, R.D. Peacock, and R.W.H. Small, J. Chem. Soc., 644 (1964).

31. A.J. Edwards and G.R. Jones, J. Chem. Soc. A, 1651 (1969).

32. B.K. Morrell, A. Zalkin, A. Tressaud, and N. Bartlett, Inorg. Chem., 12, 2640 (1973).

33. S.J. Mitchell and J.H. Holloway, J. Chem. Soc. A, 2789 (1971).

34. A. Edwards and P. Taylor, J. Chem. Soc. D, 1376 (1971).

Table II-1. Vibrational Assignments for $(NO^+)_2GeF_6^{2-}$

obs. freq. (cm^{-1})		assignment	
IR	Raman	$NO^+(C_{\infty v})$	$GeF_6^{2-}(O_h)$
2313	2317 2380	$\nu_1(\Sigma^+)$	
	620		$\nu_1(A_{1g})$
600			$\nu_3(T_{1u})$
	479		$\nu_2(E_g)$
352			$\nu_4(T_{1u})$
	330		$\nu_5(T_{2g})$

Table II-2. X-ray powder data for $NO^+GeF_5^-$ prepared in SO_2 solution.

intensity	$1/d^2$(obs.)	$1/d^2$(calc.)	hkl
w	.0217	.0211	101
vs	.0314	.0316	111
m	.0346	.0341	200
m	.0412	.0418	020
s, broad	.0454	.0446	210
w, broad	.0567	.0573	211
w, broad	.0763	.0760	220
vvs	.0872	.0874	310
m	.1032	.1027	130
m	.1139	.1138	003
vw	.1259	.1266	222
w	.1495	.1494	401
m	.1560	.1557	023

s = strong, m = medium, w = weak, v = very.

Orthorhombic, $\underline{a}$ = 10.815, $\underline{b}$ = 9.773, $\underline{c}$ = 8.891.

Table II-3. X-ray powder data for $SF_3^+GeF_5^-$.

intensity	$1/d^2$(obs.)	$1/d^2$(calc.)	hkl
s	.0167	.0170	010
vw	.0219	--	SF_3BF_4
w	.0245	.0244	110
s	.0416	.0418	011
s	.0465	.0468	210
s	.0669	.0671	300
s	.0703	.0717	211
s	.0761	.0755	120
m	.0850	--	SF_3BF_4
m	.0912	.0919	301
w	.1095	.1090	311
m	.1167	.1163	012
m, broad	.1281	.1292	202
m	.1417	.1442	401
w	.1516	.1530	030
vw	.1589	.1600	321
w	.1662	.1665	302
w	.1788	.1779	031
w, broad	.1889	.1874	420
w, broad	.2115	.2113	501
w	.2275	.2284	511
w	.2360	.2357	412
m	.2694	.2686	600
w	.2828	.2823	232
m	.3051	.3044	141
w	.3121	.3104	611
w	.3190	.3196	332
w	.3348	.3366	620
w	.3451	.3429	403
w	.3655	.3656	700
w	.3747	.3766	033
m	.3978	.3974	004
w	.4176	.4164	441

Orthorhombic, $\underline{a}$ = 11.576, $\underline{b}$ = 7.667, $\underline{c}$ = 6.345.

Table II-4. X-ray powder data for $NO_2^+GeF_5^-$

intensity	$1/d^2$(obs.)	intensity	$1/d^2$(obs.)
m	.0168	m	.0923
vw	.0223	ms	.0969
w	.0261	w	.1032
w	.0283	w	.1085
vs	.0335	m	.1225
m	.0383	w	.1225
vvw	.0430	w	.1323
m	.0486	m	.1529
s	.0627	vw	.1670
w	.0683	vw	.1769
w	.0736	vw	.1817
vw	.0767	mw	.2175
vw	.0813	m	.2241

s = strong, m = medium, w = weak, v = very.

Table II-5. Crystallographic data for $XeF_5^+GeF_5^-$ and $ClO_2^+GeF_5^-$.

	XeF_5GeF_5	ClO_2GeF_5
crystal dimensions:	.15 x .14 x .10 mm	.30 x .10 x .10 mm
space group:	Pmnb, non std. setting of Pnma, #62.	$C222_1$
volume ($\AA^3$):	683.9(5), Z = 4	987.0(4), Z = 8
cell dimensions($\AA$):	$\underline{a}$ = 7.119(2) $\underline{b}$ = 12.986(4) $\underline{c}$ = 7.398(1)	$\underline{a}$ = 14.6480(15) $\underline{b}$ = 7.5762(11) $\underline{c}$ = 8.8941(15)
radiation:	$MoK_{\bar{\alpha}}$, monochromatized (λ = .7107$\AA$)	
2θ range:	2 - 45°	
hkℓ range:	+h, +k, ±ℓ	-h, +k, ±ℓ h+k=2n
background:	¼Δθ, where Δθ = .70 + .347 tanθ	
scan rate:	variable, maximum 50 sec.	
absorption coefficient(μ):	98.9 cm^{-1}	---
transmission:	29.4% max., 11.7% min.	---
orientation and intensity standards:	(272), (442), (124) every 250 reflections	($\bar{3}$15), ($\bar{8}$21), ($\bar{4}$42) -- no decay
reflections measured:	1054	645

Table II-6. Observed and calculated structure factors for XeF_5GeF_5.

H	K	L	FOBS	FCALC
0	0	2	1355	1348
0	0	4	29*	24
0	0	6	431	426
0	1	1	499	491
0	1	2	1332	1345
0	1	3	1554	1574
0	1	4	583	578
0	1	5	1225	1238
0	1	6	745	754
0	1	7	158	154
0	2	0	1156	1165
0	2	1	1421	1479
0	2	2	974	1005
0	2	3	157*	1586
0	2	4	1293	1309
0	2	5	735	739
0	2	6	448	451
0	2	7	227	216
0	3	1	2063	2157
0	3	2	729	746
0	3	3	698	683
0	3	4	287	277
0	3	5	52*	37
0	3	6	489	493
0	3	7	732	729
0	4	0	309	318
0	4	1	697	718
0	4	2	315	344
0	4	3	147	144
0	4	4	2075	2034
0	4	5	262	258
0	4	6	207	202
0	4	7	92*	18
0	5	1	849	894
0	5	2	1473	1523
0	5	3	183	185
0	5	4	144	142
0	5	5	478	474
0	5	6	814	818
0	5	7	467	469
0	6	0	2869	2866
0	6	1	1539	1537
0	6	2	797	825
0	6	3	718	728
0	6	4	81*	60
0	6	5	218	205
0	6	6	521	525
0	6	7	185	169
0	7	1	196	193
0	7	2	112*	109
0	7	3	1657	1667
0	7	4	146	148
0	7	5	953	943
0	7	6	212	203
0	8	0	2022	1992
0	8	1	638	632
0	8	2	728	743
0	8	3	727	727
0	8	4	91	85
0	8	5	427	423
0	8	6	426	431
0	9	1	843	834
0	9	2	939	957
0	9	3	478	493
0	9	4	394	406
0	9	5	498	496
0	9	6	561	549
0	10	0	403	391
0	10	1	183	176
0	10	2	558	561
0	10	3	611	627
0	10	4	888	893
0	10	5	387	383
0	11	1	948	916
0	11	2	342	337
0	11	3	100	98
0	11	4	119	117
0	12	0	148	143
0	12	1	523	508
0	12	2	254	253
0	12	3	291	277
0	12	4	581	585
0	13	1	144	136
0	13	2	454	445
1	0	1	1619	1584
1	0	3	64*	69
1	0	5	958	969
1	0	7	316	324
1	1	1	1202	1203
1	1	2	1006	955
1	1	3	988	992
1	1	4	133	125
1	1	5	374	384
1	1	6	641	651
1	1	7	379	387
1	2	0	1915	1915
1	2	1	481	393
1	2	2	281	198
1	2	3	222	222
1	2	4	1117	1133
1	2	5	185*	39
1	2	6	298	292
1	2	7	43*	51
1	3	1	511	542
1	3	2	1023	1068
1	3	3	486	481
1	3	4	514	588
1	3	5	253	256
1	3	6	682	618
1	3	7	292	295
1	4	0	741	755
1	4	1	921	953
1	4	2	50*	51
1	4	3	1297	1317
1	4	4	479	486
1	4	5	618	618
1	4	6	58*	26
1	4	7	125	123
1	5	1	318	334
1	5	2	585	527
1	5	3	1089	1088
1	5	4	81	77
1	5	5	466	467
1	5	6	228	221
1	5	7	619	625
1	6	0	1376	1376
1	6	1	373	393
1	6	2	389	317
1	6	3	237	236
1	6	4	734	-732
1	6	5	425	425
1	6	6	183*	82
1	6	7	0*	18
1	7	1	218	201
1	7	2	1163	1288
1	7	3	224	221
1	7	4	154	153
1	7	5	142	131
1	7	6	592	586
1	8	0	625	625
1	8	1	737	748
1	8	2	167*	163
1	8	3	441	453
1	8	4	393	398
1	8	5	367	365
1	8	6	306	304
1	9	1	734	747
1	9	2	60*	65
1	9	3	663	673
1	9	4	51*	63
1	9	5	244	248
1	10	0	479	478
1	10	1	561	559
1	10	2	223	286
1	10	3	276	288
1	10	4	430	432
1	10	5	414	422
1	11	1	81*	48
1	11	2	631	648
1	11	3	156	155
1	11	4	144	145
1	12	0	632	688
1	12	1	219	285
1	12	2	35*	25
1	12	3	165	168
1	13	1	295	289
1	13	2	182	186
2	0	0	358	368
2	0	2	1011	995
2	0	4	1034	1028
2	0	6	238	228
2	1	1	1871	1836
2	1	2	777	768
2	1	3	325	322
2	1	4	458	448
2	1	5	716	711
2	1	6	478	488
2	1	7	774	797
2	2	0	1460	1478
2	2	1	862	866
2	2	2	185	128
2	2	3	131	132
2	2	4	822	889
2	2	5	1007	1001
2	2	6	514	521
2	3	0	1454	1466
2	3	2	55*	54
2	3	4	1857	1868
2	3	6	441	436
2	3	7	117*	99
2	4	0	1226	1267
2	4	1	242	192
2	4	2	74*	58
2	4	3	0*	48
2	4	4	257	247
2	4	5	439	446
2	4	6	813	814
2	4	7	123*	93
2	5	1	439	458
2	5	2	1182	1228
2	5	3	967	949
2	5	4	89	86
2	5	5	813	822
2	5	6	346	334
2	5	7	284	288
2	6	0	638	647
2	6	1	563	578
2	6	2	666	788
2	6	3	419	424
2	6	4	1068	1088
2	6	5	733	725
2	6	6	177	166
2	7	1	1292	1317
2	7	2	554	614
2	7	3	187	94
2	7	4	211	286
2	7	5	388	384
2	7	6	52*	41
2	8	0	189	182
2	8	1	711	725
2	8	2	847	881
2	8	3	58*	54
2	8	4	1122	1133
2	8	5	283	281
2	8	6	259	261
2	9	1	804	824
2	9	2	718	729
2	9	3	605	611
2	9	4	268	284
2	9	5	224	227
2	10	0	1032	1026
2	10	1	399	416
2	10	2	322	338
2	10	3	242	246
2	10	4	52*	51
2	10	5	341	335
2	11	1	93	104
2	11	2	143	133
2	11	3	817	817
2	11	4	132	138
2	12	0	729	724
2	12	1	217	222
2	12	2	428	423
2	12	3	219	218
2	13	1	373	357
2	13	2	551	548
3	0	1	589	576
3	0	3	272	271
3	0	5	1267	1258
3	0	7	325	324
3	1	1	1356	1381
3	1	2	1229	1184
3	1	3	647	684
3	1	4	136	132
3	1	5	333	337
3	1	6	291	289
3	1	7	352	362
3	2	0	1252	1249
3	2	1	832	888
3	2	2	478	455
3	2	3	172	171
3	2	4	1072	1061
3	2	5	123	111
3	2	6	221	224
3	2	7	42*	35
3	3	1	762	748
3	3	2	972	975
3	3	3	161	162
3	3	4	55*	51
3	3	5	307	299
3	3	6	579	582
3	3	7	296	308
3	4	0	278	267
3	4	1	1069	1072
3	4	2	164	153
3	4	3	569	578
3	4	4	571	575
3	4	5	611	621
3	4	6	79*	67
3	5	1	712	738
3	5	2	479	483
3	5	3	988	998
3	5	4	281	191
3	5	5	242	246
3	5	6	286	286
3	5	7	483	493
3	6	1	153	154
3	6	2	261	256
3	6	3	333	329
3	6	4	934	935
3	6	5	479	478
3	6	6	144	136
3	7	1	113	187
3	7	2	1152	1194
3	7	3	186	184
3	7	4	63*	53
3	7	5	38*	17
3	7	6	408	484
3	8	0	751	761
3	8	1	466	508
3	8	2	395	484
3	8	3	387	318
3	8	4	258	257
3	8	5	498	487
3	9	1	883	923
3	9	2	8*	18
3	9	3	411	483
3	9	4	134	138
3	9	5	388	382
3	10	0	403	489
3	10	1	458	478
3	10	2	141	159
3	10	3	239	236
3	10	4	341	343
3	11	1	97	97
3	11	2	652	671
3	11	3	243	243
3	12	0	393	398
3	12	1	185	181
3	12	2	8*	34
4	0	0	3149	3038
4	0	2	1817	988
4	0	4	385	388
4	0	6	472	478
4	1	1	169	167
4	1	2	1858	1828
4	1	3	1271	1245
4	1	4	235	229
4	1	5	818	815
4	1	6	522	525
4	2	0	593	587
4	2	1	1841	1827
4	2	2	1033	1025
4	2	3	855	851
4	2	4	844	844
4	2	5	667	666
4	2	6	422	429
4	3	1	1788	1769
4	3	2	578	562
4	3	3	165	151
4	3	4	69*	51
4	3	5	0*	27
4	3	6	358	363
4	4	0	178	166
4	4	1	318	311
4	4	2	794	798
4	4	3	213	212
4	4	4	1514	1516
4	4	5	273	278
4	4	6	258	245
4	5	1	887	897
4	5	2	1289	1232
4	5	3	371	367
4	5	4	56*	72
4	5	5	326	324
4	5	6	497	522
4	6	0	1382	1394
4	6	1	775	798
4	6	2	692	712
4	6	3	519	522
4	6	4	48*	39
4	6	5	372	377
4	7	1	34*	24
4	7	2	185	194
4	7	3	1255	1241
4	7	4	89	99
4	7	5	714	713
4	8	0	1274	1302
4	8	1	505	597
4	8	2	499	518
4	8	3	412	483
4	8	4	0*	19
4	8	5	291	294
4	9	1	546	576
4	9	2	789	742
4	9	3	363	378
4	9	4	166	173
4	10	0	211	213
4	10	1	238	251
4	10	2	471	492
4	10	3	327	319
4	11	1	818	838
4	11	2	237	244
5	0	1	1118	1096
5	0	3	183	163
5	0	5	582	497
5	1	1	527	508
5	1	2	534	525
5	1	3	689	685
5	1	4	45*	53
5	1	5	258	254
5	1	6	511	522
5	2	0	1225	1229
5	2	1	42*	32
5	2	2	228	223
5	2	3	308	297
5	2	4	717	721
5	2	5	182	95
5	3	1	258	249
5	3	2	671	676
5	3	3	413	411
5	3	4	431	432
5	3	5	146	153
5	4	0	558	553
5	4	1	551	551
5	4	2	117	111
5	4	3	892	914
5	4	4	227	225
5	4	5	393	401
5	5	1	183	183
5	5	2	274	271
5	5	3	788	788
5	5	4	155	162
5	5	5	344	354
5	6	0	1097	1119
5	6	1	336	347
5	6	2	122	122
5	6	3	189	188
5	6	4	415	412
5	7	1	169	171
5	7	2	699	721
5	7	3	135	131
5	7	4	156	153
5	8	0	328	325
5	8	1	478	506
5	8	2	24*	6
5	8	3	337	344
5	9	1	426	437
5	9	2	48*	51
5	9	3	548	548
5	10	0	326	336
5	10	1	371	382
6	0	0	662	661
6	0	2	688	693
6	0	4	968	953
6	1	1	827	822
6	1	2	446	433
6	1	3	228	219
6	1	4	336	329
6	2	0	571	555
6	2	1	535	526
6	2	2	548	533
6	2	3	417	418
6	2	4	378	362
6	3	1	271	278
6	3	2	318	315
6	3	3	1157	1158
6	3	4	159	162
6	4	0	1068	1063
6	4	1	164	159
6	4	2	551	554
6	4	3	69	57
6	4	4	134*	121
6	5	1	429	419
6	5	2	574	584
6	5	3	773	761
6	5	4	181	184
6	6	0	158	193
6	6	1	538	557
6	6	2	588	588
6	6	3	249	246
6	7	1	714	725
6	7	2	282*	282
6	8	0	141	133
6	8	1	255	255
7	0	1	424	426
7	0	3	243	239
7	1	1	587	612
7	1	2	553	555
7	1	3	364	369
7	2	0	672	679
7	2	1	249	247
7	2	2	157	161
7	2	3	53*	24
7	3	1	334	336
7	3	2	542	541
7	4	0	213	218
7	4	1	521	525
7	4	2	31*	23
7	5	1	368	376

Table II-7. Positional and thermal parameters for XeF_5GeF_5.

Atom	x	y	z	B_{11}	B_{22}	B_{33}	B_{12}	B_{13}	B_{23}
Xe	.25	.13903(3)	.36600(5)	.00810(5)	.00386(2)	.01087(7)	0	0	-.00363(7)
Ge	0	0	0	.00243(8)	.00318(3)	.00818(9)	-.00007(8)	-.0006(2)	-.0007 (1)
F1	.0597(2)	-.0269 (1)	.2242 (3)	.0059 (3)	.0054 (1)	.0094 (4)	.0035 (4)	-.0013(6)	.0014 (5)
F2	.0567(2)	.1283 (1)	.0423 (3)	.0070 (3)	.0032 (1)	.0160 (4)	.0014 (4)	-.0001(7)	-.0009 (5)
F3	.25	-.0269 (2)	-.0708 (4)	.0028 (6)	.0040 (2)	.0100 (6)	0	0	-.0018 (7)
F4	.25	.2688 (2)	.2698 (6)	.0208 (7)	.0040 (2)	.0249 (8)	0	0	-.0034 (10)
F5	.5030(2)	.1530 (2)	.4057 (3)	.0094 (4)	.0062 (1)	.0196 (5)	-.0029 (4)	-.0053(8)	-.0061 (6)
F6	.25	.0342 (2)	.5314 (5)	.0150 (6)	.0064 (2)	.0118 (6)	0	0	.0024 (8)
F7	.25	.2136 (3)	.5741 (5)	.0194 (7)	.0084 (3)	.0186 (7)	0	0	-.0157 (9)

Table II-8. Observed and calculated structure factors for ClO_2GeF_5.

H	K	L	FOBS	FCALC
0	0	2	379	351
0	0	4	248	266
0	0	6	718	740
0	0	8	174	170
0	0	9	771	739
0	2	1	1134	1072
0	2	2	258	266
0	2	3	324	318
0	2	4	801	655
0	2	5	741	715
0	2	6	363	351
0	2	7	551	576
0	2	8	249	243
0	2	9	402	402
0	4	0	421	415
0	4	1	265	285
0	4	2	951	937
0	4	3	125	115
0	4	4	465	457
0	4	5	253	255
0	4	6	132	120
0	4	7	121	119
0	4	8	704	718
0	6	0	174	178
0	6	1	426	411
0	6	2	672	692
0	6	3	72	72
0	6	4	298	307
0	6	5	260	288
0	6	6	42	31
0	8	0	410	397
0	8	1	213	229
1	1	-9	258	268
1	1	-8	365	393
1	1	-7	356	363
1	1	-6	266	274
1	1	-5	519	531
1	1	-4	273	274
1	1	-3	393	419
1	1	-2	826	894
1	1	-1	636	709
1	1	0	547	508
1	1	1	887	788
1	1	2	1047	981
1	1	3	501	452
1	1	4	773	733
1	1	5	577	547
1	1	6	328	284
1	1	7	355	339
1	1	8	439	422
1	1	9	279	277
1	3	-8	253	276
1	3	-7	535	579
1	3	-6	418	442
1	3	-5	175	186
1	3	-4	466	518
1	3	-3	429	484
1	3	-2	331	366
1	3	-1	321	336
1	3	0	362	368
1	3	1	294	274
1	3	2	418	388
1	3	3	575	588
1	3	4	576	517
1	3	5	288	188
1	3	6	493	451
1	3	7	629	598
1	3	8	303	288
1	5	-7	117	126
1	5	-6	354	384
1	5	-5	367	385
1	5	-4	139	151
1	5	-3	451	496
1	5	-2	457	488
1	5	-1	311	307
1	5	0	584	582
1	5	1	385	318
1	5	2	488	453
1	5	3	557	513
1	5	4	195	175
1	5	5	442	488
1	5	6	392	363
1	5	7	154	141
1	7	-4	377	417
1	7	-3	227	221
1	7	-2	215	217
1	7	-1	298	297
1	7	0	148	128
1	7	1	266	264
1	7	2	219	218
1	7	3	224	218
1	7	4	474	446
2	0	0	95	99
2	0	1	584	488
2	0	2	305	307
2	0	3	975	934
2	0	4	57	59
2	0	5	562	545
2	0	6	51	11
2	0	7	216	226
2	0	8	118	116
2	0	9	328	321
2	2	-9	145	153
2	2	-8	282	269
2	2	-7	129	135
2	2	-6	393	424
2	2	-5	174	182
2	2	-4	717	592
2	2	-3	483	533
2	2	-2	619	601
2	2	-1	86	70
2	2	0	39	42
2	2	1	70	75
2	2	2	687	626
2	2	3	583	519
2	2	4	883	793
2	2	5	198	167
2	2	6	479	442
2	2	7	158	147
2	2	8	237	222
2	2	9	178	164
2	4	-8	118	121
2	4	-7	155	166
2	4	-6	224	250
2	4	-5	589	643
2	4	-4	208	387
2	4	-3	687	764
2	4	-2	399	413
2	4	-1	534	533
2	4	0	43	45
2	4	1	681	565
2	4	2	427	427
2	4	3	823	746
2	4	4	341	308
2	4	5	717	652
2	4	6	292	273
2	4	7	186	172
2	4	8	134	128
2	6	-6	171	187
2	6	-5	315	353
2	6	-4	488	542
2	6	-3	228	241
2	6	-2	584	683
2	6	-1	188	180
2	6	0	154	152
2	6	1	185	174
2	6	2	593	578
2	6	3	292	277
2	6	4	574	532
2	6	5	408	365
2	6	6	195	181
2	8	-1	70	71
2	8	0	44	38
2	8	1	85	82
3	1	-9	136	136
3	1	-8	369	381
3	1	-7	443	456
3	1	-6	168	178
3	1	-5	845	878
3	1	-4	443	485
3	1	-3	284	223
3	1	-2	671	757
3	1	-1	872	952
3	1	0	335	321
3	1	1	1032	938
3	1	2	826	741
3	1	3	176	158
3	1	4	535	497
3	1	5	959	871
3	1	6	154	148
3	1	7	451	426
3	1	8	390	371
3	1	9	197	185
3	3	-8	181	198
3	3	-7	524	542
3	3	-6	246	263
3	3	-5	268	285
3	3	-4	534	594
3	3	-3	518	583
3	3	-2	634	698
3	3	-1	652	662
3	3	0	1084	951
3	3	1	657	687
3	3	2	741	677
3	3	3	673	685
3	3	4	668	598
3	3	5	332	297
3	3	6	268	246
3	3	7	656	633
3	3	8	167	158
3	5	-7	188	186
3	5	-6	279	289
3	5	-5	93	96
3	5	-4	447	498
3	5	-3	938	1018
3	5	-2	272	296
3	5	-1	370	376
3	5	0	483	473
3	5	1	391	389
3	5	2	288	272
3	5	3	1117	1016
3	5	4	587	464
3	5	5	188	94
3	5	6	321	296
3	5	7	228	213
3	7	-4	384	412
3	7	-3	122	142
3	7	-2	406	425
3	7	-1	342	391
3	7	0	165	161
3	7	1	434	423
3	7	2	489	424
3	7	3	127	128
3	7	4	484	386
4	0	0	1169	1167
4	0	1	197	209
4	0	2	742	728
4	0	3	186	191
4	0	4	153	149
4	0	5	331	286
4	0	6	844	817
4	0	7	26	24
4	0	8	475	462
4	0	9	246	256
4	2	-8	165	174
4	2	-7	699	742
4	2	-6	332	361
4	2	-5	598	639
4	2	-4	351	378
4	2	-3	383	378
4	2	-2	339	362
4	2	-1	679	714
4	2	0	128	138
4	2	1	818	762
4	2	2	488	357
4	2	3	344	311
4	2	4	435	405
4	2	5	416	383
4	2	6	429	427
4	2	7	541	511
4	4	-6	286	308
4	4	-5	165	180
4	4	-4	248	266
4	4	-3	464	502
4	4	-2	432	446
4	4	-1	42	38
4	4	0	364	322
4	4	1	74	69
4	4	2	517	482
4	4	3	507	469
4	4	4	292	266
4	4	5	142	133
4	4	6	368	332
4	6	-4	213	226
4	6	-3	208	218
4	6	-2	297	309
4	6	-1	260	259
4	6	0	27	24
4	6	1	308	308
4	6	2	299	289
4	6	3	231	212
4	6	4	249	233
4	6	5	153	159
4	6	6	279	309
4	8	0	167	158
4	8	1	133	133
4	8	2	153	159
4	8	3	233	258
4	8	4	520	527
4	8	5	689	587
4	8	6	678	642
5	1	0	281	258
5	1	1	652	591
5	1	2	195	174
5	1	3	204	198
5	1	4	292	268
5	1	5	276	295
5	3	-4	142	154
5	3	-3	145	151
5	3	-2	255	271
5	3	-1	821	845
5	3	0	829	811
5	3	1	877	844
5	3	2	331	386
5	3	3	192	176
5	3	4	166	152
5	3	5	337	316
5	3	6	457	420
5	3	7	278	251
5	5	-5	184	194
5	5	-4	126	115
5	5	-3	106	106
5	5	-2	71	72
5	5	-1	108	105
5	5	0	605	596
5	5	1	216	218
5	5	2	55	58
5	5	3	138	125
5	5	4	136	129
5	5	5	201	188
5	7	-4	282	289
5	7	-3	192	196
5	7	-2	151	148
5	7	-1	471	463
5	7	0	89	98
6	0	0	491	482
6	0	7	367	361
6	0	8	148	149
6	2	-8	177	188
6	2	-7	224	241
6	2	-6	587	652
6	2	-5	274	298
6	2	-4	669	737
6	2	-3	569	648
6	2	-2	608	662
6	2	-1	349	395
6	2	0	89	87
6	2	1	422	397
6	2	2	665	687
6	2	3	714	652
6	2	4	836	761
6	2	5	368	326
6	2	6	555	515
6	2	7	229	216
6	2	8	192	181
6	4	-7	193	205
6	4	-6	83	82
6	4	-5	686	652
6	4	-4	336	362
6	4	-3	427	467
6	4	-2	447	475
6	4	-1	634	643
6	4	0	84	82
6	4	1	684	645
6	4	2	503	472
6	4	3	587	473
6	4	4	428	389
6	4	5	717	652
6	4	6	271	265
6	4	7	206	198
6	6	-5	288	296
6	6	-4	491	526
6	6	-3	87	87
6	6	-2	444	454
6	6	-1	527	535
6	6	0	220	216
6	6	1	565	543
6	6	2	494	465
6	6	3	88	86
6	6	4	518	499
6	6	5	315	296
7	1	-10	94	95
7	1	-7	277	286
7	1	-6	233	253
7	1	-5	445	492
7	1	-4	438	475
7	1	-3	529	575
7	1	-2	584	658
7	1	-1	488	507
7	1	0	633	631
7	1	1	516	491
7	1	2	578	527
7	1	3	659	588
7	1	4	513	467
7	1	5	498	465
7	1	6	246	232
7	1	7	297	274
7	1	8	137	131
7	3	-7	122	126
7	3	-6	273	286
7	3	-5	185	286
7	3	-4	551	608
7	3	-3	395	431
7	3	-2	629	662
7	3	-1	213	228
7	3	0	139	137
7	3	1	122	217
7	3	2	712	650
7	3	3	502	461
7	3	4	601	583
7	3	5	237	221
7	3	6	281	258
7	3	7	114	103
7	5	-6	110	126
7	5	-5	355	379
7	5	-4	293	283
7	5	-3	558	588
7	5	-2	201	212
7	5	-1	184	189
7	5	0	212	215
7	5	1	166	158
7	5	2	212	204
7	5	3	658	683
7	5	4	201	187
7	5	5	422	386
7	5	6	105	99
7	7	-2	243	252
7	7	-1	167	169
7	7	0	182	189
7	7	1	172	166
7	7	2	364	343
8	0	0	674	707
8	0	1	459	477
8	0	2	462	456
8	0	3	335	339
8	0	4	352	346
8	0	5	287	207
8	0	6	712	689
8	0	7	75	88
8	0	8	415	417
8	2	-7	476	518
8	2	-6	151	160
8	2	-5	332	354
8	2	-4	412	413
8	2	-3	274	284
8	2	-2	482	434
8	2	-1	619	644
8	2	0	247	248
8	2	1	575	651
8	2	2	488	445
8	2	3	344	311
8	2	4	435	405
8	2	5	416	383
8	2	6	429	427
8	2	7	541	511
8	4	-6	286	308
8	4	-5	165	180
8	4	-4	248	266
8	4	-3	464	502
8	4	-2	432	446
8	4	-1	42	38
8	4	0	364	322
8	4	1	74	69
8	4	2	517	482
8	4	3	507	469
8	4	4	292	266
8	4	5	142	133
8	4	6	368	332
8	6	-4	213	226
8	6	-3	208	218
8	6	-2	297	309
8	6	-1	260	259
8	6	0	27	24
8	6	1	308	308
8	6	2	299	289
8	6	3	231	212
8	6	4	249	233
8	6	5	153	159
8	6	6	279	309
8	8	0	167	158
8	8	1	133	133
8	8	2	153	159
8	8	3	233	258
8	8	4	520	527
8	8	5	689	587
8	8	6	678	642
9	1	0	281	258
9	1	1	652	591
9	1	2	195	174
9	1	3	204	198
9	1	4	292	268
9	1	5	276	295
9	3	-4	142	154
9	3	-3	145	151
9	3	-2	255	271
9	3	-1	821	845
9	3	0	829	811
9	3	1	877	844
9	3	2	331	386
9	3	3	192	176
9	3	4	166	152
9	3	5	337	316
9	3	6	457	420
9	3	7	278	251
9	5	-5	184	194
9	5	-4	126	115
9	5	-3	106	106
9	5	-2	71	72
9	5	-1	108	105
9	5	0	605	596
9	5	1	216	218
9	5	2	55	58
9	5	3	138	125
9	5	4	136	129
9	5	5	201	188
9	7	-4	282	289
9	7	-3	192	196
9	7	-2	151	148
9	7	-1	471	463
9	7	0	89	98
10	0	0	491	482
10	0	7	367	361
10	0	8	148	149
10	2	-8	177	188
10	2	-7	224	241
10	2	-6	587	652
10	2	-5	274	298
10	2	-4	669	737
10	2	-3	569	648
10	2	-2	608	662
10	2	-1	349	395
10	2	0	89	87
10	2	1	422	397
10	2	2	665	687
10	2	3	714	652
10	2	4	836	761
10	2	5	368	326
10	2	6	555	515
10	2	7	229	216
10	2	8	192	181
10	4	-7	193	205
10	4	-6	83	82
10	4	-5	686	652
10	4	-4	336	362
10	4	-3	427	467
10	4	-2	447	475
10	4	-1	634	643
10	4	0	84	82
10	4	1	684	645
10	4	2	503	472
10	4	3	587	473
10	4	4	428	389
10	4	5	717	652
10	4	6	271	265
10	4	7	206	198
10	6	-5	288	296
10	6	-4	491	526
10	6	-3	87	87
10	6	-2	444	454
10	6	-1	527	535
10	6	0	220	216
10	6	1	565	543
10	6	2	494	465
10	6	3	88	86
10	6	4	518	499
10	6	5	315	296
10	8	0	94	95
10	8	1	584	488
10	8	2	305	307
10	8	3	975	934
10	8	4	57	59
10	8	5	562	545
10	8	6	51	11
10	8	7	216	226
10	8	8	118	116
10	8	9	328	321
11	3	-5	59	58
11	3	-4	475	494
11	3	-3	419	446
11	3	-2	392	413
11	3	-1	142	146
11	3	0	353	351
11	3	1	165	162
11	3	2	487	393
11	3	3	483	458
11	3	4	563	518
11	3	5	37	67
11	5	-3	453	463
11	5	-2	188	196
11	5	-1	0	9
11	5	0	178	156
11	5	1	33	32
11	5	2	218	218
11	5	3	504	472
11	5	4	446	459
12	0	0	49	47
12	0	2	120	117
12	0	3	716	725
12	0	4	221	225
12	0	5	134	143
12	0	6	429	427
12	2	-5	338	352
12	2	-4	405	424
12	2	-3	324	335
12	2	-2	435	459
12	2	-1	452	472
12	2	0	124	138
12	2	1	491	486
12	2	2	497	473
12	2	3	348	322
12	2	4	443	415
12	2	5	329	310
12	4	-4	98	101
12	4	-3	198	208
12	4	-2	278	280
12	4	-1	356	356
12	4	0	310	322
12	4	1	376	375
12	4	2	294	284
12	4	3	174	166
12	4	4	180	94
13	1	-5	156	163
13	1	-4	216	226
13	1	-3	189	197
13	1	-2	235	245
13	1	-1	325	329
13	1	0	257	256
13	1	1	233	227
13	1	2	227	218
13	1	3	220	205
13	1	4	238	222
13	1	5	208	188
13	3	-4	0	38
13	3	-3	172	179
13	3	-2	182	192
13	3	-1	503	508
13	3	0	306	313
13	3	1	525	509
13	3	2	221	209
13	3	3	230	192
13	3	4	42	37
14	0	0	189	194
14	0	2	67	78
14	0	3	218	204
14	0	4	508	505
14	0	4	32	23
14	2	-3	277	281
14	2	-2	175	188
14	2	-1	481	413
14	2	0	211	209
14	2	1	388	377
14	2	2	178	164
14	2	3	311	290
15	1	-2	266	281
15	1	-1	181	198
15	1	0	0	38
15	1	1	211	211
15	1	2	312	308

Table II-9. Positional and thermal parameters for ClO_2GeF_5.

Atom	x	y	z	B_{11}	B_{22}	B_{33}	B_{12}	B_{13}	B_{23}
Ge	0.11474(7)	0.1118(1)	0.3194(1)	.00085(5)	.0027(2)	.0015(1)	.0000(1)	.0000(1)	.0004(2)
CL1	-.3858 (3)	0	0	.0017(2)	.0060(6)	.0041(5)	0	0	.0025(8)
CL2	0.2708 (3)	0	0	.0013(2)	.0063(5)	.0034(5)	0	0	-.0004(9)
F1	0.1386 (4)	0.2148(8)	0.1444(7)	.0016(3)	.0081(10)	.0026(7)	.0009(9)	.0007(8)	.006 (2)
F2	0	0.0331(10)	.25	.0008(4)	.0041(13)	.0003(11)	0	-.0015(12)	0
F3	0.0601 (4)	0.2980(7)	0.3863(8)	.0017(3)	.0033(9)	.0059(8)	.0017(8)	-.0007(9)	-.005 (2)
F4	0.2196 (4)	0.1734(7)	0.4027(7)	.0013(3)	.0048(8)	.0042(8)	-.0001(8)	.0000(8)	-.002 (2)
F5	0.1571 (4)	-.0890(8)	0.2558(8)	.0018(3)	.0047(10)	.0047(8)	.0017(9)	.0008(8)	-.001 (1)
F6	0.0793 (6)	0	.5	.0012(4)	.0084(15)	.0026(12)	0	0	.004 (2)
O1	-.4339 (5)	0.0864(10)	0.1144(9)	.0032(4)	.005 (1)	.0040(9)	-.000 (1)	-.001 (1)	.000 (2)
O2	0.3189 (5)	0.0669(9)	0.1231(9)	.-022(4)	.005 (1)	.0025(9)	-.001 (1)	-.001 (1)	-.000 (2)

Table II-10. Selected internuclear distances and angles for XeF_5GeF_5.

Distances:

Ge	F1	1.745(2)	Xe	F3	3.890(3)
Ge	F2	1.745(2)	Xe	F4	1.828(5)
Ge	F3	1.890(1)	Xe	F5	1.831(3)
Xe	F1	2.752(3)	Xe	F6	1.826(4)
Xe	F2	2.764(3)	Xe	F7	1.813(4)

Angles:

F1-Ge-F1	180	F5-Xe-F5	158.26(20)
F1-Ge-F2	87.86(13)	F5-Xe-F6	88.18(11)
F1-Ge-F3	90.07(13)	F5-Xe-F7	79.13(10)
F2-Ge-F2	180	F6-Xe-F7	79.70(23)
F2-Ge-F3	90.48(13)	Ge-F3-Ge	140.70(20)
F4-Xe-F5	88.25(12)	Xe-F1-Ge	109.09(12)
F4-Xe-F6	160.94(21)	Xe-F2-Ge	108.58(11)
F4-Xe-F7	81.25(24)		

Table II-11. Selected internuclear distances and angles for ClO_2GeF_5.

Distances:

Ge	F1	1.776(3)	Cℓ1	F4	2.898(4)
Ge	F2	1.887(1)	Cℓ1	O1	1.401(5)
Ge	F3	1.728(3)	Cℓ2	F1	2.837(4)
Ge	F4	1.768(3)	Cℓ2	F4	2.625(3)
Ge	F5	1.737(4)	Cℓ2	F5	2.900(4)
Ge	F6	1.888(2)	Cℓ2	O2	1.396(5)
Cℓ1	F1	2.539(3)			

Angles:

F1-Ge-F2	91.57(12)	F3-Ge-F5	172.92(17)
F1-Ge-F3	91.97(18)	F3-Ge-F6	86.89(16)
F1-Ge-F4	94.60(17)	F4-Ge-F5	93.31(16)
F1-Ge-F5	91.66(18)	F4-Ge-F6	90.04(18)
F1-Ge-F6	175.26(18)	F5-Ge-F6	88.99(15)
F2-Ge-F3	87.59(16)	O1-Cℓ1-O1	119.5(4)
F2-Ge-F4	173.82(14)	O2-Cℓ2-O2	119.5(4)
F2-Ge-F5	86.24(16)	Ge-F2-Ge	143.2(2)
F2-Ge-F6	83.79(15)	Ge-F6-Ge	148.1(3)
F3-Ge-F4	92.46(16)		

Table II-12. Vibrational assignments for XeF_5GeF_5.

observed freq. (cm^{-1})		assignment	
IR	Raman	$XeF_5^+(C_{4v})$	$(GeF_5)_n^{n-}(D_{4h})$
700			$\nu_6(E_u)$
680 645	675 648	$\nu_7(E)$	
	669	$\nu_1(A_1)$	
	654		$\nu_1(A_{1g})$
	622	$\nu_4(B_2)$	
	602	$\nu_2(A_1)$	
600			
	526 518		stretching vibrations of the chains
500			
	463		$\nu_4(B_{2g})$
413 400	417 402	$\nu_8(E)$	
	381		deformation of the chain-square plane angle
355	354	$\nu_3(A_1)$	
	339 331		$\nu_2(B_{1g})$
	300	$\nu_6(B_1)$	
	263	$\nu_5(B_2)$	
	220 208	$\nu_9(E)$	
	184 124		chain torsional-rotational modes

Table II-13. Vibrational assignments for ClO_2GeF_5 and $NOGeF_5$.

ClO_2GeF_5		$NOGeF_5$				
observed freq. (cm^{-1})				assignment		
IR	Raman	IR	Raman	$ClO_2^+(C_{2v})$	$NO^+(C_{\infty v})$	$(GeF_5)_n^{n-}$
		2322	2320		$\nu_1(\Sigma^+)$	
1303 1293	1307 1294			$\nu_3(B_1)$		
1086						
	1065 1057			$\nu_1(A_1)$		
1040 1018				$2 \times \nu_2$		
	713					Ge-non-bridging F stretching vibrations
695		695				
650	657	635	645			
	603					stretching vibrations of the chains
595	590		578			
		480	490			
	525 512			$\nu_2(A_1)$		
395	399					chain-GeF_4 group angle def.
	337		338			GeF_4 group bending modes
	303		323			
290	292					
	232 160					chain torsion-rotations

Table II-14. Vibrational assignments for NO_2GeF_5 and SF_3GeF_5.

NO_2GeF_5		SF_3GeF_5			
observed freq. (cm^{-1})			assignment		
IR	Raman	Raman	$NO_2^+(D_{\infty h})$	$SF_3^+(C_{3v})$	$(GeF_5)_n^{n-}$
3765			$\nu_1 + \nu_3$		
2388 2378	}		$\nu_3(\Sigma_u^+)$		
	1409 1405 }		$\nu_1(\Sigma_g^+)$		
		945 932 }		$\nu_1(A_1)$	
		916 904 887 }		$\nu_3(E)$	
		874			
687		708 669 }			Ge-non-bridging F stretching vibrations
660	654				
618					stretching vibrations of the chains
	606	583 }			
587	592		$\nu_2(\P_u)$		
		538		$\nu_4(E)$	
	501	507			stretching vibrations of the chain
		410		$\nu_2(A_1)$	
382 362 343	354	353 }			bending modes of the GeF_4 group
	265 156 }				chain torsional-rotational modes

Table II-15. Vibrational assignments for GeF_5^- in $(n\text{-}Bu)_4N^+GeF_5^-$.

	GeF_5^- (this work)	SiF_5^- (ref. 25)	$GeCl_5^-$ (ref. 26)
ν_1 (cm^{-1})	665	708	348
ν_2	520	519	236
ν_3	654	785	310
ν_4	345	481	200
ν_5	690	874	395
ν_6	317	449	200
ν_7	≃117	-	-
ν_8	337	-	-

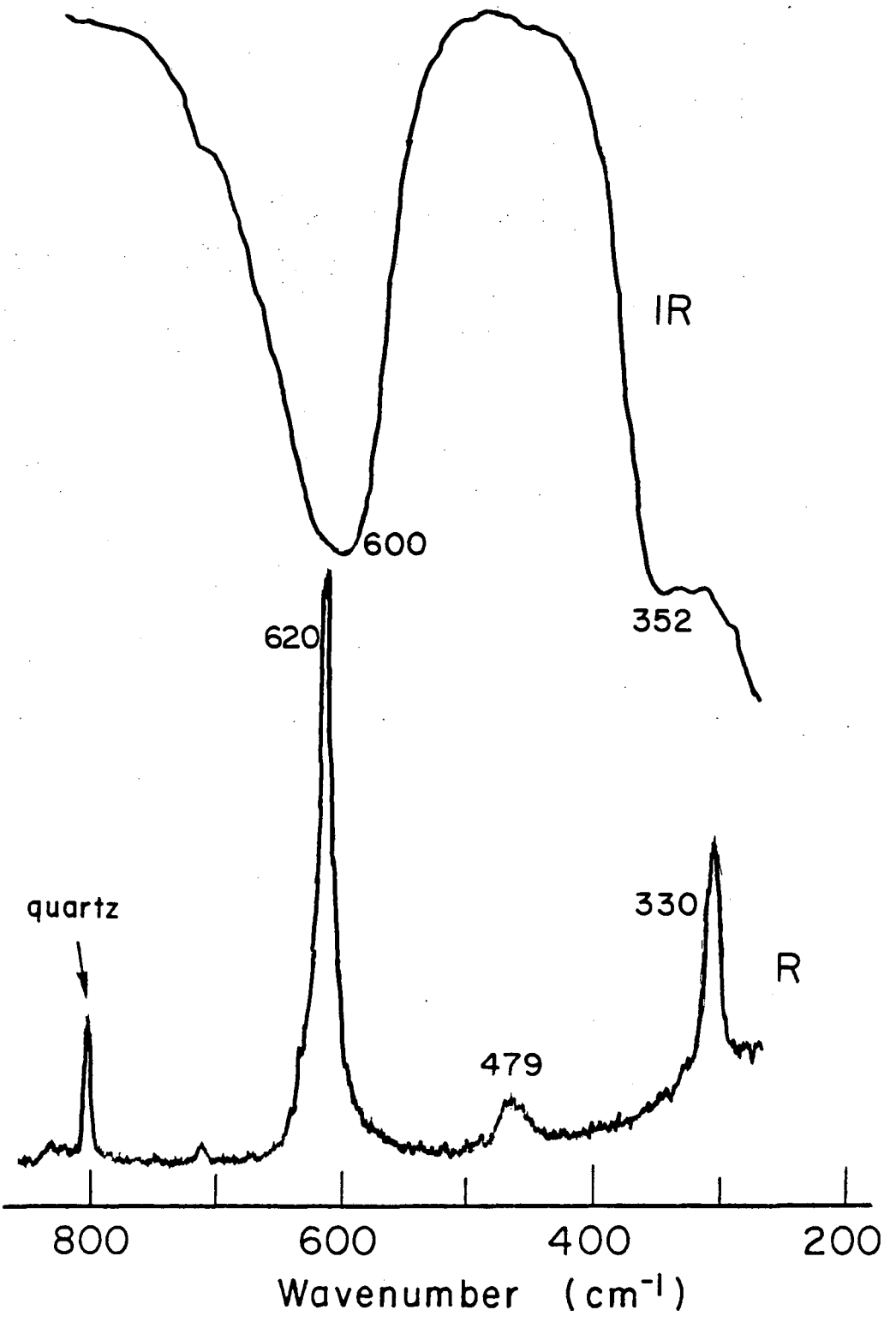

Figure II-1. Raman and infrared spectra of $(NO^{+})_2GeF_6^{2-}$.

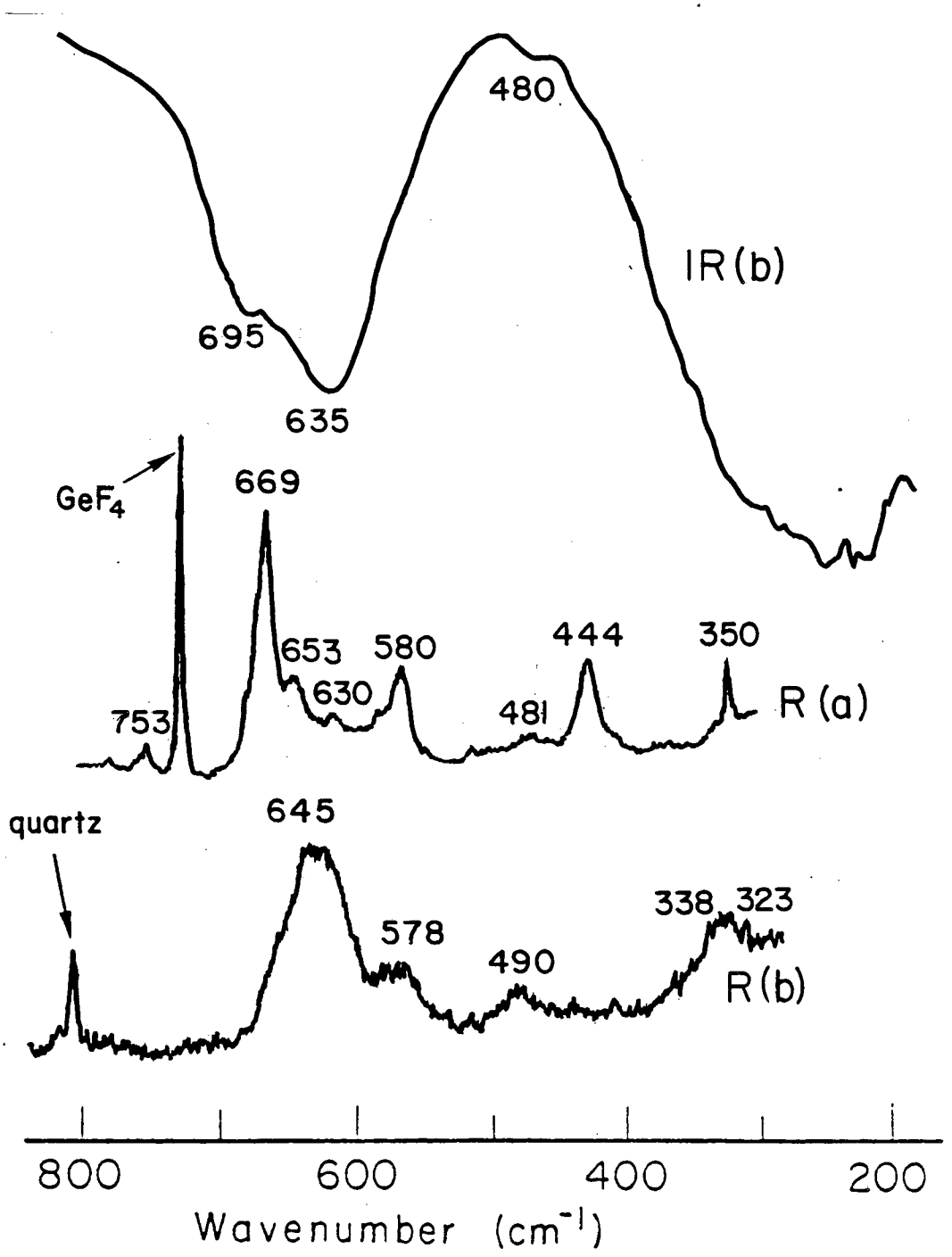

XBL 836-9977

Figure II-2. Vibrational spectra of $NO^{+}GeF_5^{-}$: (a) from sublimation of $(NO)_2GeF_6$ in GeF_4 vapor, (b) prepared in SO_2 solution.

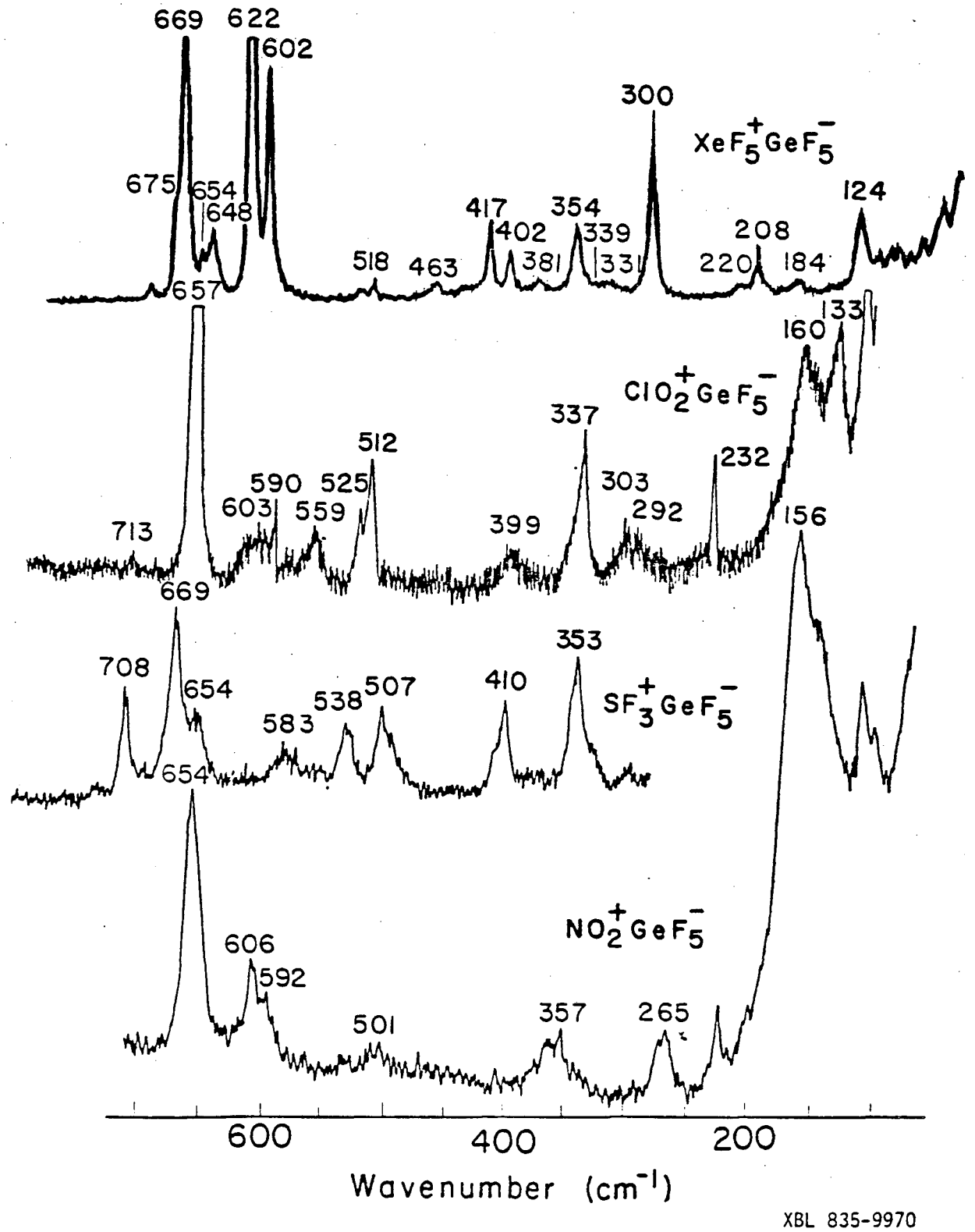

Figure II-3. Raman spectra of GeF_5^- salts.

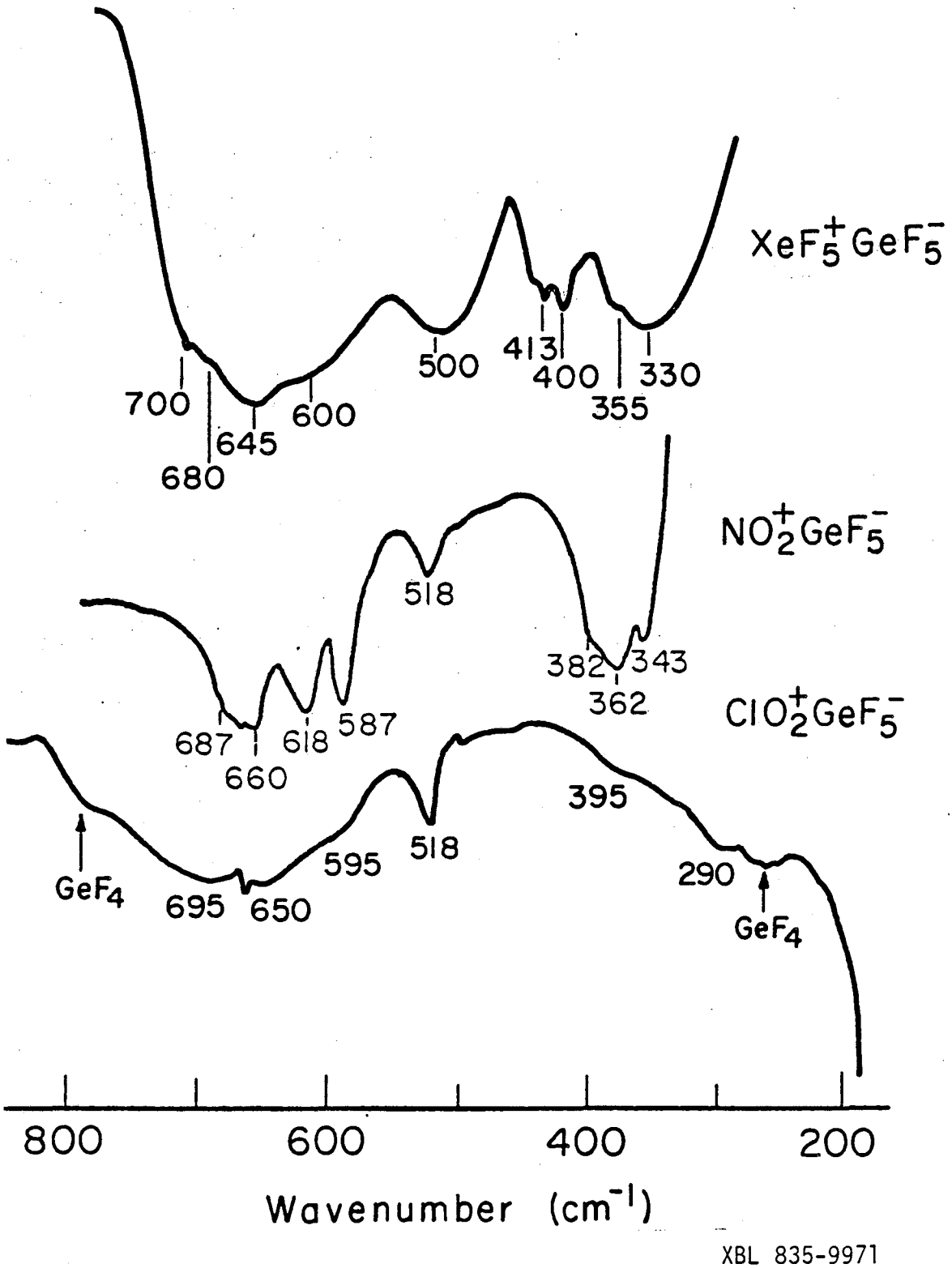

Figure II-4. Infrared spectra of GeF_5^- salts.

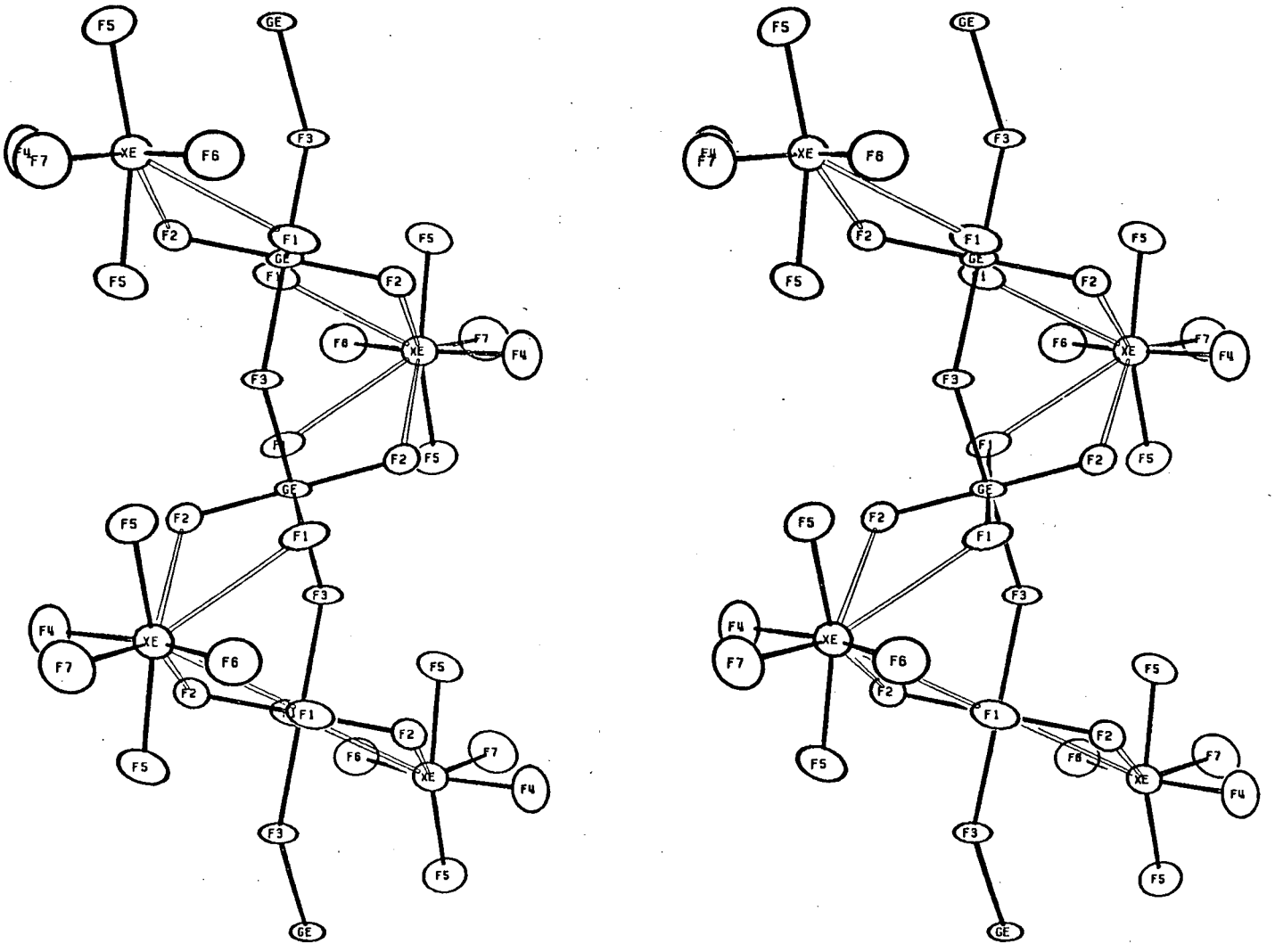

Figure II-5. The $XeF_5^+GeF_5^-$ crystal structure.

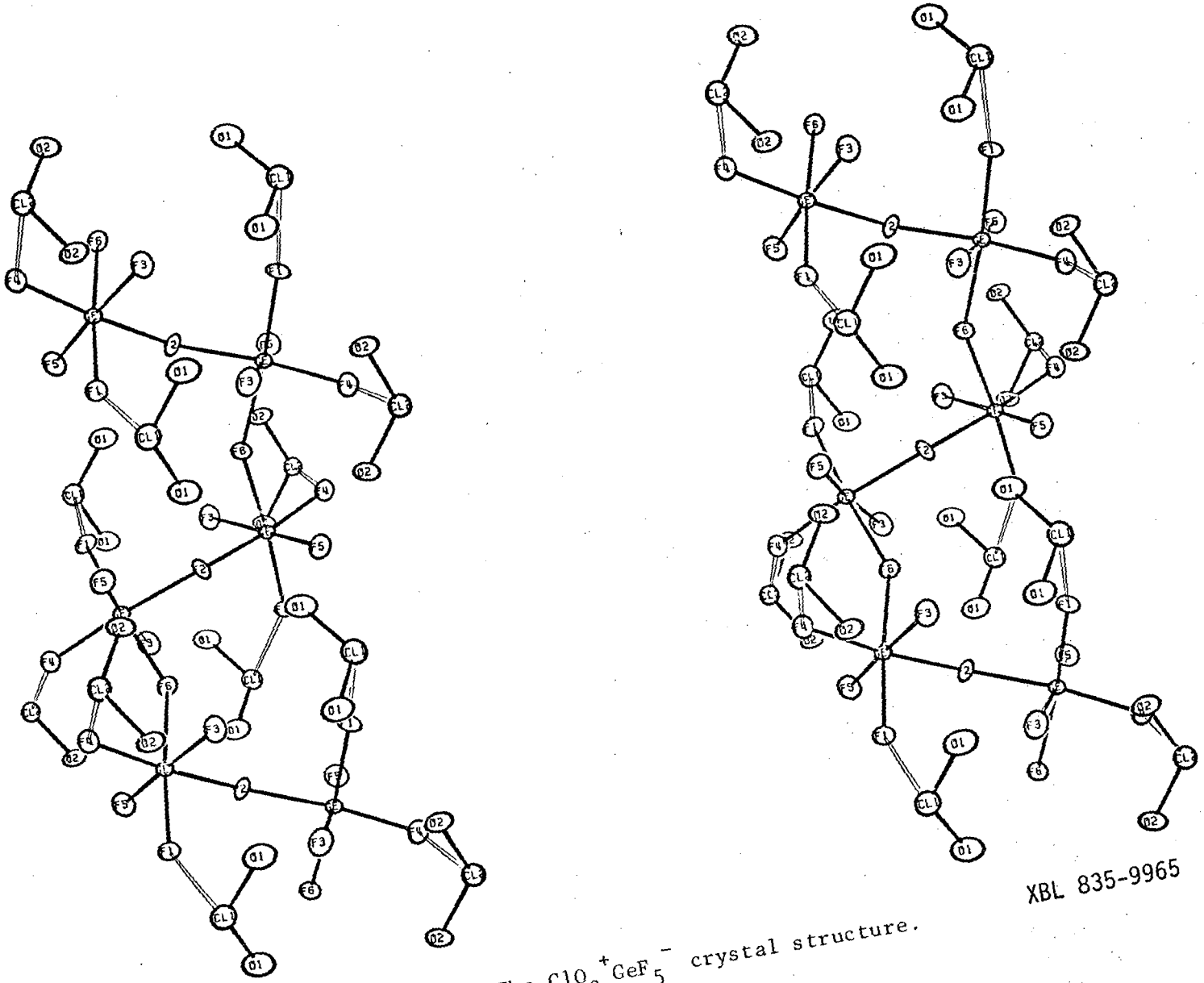

Figure II-6. The $ClO_2^+GeF_5^-$ crystal structure.

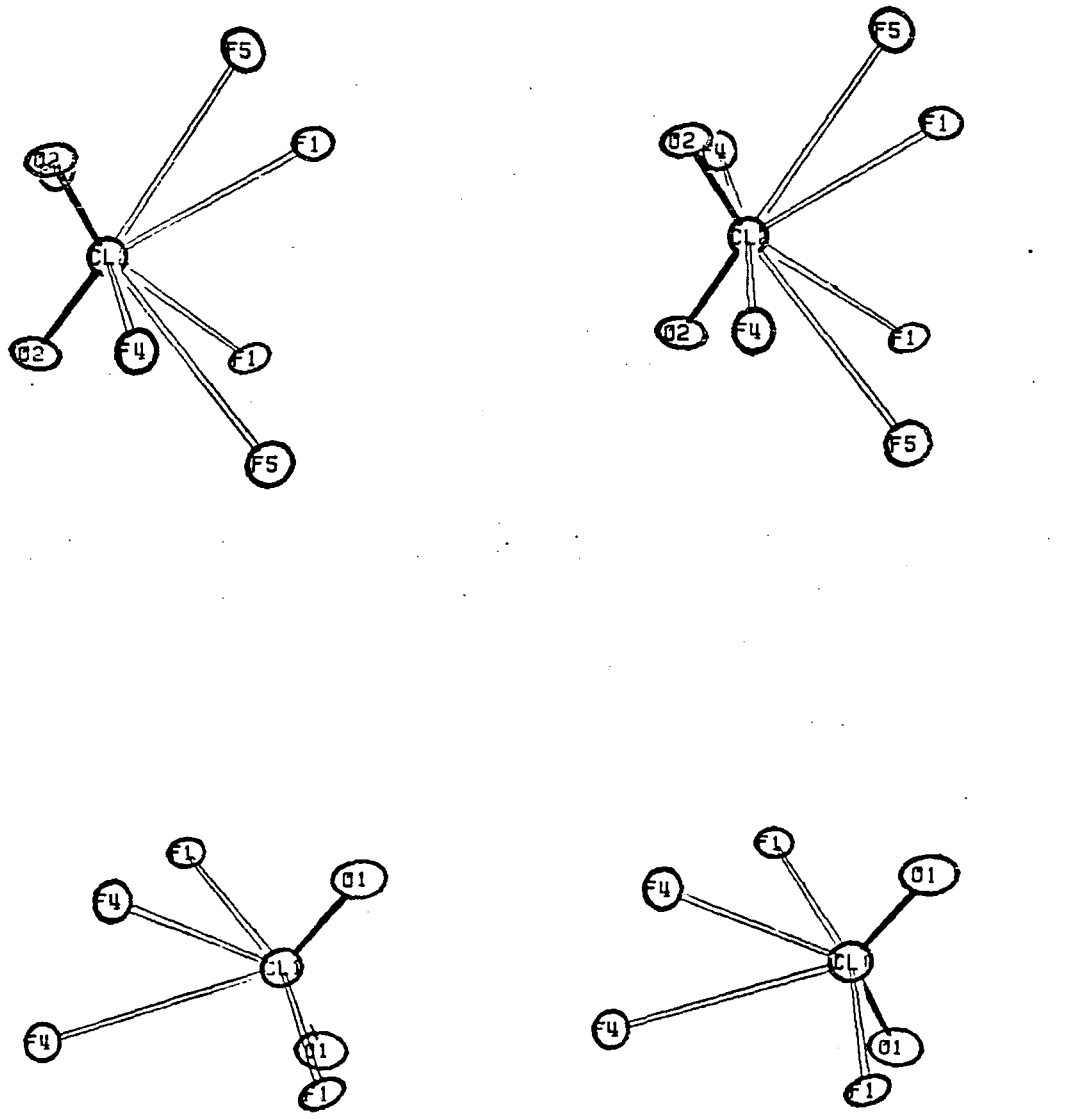

XBL 835-9962

Figure II-7. Chlorine coordination environments in $ClO_2^+GeF_5^-$.

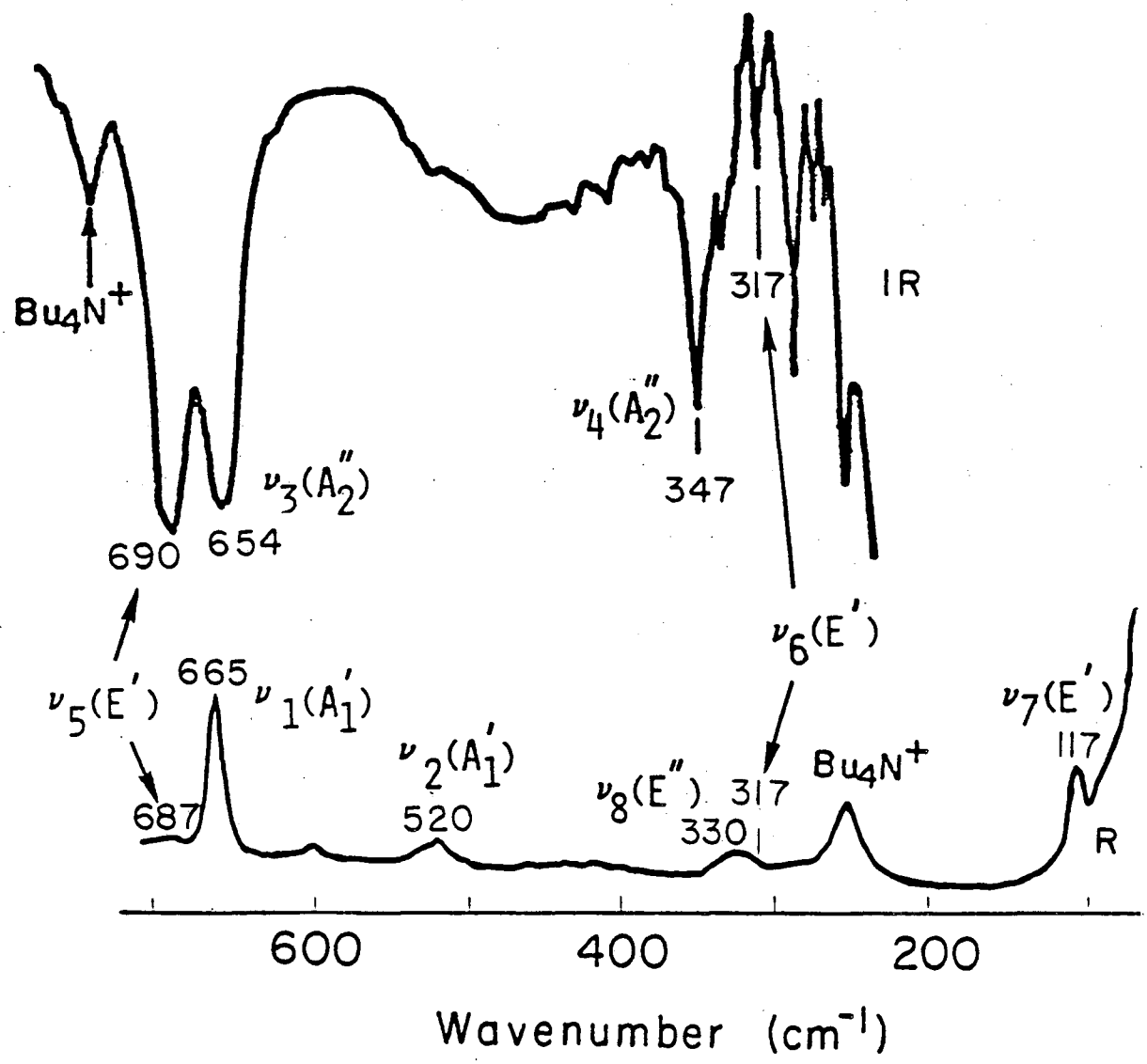

Figure II-8. Vibrational spectra of $(n\text{-}C_4H_9)_4N^+GeF_5^-$.

CHAPTER III

THE FLUORIDE ION AFFINITIES OF GeF_4 AND BF_3 AS CALCULATED FROM BORN-HABER CYCLES

A. Introduction

A thermodynamic model for the intercalation of graphite by fluoroanions has recently been advanced[1]. It states that the free energy change associated with the half-cell reaction which produces a fluoroanion (from the reactants in the intercalation) must exceed a threshold of ca. 120 kcal $mole^{-1}$ for the reaction to proceed. Since it has been reported that germanium tetrafluoride and fluorine are intercalated, in combination, by graphite[2] to form both GeF_5^- and GeF_6^{2-}, the first and second fluoride-ion affinities of that molecule are each of interest. Evaluation of the fluoride ion affinity of boron trifluoride by Altschuler[3] has yielded a value of -71 kcal $mole^{-1}$. This has been accepted by several authors[4,5] as the basis for other fluoride ion affinities and electron affinities. Sharpe[6], however, has preferred a value of -91 kcal $mole^{-1}$, based upon the data of Bills and Cotton[7]. Although the latter value is in harmony with other fluoride ion affinities and electron affinities, its confirmation was clearly desirable to provide a firm basis for correction of affinities based upon the erroneous value. This chapter describes the studies which have provided these fluoride ion affinities.

The salts $ClO_2^+GeF_5^-$ and $(SF_3^+)_2GeF_6^{2-}$, each of which dissociates to stable component species at easily accessible temperatures, have provided for the determination of the following enthalpy changes:

$$\Delta H°(ClO_2GeF_5(s) = ClO_2F(g) + GeF_4(g))$$

$$\Delta H°((SF_3)_2GeF_6(s) = 2\ SF_4(g) + GeF_4(g))$$

The salt $ClO_2^+BF_4^-$ also dissociates extensively at ordinary temperatures, and the enthalpy change:

$$\Delta H°(ClO_2BF_4(s) = ClO_2F(g) + BF_3(g))$$

has been reported[8] to be -24(1) kcal mole^{-1}. This finding has been confirmed in measurements carried out by Mr. Guy Rosenthal in these laboratories.

The crystal structures of the salts have been determined, ClO_2GeF_5 being described in the previous chapter and $(SF_3)_2GeF_6$ in the present chapter. The crystal structure of $ClO_2^+BF_4^-$ was determined by Mr. Rosenthal and appears elsewhere[9]. From this structural information, lattice energies for the salts have been derived; the Madelung term was calculated by the method of Bertaut[10] as modified by Templeton[11], and standard methods of calculation were applied to determine the other terms. The fluoride ion affinities of BF_3 and GeF_4 follow from these calculations by completing Born-Haber cycles.

There is evidence that the graphite lattice acts as a "macro-cation" when it is intercalated, and so stabilizes[9] such uncommon species as SiF_5^-, $B_2F_7^-$, and $P_2F_{11}^-$. It was hoped that a generalized method could be found whereby the thermodynamic stability of fluoro-anions and fluoro-cations could be evaluated. Central to this goal was the development of a method of calculation or accurate estimation of lattice energies of complex molecular fluoride salts; such a method is proposed in this chapter, and will be discussed further in Chapter IV.

B. Experimental

1. $(SF_3)_2GeF_6$

SF_4 and GeF_4 were brought together in a 2:1 molar ratio to produce a colorless solid $2SF_4 \cdot GeF_4$ which was purified by sublimation at room

temperature. Single crystals were grown by sublimation in quartz x-ray capillaries at 30-35°C. Precession photographs indicated space group Pnn2 or Pnnm. A crystal mounted on a CAD-4 four circle diffractometer provided a data set collected in the manner described in Chapter II. Because of the ready dissociation of this compound, data were gathered at -97 ± 7°. The crystallographic data for this compound are given in Table III-1.

The structure was successfully refined in the centric space group Pmnn (no. 58). Full matrix least squares refinement with anisotropic thermal parameters gave final convergence with weighted R = .025, unweighted R = .016, e.s.d.o.u.w. = 1.463 for 42 variables and 299 independent data. The largest parameter shift in the final refinement cycle was < 0.1 σ. A final difference Fourier synthesis gave no peaks with density greater than 0.141 e/$Å^3$. The observed and calculated structure factors for $(SF_3)_2GeF_6$ appear in Table III-2; positional and thermal parameters are given in Table III-3.

2. Dissociation pressure measurements for ClO_2GeF_5 and $(SF_3)_2GeF_6$

Vapor pressure measurements were made using a Monel diaphragm gauge as described by Cromer[12]. Each sample (1-2g.) was sublimed into a thin-walled quartz bulb partially collapsed to increase the surface area for good thermal contact. This was attached via Monel compression fittings to the gauge as shown in figure III-1.

The null point (no pressure difference across the nickel diaphragm) was established by closing A and C and opening B and D. For vapor pressure readings, the sample system and gauge were fully immersed in a water bath. Valve B was closed, A and C were opened, and E and D were

adjusted to find the null point at each bath temperature at equilibrium, the pressure being determined from a mercury column. The sample was pumped out briefly between pressure readings, which were reproducible within 1 or 2 torr at low temperature (0 - 10°C) and within 4 or 5 torr at higher temperatures (25 - 30°C). Log P vs. 1/T data for ClO_2GeF_5 and $(SF_3)_2GeF_6$ are given in Table III-4. Since for ClO_2GeF_5, $K_p = [P_{ClO_2F}][P_{GeF_4}] = {}^1/_4 P^2$, and for $(SF_3)_2GeF_6$, $K_p = [P_{SF_4}]^2[P_{GeF_4}] = 4P^3/27$, we have from the van't Hoff relation, $d(\ln K_p)/d(1/T) = -\Delta H°/R$:

$$ClO_2GeF_5(s) = ClO_2F(g) + GeF_4(g) \qquad \Delta H°=29.1(4) \text{ kcal/mole}$$
$$\Delta S°= 90(1) \text{ cal/mole°K}$$

$$(SF_3)_2GeF_6(s) = 2SF_4(g) + GeF_4(g) \qquad \Delta H°=42.9(6) \text{ kcal/mole}$$
$$\Delta S°=125(2) \text{ cal/mole°K}$$

The identities of the gaseous species in equilibrium with the solids were established by infrared spectroscopy.

C. Lattice Energy Calculations

1. Electrostatic Terms

The electrostatic energy of a lattice of atoms of zero polarizability may be calculated exactly by the method of Bertaut[10], provided the position and charge of each atom in the structure is known. This method involves the infinite sum in reciprocal space:

$$U_{elec} = \frac{18\pi R^2}{V} \sum_{hk\ell} |F(hk\ell)|^2 \frac{(\sin\alpha-\alpha\cos\alpha)^2}{\alpha^8} - \frac{3}{5R} \sum_j q_j^2$$

where $F(hkl) = \sum q_j \exp(2\pi i \underline{h}\cdot\underline{r}_j)$, $\alpha = 2\pi R/d_{hk\ell}$, q_j is the charge on atom j, $\underline{h}\cdot\underline{r}_j = hx_j + ky_j + lz_j$, (x_j,y_j,z_j) are the fractional coordinates of atom j, R is one-half the shortest interatomic distance in the crystal, $d_{hk\ell}$ is the distance between lattice planes hkℓ, and V is the volume of the unit cell. In practice the sum must be terminated at some finite

value of h,k, and ℓ, and to estimate the error introduced thereby, the modification introduced by Templeton[11] has been used. In all calculations the termination of the series was chosen so as to insure that this error was no greater that 0.2 kcal mole^{-1}. Fractional charges were assigned to atoms using the electronegativity equalization procedure of Jolly and Perry[13]. Variation of these charges, within reasonable limits, produced small (1-3%) variations in the electrostatic part of the lattice energy; This is as expected since the multipolar interactions of complex ions in ionic crystals only amount to a few percent of the total lattice energy.

2. London energy terms

The dipole-induced dipole dispersion energy term (U_{dd}) is given by:

$$U_{dd} = -\frac{3}{2} \sum_{i \neq j} \frac{\alpha_i \alpha_j \varepsilon_i \varepsilon_j}{(\varepsilon_i + \varepsilon_j)} r_{ij}^{-6}$$

where α and ε are respectively the polarizability and characteristic energy of the ion. The dipole-induced quadrupole energy (U_{dq}) is likewise given by a summation in r_{ij}^{-8}; it is however generally 10 - 15% of U_{dd}, and so is taken here as simply 0.12 U_{dd}.

3. The zero point vibrational energy and associated terms

A complete lattice enthalpy at 298 K must include the enthalpy of cooling the gaseous ions to 0 K, the enthalpy of warming the crystal from 0 K to 298 K, and the zero point vibrational energy of the crystal.

For crystals containing relatively large, massive ions (SF_3^+, UF_6^-, GeF_6^{2-}, etc.), the zero point energy (U_z) is small (0.2 - 0.4 kcal mole^{-1}). For crystals containing small ions this term is more important and may be estimated from Waddington's correlation[14] of $S°_{298K}$ with U_z. The specific heat (C_p) of the crystal is taken to be 3R per ion; C_p is

assumed to be 5/2R for monatomic, 7/2R for diatomic, and 4R for nonlinear polyatomic ions in the gas phase.

4. The repulsion energy term

A number of approaches to the calculation of closed shell repulsion energies may be found in the literature. Ladd and Lee[15] have successfully used the expression:

$$U_r = B \exp(-r_o/\rho)$$

where B is a constant eliminated by the criterion of energy minimization, r_o is the shortest interatomic distance, and ρ is a parameter determined from compressibility data. In the absence of such data, Born and Mayer's equation[16] may be used:

$$U_r = b \sum_{i \neq j} (1 + q_i/n_i + q_j/n_j)\exp\{(r_i + r_j - r_{ij})/\rho\}$$

Here n is the number of electrons in the outer shell of the ion, q is the charge on the ion, r is its "basic radius", r_{ij} is the distance between ions i and j, and b and ρ are constants (10^{-12} erg molecule^{-1} and 0.32 -0.36 Å, respectively). The range of variation of the parameter ρ is smaller when this expression for U_r is used.

5. Derivation of parameters and calculations

The assignment of polarizabilities, characteristic energies, and basic radii to the atoms in a crystal is not straightforward. Although readily accepted values for these quantities for alkali and halide ions are available, serious errors (vide infra) can arise if the values of α, r, and ε of fluoride ions are applied to fluorine atoms in a complex ion or molecule. The present approach has been, instead, to calculate the lattice energies of molecular fluoride crystals (ignoring M - F interactions in the calculation of the repulsion energy, since the

forces giving rise to it are of extreme short range). The sublimation enthalpies (and hence the lattice energies) are known for these compounds, and ε_F and r_F are derived parametrically if values are assumed for α_F, α_M, and ε_M. The last two terms are of reduced parametric importance since M - F interactions account for only a small fraction of the dispersion energies of these compounds. The derived values of ε_F and r_F are used in subsequent calculations.

It is hoped that accurate lattice enthalpies may be calculated, within the limits of a large simplification: that is, that the London and repulsive interactions in the crystals under consideration arise from potentials which are radially symmetric about the fluorine atoms. Departures from spherical symmetry in the valence electron distributions, induced by molecular bonding, are ignored. This approximation is to a large extent justified when one considers that van der Waals' contacts are generally made in a direction away from the M - F bonds, and in this direction the fluorine valence electron distribution may look radially symmetric. Within this assumption one may calculate the fluorine parameters ε_F and r_F.

For the compounds SiF_4 and UF_6 we have:

$$U_r = b(1 + 2q_F/n_F)\exp(2r_F/\rho) \sum_{i\neq j} \exp(-r_{ij}/\rho)$$

The lattice energy (U_L) is given by:

$$U_L = U_{elec} + U_{dd} + U_{dq} - U_r - U_z$$

Since $(dU_L/dr)_{r=r_o} = 0$,

$$U_{elec} + 6U_{dd} + 8U_{dq} = b(1 + 2q_F/n_F)\exp(2r_F/\rho) \sum_{i\neq j} r_{ij}/\rho\exp(-r_{ij}/\rho)$$

Substituting $U_{dq} = 0.12U_{dd}$, it follows that

$$U_r = \frac{U_L + U_z - .8391\, U_{elec}}{\sum_{i\neq j} (.1609 r_{ij}/\rho - 1)\exp(-r_{ij}/\rho)} \sum_{i\neq j} \exp(-r_{ij}/\rho)$$

$$r_F = \rho/2\ \ell n\{ \frac{U_L + U_z - .8391\, U_{elec}}{b(1 + 2q_F/n_F) \sum_{i\neq j} (.1609 r_{ij}/\rho - 1)\exp(-r_{ij}/\rho)} \}$$

Note that U_r (and thus $U_{dd} + U_{dq}$) is independent of the constant b and thus depends only on the choice of ρ, the calculated electrostatic energy, and the measured sublimation enthalpy. However, r_F depends on both b and ρ.

The crystal structures of SiF_4 and UF_6 are accurately known[17,18], and the polarizabilities, characteristic energies, and fractional charges assigned to each atom are shown in Table III-5. From the latter one calculates U_{elec} = 1.1(1) kcal mole^{-1} for SiF_4 and 2.0(1) kcal mole^{-1} for UF_6. The heats of sublimation are 6.2 kcal mole^{-1} (at 177K) for SiF_4[19] and 11.8 kcal mole^{-1} (at 298K) for UF_6[20]. The calculated values of ε_F and r_F (using a polarizability of 0.80 Å^3 for F) are shown for three choice of ρ in Table III-5. Since the characteristic energy of an atom is related to its ionization potential, it is not surprising that the derived value of ε_F for these (nearly electroneutral) fluorine atoms is significantly higher than that calculated by Mayer[21] for the fluoride ion in the alkali fluorides. r_F is likewise slightly smaller than the fluoride ion value determined by Jenkins and Pratt[22]. The agreement between the parameters derived from SiF_4 and UF_6 is reasonably good; when the lattice energy of SF_3BF_4 was calculated using the two sets of parameters, the calculations differed by 1.3 kcal mole^{-1}. Average values of r_F and ε_F are adopted for subsequent calculations.

These derived fluorine parameters may now be applied to the more complex salts $SF_3^+BF_4^-$, $NO^+UF_6^-$, $(SF_3^+)_2GeF_6^{2-}$, $ClO_2^+BF_4^-$, $K^+BF_4^-$, and $IF_6^+AsF_6^-$. If the central atom in the anion is again assumed to make no contribution to U_r, the lattice energy of the salt and the basic radius of the central atom in the cation may be calculated (in the case of $IF_6^+AsF_6^+$, the fluorine basic radius is calculated). The following details for the salt $SF_3^+BF_4^-$ exemplify this approach:

From $(dU_L/dr)_{r=r_o} = 0$, we have

$$U_{elec} + 6U_{dd} + 8U_{dq} = b\{\exp(2r_S/\rho)_{\Sigma\underline{A}} + \exp((r_S + r_F)/\rho)_{\Sigma\underline{B}} + \exp(2r_F/\rho)_{\Sigma\underline{C}}$$

where

$$\Sigma_{\underline{A},\underline{B},\underline{C}} = \sum_{i\neq j} (1 + q_i/n_i + q_j/n_j)r_{ij}/\rho \exp(-r_{ij}/\rho)$$

Here $\underline{A}$ refers to the sum over S - S, $\underline{B}$ over S - F, and $\underline{C}$ over F - F interactions. As pointed out by previous workers[22], this equation is quadratic in $\exp(r_S/\rho)$, and so r_S and hence U_r follow from Born and Mayer's equation.

Calculation for the dispersion energy terms U_{dd} and U_{dq} requires that ε and α be assigned to the central atom of the cation (S in SF_3^+, Cl in ClO_2^+, NO^+, and K^+). The polarizability of cationic sulfur and chlorine atoms should be less than that of the neutral argon atom[23], 1.6 $Å^3$, and slightly larger than that of K^+, for which a preferred value[24] of 1.029 $Å^3$ has been given. These are assumed to have a polarizability of 1.2 $Å^3$ and NO^+ (which occupies about the same volume as a K^+ ion in its salts) to have a polarizability of 1.0$Å^3$. The characteristic energy is taken as 9/10 of the second ionization potential of the free atom. The oxygen parameters r_0 and ε_0 are

calculated from the OsO_4 structure[25] (for which the heat of sublimation[26] is 11.6 kcal $mole^{-1}$ at 300 K and U_{elec} =2.5(1) kcal $mole^{-1}$), assuming a polarizability of 0.90Å^3 for the O atoms. Thus we obtain r_0 = 1.144 Å and ε_0 = 58.5 eV $molecule^{-1}$. The values of α and ε assigned to the central atom in the anion again have little impact on the result of the calculation. These are given in Table III-6.

Table III-6 shows the calculated lattice enthalpies for $SF_3^+BF_4^-$, $NO^+UF_6^-$, $(SF_3^+)_2GeF_6^{2-}$, $ClO_2^+BF_4^-$, $K^+BF_4^-$, and $IF_6^+AsF_6^-$, and the derived basic radii for $S^{+.9442}$, $Cl^{+1.083}$, NO^+, K^+, and $F^{\sim-.27}$. In these calculations a value of ρ = .333 Å was chosen, since this is the preferred value for the alkali fluorides[22]. Variation of ρ between .333 and .360 Å produced a variation of 1.5 kcal $mole^{-1}$ in the $SF_3^+BF_4^-$ lattice enthalpy. Likewise a variation of $U_{dd} + U_{dq}$ by 25% (= 9.5 kcal) produced a change in the calculated lattice enthalpy of only 2.4 kcal $mole^{-1}$, because of a compensating change induced in U_r. In these calculations the charge distributions of the individual atoms were taken to be spherical. However, since the atoms are polarizable, they will in fact have multipolar charge distributions arising from the non-spherical arrangement of their (charged) near neighbors. The interactions of these multipoles will contribute another term to the electrostatic part of the lattice energy, which should be greater for NO^+, ClO_2^+, and SF_3^+ salts than for simple alkali halide salts. The largest of these, the dipole–monopole interaction term, was evaluated for $SF_3^+BF_4^-$ by allowing each atom to become a permanent dipole (by virtue of its polarizability and the field created by the other point charges in the ion); the energy of this interaction is found to be ca. 0.1 kcal $mole^{-1}$. While this model is crude, it nevertheless provides an estimate of the order of

magnitude of such interactions, which is indeed small.

The computer programs used for these lattice energy calculations are listed out in the appendix to this thesis.

6. An empirical lattice energy determination for ClO_2GeF_5

For $ClO_2^+GeF_5^-$ the method of calculation of the lattice enthalpy outlined above cannot be applied since the anion rearranges from a monomer in the gas phase to a cis - bridged polymer in the crystal. The lattice energy of this salt may be estimated from its formula-unit volume. Since the lattice energy of a simple A^+B^- salt is dominated by the coulombic term (the repulsion energy and the dispersion energy terms being largely mutually cancelling over a fairly wide range of formula-unit volumes), a roughly linear correlation between the lattice energy and $M/(r_{A^+-B^-})$ is expected, where M is the Madelung constant and $r_{A^+-B^-}$ is the shortest cation - anion distance in the crystal. Kapustinskii has shown[27], however, that $M/(r_{A^+-B^-})$ is relatively invariant with transformation from one structural type to another for the same ions A^+ and B^-; and so one should expect a linear correlation between the lattice energy and the inverse of the average primitive unit cell edge, i.e., the cube root of the formula-unit volume in the crystal. This linear correlation is shown in figure III-2. The correlation is particularly good among members of a given structural family, e.g., NaCl or CsCl. Where the dispersion energy term is expected to be large because of highly polarizable or strongly coordinating ions (e.g., TlCl, ClO_2BF_4, SF_3BF_4), a positive deviation is seen. The lattice enthalpy of $ClO_2^+GeF_5^-$ is therefore calculated simply from the U_L vs. $V^{-1/3}$ plot, allowing the same positive deviation as for $ClO_2^+BF_4^-$, to give $\Delta H°_L(ClO_2GeF_5) = 146(5)$ kcal mole^{-1}. This lattice enthalpy value is,

however, of limited physical meaning since it does not represent the enthalpy change:

$$\Delta H°(ClO_2^+(g) + GeF_5^-(\text{monomer, g}) = ClO_2GeF_5(s)),$$

and so cannot be used in a Born-Haber cycle to evaluate $\Delta H°(GeF_4(g) + F^-(g) = GeF_5^-(\text{monomer, g}))$. While the monomeric form of GeF_5^- has been established in the solid state[28], it only occurs when it is stabilized by very large cations such as tetra n-butylammonium. The diameter of such a cation (~8.3 Å) is too large to be accomodated by cis or trans-bridging GeF_5^-, since the F-Ge-F-Ge-F unit has a maximum extension of about 7.6 Å. Rearrangement to polymeric GeF_5^- occurs when it is made possible by the presence of small cations. The enthalpy change associated with this rearrangement, while it is certainly exothermic, is as yet uncertain.

D. Results and discussion

1. $(SF_3)_2GeF_6$ structure

The sulfur and germanium coordination environments in the $(SF_3)_2GeF_6$ structure are shown in figure III-3. While the space group requires only C_s symmetry at S and C_{2v} symmetry at Ge, the SF_3^+ ion has essentially C_{3v} symmetry with all the S - F bonds of equal length and all the F - S - F angles equal within one standard deviation; the GeF_6^{2-} ion is almost a regular octahedron with all the Ge - F bond lengths equal within 1σ and with the F - Ge - F angles differing from 90° by about 3σ. Each sulfur atom makes close contacts with one fluorine atom from each of three different anions, and so the cation-to-anion coordination in $(SF_3)_2GeF_6$ is 6:3, with each fluorine atom in the GeF_6^{2-} octahedron making a bridging contact (2.37 - 2.42 Å) to a sulfur atom. Fluorine atoms in the SF_3^+ ion make only van der Waals'

contacts (≥2.65 Å) with other fluorine atoms in the structrure. The bridging of fluorine in this structure resembles that found in SF_3BF_4, where the coordination is 3:3. The dimensions of SF_3^+ in $SF_3^+BF_4^-$ and $(SF_3)_2GeF_6^{2-}$ are not significantly different, and as has been remarked earlier[29], the F-S-F bond angle has the same value as that of F-P-F in the isoelectronic relative PF_3. Bond lengths and angles for $(SF_3)_2GeF_6$ are given in Table III-7.

2. Fluoride ion and electron affinities

i) Boron trifluoride: The enthalpy change (2σ in parentheses) for the reaction:

$$ClO_2F(g) + BF_3(g) = ClO_2BF_4(s)$$

has been reported[8] to be -24(1) kcal mole^{-1}. Since $\Delta H°_L(ClO_2BF_4)$ = 149(5) kcal, then we have from $\Delta H°_f(ClO_2F)$ = -8.0(5) kcal[30], $\Delta H°_f(ClO_2)$ = 24.5(8) kcal[31], $\Delta H°(ClO_2 = ClO_2^+ + e^-)$ = 246.6(23) kcal[32], and $\Delta H°_f(F^-)$ = -62 kcal, that for $BF_3(g) + F^-(g) = BF_4^-(g)$, $\Delta H°$ = -92(6) kcal mole^{-1}. This is in agreement with the value calculated by Sharpe[6] from the data originally published by Bills and Cotton[7], but disagrees with the often cited value of -71 kcal which derives[4] from the enthalpy change for the reaction $KBF_4(s) = KF(s) + BF_3(g)$.

ii) Uranium hexafluoride: The electron affinity of UF_6 has been evaluated at 113 kcal mole^{-1} by Beauchamp and coworkers[33] from measurement of the enthalpy of the reaction:

$$UF_6^-(g) + BF_3(g) = BF_4^-(g) + UF_5(g),\ \Delta H° = +37(4) \text{ kcal}$$

Substituting the revised value of -92 kcal for $\Delta H°(BF_3(g) + F^-(g) = BF_4^-(g))$ in place of the -71 assumed by Beauchamp, et al., and using -62 kcal for the heat of formation of F^-, we obtain $EA(UF_6)$ = 135 kcal mole^{-1}.

Since $\Delta H°(NO(g) + UF_6(g) = NOUF_6(s)) = -52$ kcal[34], from the ionization potential of NO (213 kcal) and our calculated lattice enthalpy for $NOUF_6$ (132 kcal), we obtain $EA(UF_6) = 133$ kcal. This agreement of the cyclotron resonance and lattice energy evaluations of $EA(UF_6)$ points to the correctness of the -92 kcal value for $\Delta H°(BF_3(g) + F^-(g) = BF_4^-(g))$ and also indicates that the lattice energy evaluations are reliable.

iii) Sulfur tetrafluoride: One may now calculate $\Delta H°(SF_4(g) = SF_3^+(g) + F^-(g)) = +211(8)$ kcal from $\Delta H°_L(SF_3BF_4) = 144(5)$, $\Delta H°(BF_3(g) + F^-(g) = BF_4^-(g)) = -92(6)$ and $\Delta H°(SF_4(g) + BF_3(g) = SF_3BF_4(s)) = -25(1)$ kcal[35].

iv) Germanium tetrafluoride: The first fluoride ion affinity of GeF_4 is obtained from $\Delta H°(ClO_2F(g) = ClO_2^+(g) + F^-(g)) = 217(3)$, $\Delta H°(ClO_2F(g) + GeF_4(g) = ClO_2GeF_5(s)) = -29(1)$, and $\Delta H°_L(ClO_2GeF_5) = 146(5)$ kcal mole^{-1}. Thus $\Delta H°(GeF_4(g) + F^-(g) = GeF_5^-(g, \text{polymer})) = 100(6)$ kcal mole^{-1}.

From $\Delta H°(2SF_4(g) = 2SF_3^+(g) + 2F^-(g)) = 422(16)$, $\Delta H°(2SF_4 + GeF_4(g) = (SF_3)_2GeF_6(s)) = -43(1)$, and $\Delta H°_L((SF_3)_2GeF_6) = -383(12)$ kcal mole^{-1}, the double fluoride ion affinity $\Delta H°(GeF_4(g) + 2F^-(g) = GeF_6^{2-}(g)) = -82(18)$ kcal mole^{-1} is obtained.

Summary

From thermodynamic data pertaining to the dissocation of GeF_5^-, GeF_6^{2-}, and BF_4^- salts, and from lattice energy calculations, it has been possible to evaluate the fluoride ion affinities of GeF_4 and BF_3. The first fluoride ion affinity of GeF_4 exceeds that of BF_3 by 8 kcal mole^{-1}. Because of the smaller volume of BF_4^- relative to that of GeF_5^-, the more favorable lattice energy of the former approximately

offsets the higher fluoride ion affinity of GeF_4 relative to BF_3, at least in salts with small cations. In cases where cations are large and the values of the lattice energies of the GeF_5^- and BF_4^- salts are therefore closer, the thermodynamic stability of GeF_5^- salts appreciably exceeds that of the corresponding fluoborates.

References

1. N. Bartlett and B.W. McQuillan, in "Intercalation Chemistry", S. Wittingham and A. Jacobsen, Eds., Academic Press, London and N.Y., vol. I, 19 (1982).

2. E.M. McCarron, Y.J. Grannec, and N. Bartlett, J. Chem. Soc. Chem. Comm., 890 (1980).

3. A.P. Altschuler, J. Amer. Chem. Soc., 77, 6187 (1955).

4. J.C. Haartz and D.H. McDaniel, J. Amer. Chem. Soc., 95, 8562 (1973).

5. M.K. Murphy and J.L. Beauchamp, J. Amer. Chem. Soc., 99, 4992 (1977).

6. A.G. Sharpe in "Halogen Chemistry", V. Gutman, Ed., Academic Press, London and N.Y., vol.I, 1 (1967).

7. J.L. Bills and F.A. Cotton, J. Chem. Phys., 64, 1477 (1960).

8. K.O. Christe, C. Shack, D. Pilipovich, and W. Sawodny, Inorg. Chem., 8, 2489 (1969).

9. G.L. Rosenthal and N. Bartlett, to be submitted for publication.

10. E.F. Bertaut, J. Phys. Radium., 13, 499 (1952).

11. D.H. Templeton, J. Chem. Phys., 21, 1629 (1955).

12. S. Cromer, U.S. At. En Comm., MDDC-803, June 20, 1944.

13. W.L. Jolly and W.B. Perry, Inorg. Chem., 13, 2686 (1974).

14. (a) T.C. Waddington, Ph.D. thesis, Cambridge (1959).
(b) M.F.C. Ladd and W.H. Lee, J. Inorg. Nucl. Chem., 14, 14 (1960).

15. M.F.C. Ladd and W.H. Lee, Trans. Faraday Soc., 54, 34 (1958).

16. M. Born and J.E. Mayer, Z. Physik, 75, 1 (1932).

17. M. Atoji and W.N. Lipscomb, Acta Crys., 7, 579 (1954).

18. J.H. Levy, J.C. Taylor, and P.W. Wilson, J. Chem. Soc. Dalton, 219

(1976).

19. W.I. Patrode and J. Papish, J. Phys. Chem., 34, 1494 (1930).

20. G.D. Oliver, H.T. Milton, and J.W. Grisard, J. Amer. Chem. Soc., 75, 2827 (1953).

21. J.E. Mayer, J. Chem. Phys., 1, 270 (1933).

22. H.D.B. Jenkins and K.F. Pratt, Proc. Roy. Soc. Lond. A, 356, 115 (1977).

23. W.F. Edgell in "Argon, Helium, and the Rare Gases", G.A. Cook, Ed., Interscience, New York, vol. I, 151 (1961).

24. J Pirenne and E. Kartheuser, Physica, 30, 2005 (1964).

25. B. Krebs and K. Haase, Acta Crys. B, 32, 1334 (1976).

26. E. Ogawa, Bull. Chem. Soc. Japan, 6, 302 (1931).

27. A.F. Kapustinskii, Zh. Fiz. Khim., 5, 59 (1934).

28. I. Wharf and M. Onyszchuk, Can. J. Chem., 48, 2250 (1970).

29. D.D. Gibler, C.J. Adams, M. Fischer, A. Zalkin, and N. Bartlett, Inorg. Chem., 11, 2325 (1972).

30. P. Barberi, Bull. Inform. Sci. Tech. Comm. Energ. At., 180, 55 (1973).

31. M.A.A. Clyne, J. Chem. Soc. Faraday I, 71, 322 (1975).

32. I.P. Fisher, Trans. Faraday Soc., 63, 684 (1967).

33. J.L. Beauchamp, J. Chem. Phys., 64, 929 (1976).

34. J. Chatelet, private communication.

35. N. Bartlett and P.L. Robinson, Chem. and Ind., 1351 (1956) and J. Chem. Soc., 3417 (1961).

Table III-1. Crystallographic data for $(SF_3^+)_2GeF_6^{2-}$.

---

crystal dimensions: .022 x .018 x .020 cm.

space group: Pmnn (non-standard setting of Pnnm, #58)

vol. ($\AA^3$) = 439.4(2) ρ (calc'd) = 2.756

$\underline{a}$($\AA$) = 6.142(1) $\underline{b}$($\AA$) = 9.593(1) $\underline{c}$($\AA$) = 7.458(1)

data collection at -92°

radiation: $MoK\bar{\alpha}$, graphite monochrometer (λ = .71073$\AA$)

2θ range: 3-45°

hkl range: $\pm h$, $+k$, $+l$

scan mode: θ - 2θ

background: .25 x $\Delta\theta$, where $\Delta\theta$ = .50 + .347tanθ

scan rate: variable, maximum 50 sec.

absorption coefficient (μcalc.): 43.27 cm^{-1}

transmission: 47.4% min., 64.7% max.

orientation and intensity stds.: ($\bar{4}$ 1 1), ($\bar{1}$ 6 1), (0 0 6) every 250 reflections, no decay

reflections measured: 687

Table III-2. Observed and calculated structure factors for $(SF_3)_2GeF_6$.

H	K	L	FOBS	FCALC	H	K	L	FOBS	FCALC	H	K	L	FOBS	FCALC	H	K	L	FOBS	FCALC	H	K	L	FOBS	FCALC	H	K	L	FOBS	FCALC
0	0	2	1083	1088	0	6	6	428	428	1	4	4	56	53	2	2	4	667	673	3	0	7	378	367	3	8	3	88	87	5	0	3	69	72
0	0	4	55	50	0	7	1	35	32	1	4	5	446	448	2	2	5	403	408	3	1	0	41	35	3	9	0	254	260	5	0	5	226	228
0	0	6	326	331	0	7	2	371	369	1	4	6	14*	7	2	2	6	441	443	3	1	1	213	212	3	9	1	58	58	5	1	0	571	571
0	0	8	260	263	0	7	3	170	172	1	4	7	352	348	2	2	7	146	149	3	1	2	197	206	4	0	0	965	1000	5	1	1	44	47
0	1	1	792	753	0	7	4	177	177	1	5	0	184	112	2	3	1	139	131	3	1	3	170	170	4	0	2	472	480	5	1	2	320	322
0	1	2	327	331	0	7	5	262	263	1	5	1	0*	13	2	3	2	646	624	3	1	4	393	402	4	0	4	45	29	5	1	3	150	161
0	1	3	293	276	0	8	0	455	451	1	5	2	393	384	2	3	3	447	448	3	1	5	19*	16	4	0	6	110	113	5	1	4	169	166
0	1	4	547	552	0	8	1	273	274	1	5	3	243	238	2	3	4	235	227	3	1	6	246	254	4	1	1	656	657	5	1	5	241	241
0	1	5	79	74	0	8	2	442	437	1	5	4	582	491	2	3	5	326	332	3	1	7	0*	21	4	1	2	58	58	5	2	1	633	639
0	1	6	318	315	0	8	3	287	285	1	5	5	231	230	2	3	6	11*	8	3	2	1	567	567	4	1	3	194	188	5	2	2	178	177
0	1	7	398	408	0	8	4	332	335	1	5	6	265	269	2	3	7	141	143	3	2	2	354	349	4	1	4	261	264	5	2	3	310	302
0	2	0	152	160	0	8	5	23*	28	1	6	1	447	458	2	4	0	849	858	3	2	3	435	444	4	1	5	284	283	5	2	4	80	84
0	2	1	99	100	0	9	1	385	392	1	6	2	65	65	2	4	1	73	69	3	2	4	19*	10	4	1	6	178	165	5	2	5	111	107
0	2	2	37	31	0	9	2	16*	7	1	6	3	394	391	2	4	2	786	778	3	2	5	142	147	4	2	0	42	44	5	3	0	172	170
0	2	3	112	113	0	9	3	390	384	1	6	4	129	131	2	4	3	115	115	3	2	6	16*	21	4	2	1	80	90	5	3	1	176	174
0	2	4	212	206	0	10	0	67	67	1	6	5	224	222	2	4	4	489	496	3	3	0	759	748	4	2	2	161	158	5	3	2	200	196
0	2	5	152	148	0	10	1	20*	16	1	6	6	65	70	2	4	5	71	72	3	3	1	122	123	4	2	3	0*	16	5	3	3	258	258
0	2	6	457	464	1	0	1	107	116	1	7	0	545	552	2	4	6	91	91	3	3	2	697	698	4	2	4	323	325	5	3	4	151	149
0	2	7	150	149	1	0	3	30	32	1	7	1	143	143	2	5	1	696	691	3	3	3	143	141	4	2	5	72	74	5	4	1	87	83
0	3	1	612	617	1	0	5	491	504	1	7	2	396	400	2	5	2	391	388	3	3	4	419	422	4	2	6	359	356	5	4	2	93	98
0	3	2	179	162	1	0	7	478	491	1	7	3	243	246	2	5	3	228	223	3	3	5	388	381	4	3	1	153	162	5	4	3	333	336
0	3	3	1015	986	1	1	0	800	802	1	7	4	295	286	2	5	4	297	296	3	3	6	216	212	4	3	2	111	110	5	4	4	65	60
0	3	4	247	250	1	1	1	107	100	1	7	5	149	145	2	5	5	135	128	3	4	1	59	50	4	3	3	405	410	5	5	0	60	61
0	3	5	619	605	1	1	2	527	530	1	8	1	141	140	2	5	6	160	166	3	4	2	141	145	4	3	4	193	194	5	5	1	10*	17
0	3	6	304	299	1	1	3	269	276	1	8	2	16*	10	2	6	0	336	334	3	4	3	117	110	4	3	5	286	295	5	5	2	253	253
0	3	7	216	219	1	1	4	382	388	1	8	3	189	110	2	6	1	71	67	3	4	4	93	92	4	4	0	445	441	5	5	3	99	96
0	4	0	49	48	1	1	5	295	294	1	8	4	137	141	2	6	2	17*	27	3	4	5	216	210	4	4	1	154	156	5	6	1	200	203
0	4	1	520	530	1	1	6	412	410	1	9	0	195	193	2	6	3	30	30	3	4	6	100	109	4	4	2	621	510	5	6	2	0*	7
0	4	2	467	470	1	1	7	107	100	1	9	1	193	196	2	6	4	66	65	3	5	0	330	323	4	4	3	107	100	6	0	0	655	664
0	4	3	422	411	1	2	1	1022	1025	1	9	2	176	177	2	6	5	0*	12	3	5	1	156	157	4	4	4	372	365	6	0	2	414	420
0	4	4	481	470	1	2	2	132	120	1	9	3	232	235	2	6	6	351	347	3	5	2	272	276	4	4	6	114	112	6	1	1	244	241
0	4	5	190	193	1	2	3	536	536	1	10	1	406	412	2	7	1	535	532	3	5	3	366	360	4	5	1	309	304	6	1	2	69	71
0	4	6	25*	27	1	2	4	173	167	2	0	0	630	664	2	7	2	207	210	3	5	4	225	226	4	5	2	350	346	6	1	3	127	124
0	4	7	36	42	1	2	5	122	122	2	0	2	402	421	2	7	3	166	164	3	5	5	263	260	4	5	3	200	201	6	2	0	22*	31
0	5	1	202	200	1	2	6	34	34	2	0	4	205	212	2	7	4	240	249	3	5	6	249	240	4	5	4	150	159	6	2	1	72	60
0	5	2	555	556	1	2	7	100	99	2	0	6	99	99	2	7	5	242	239	3	6	1	760	767	4	5	5	190	103	6	2	2	80	82
0	5	3	526	504	1	3	0	354	363	2	1	1	506	506	2	0	0	550	559	3	6	2	99	99	4	6	0	109	113	6	3	1	213	215
0	5	4	52	49	1	3	1	140	147	2	1	2	376	364	2	0	1	0*	5	3	6	3	371	369	4	6	1	63	62	6	3	2	110	115
0	5	5	293	206	1	3	2	403	415	2	1	3	575	590	2	0	2	301	304	3	6	4	45	43	4	6	2	116	116	6	4	0	247	247
0	5	6	137	130	1	3	3	341	336	2	1	4	251	256	2	0	3	0*	5	3	6	5	215	207	4	6	3	30	39	6	4	1	44	40
0	5	7	120	117	1	3	4	246	250	2	1	5	434	444	2	0	4	200	190	3	7	0	374	302	4	6	4	199	200					
0	6	0	300	307	1	3	5	220	226	2	1	6	257	261	2	9	1	169	170	3	7	1	202	206	4	7	1	225	226					
0	6	1	112	113	1	3	6	132	134	2	1	7	211	213	2	9	2	106	101	3	7	2	144	144	4	7	2	205	201					
0	6	2	416	409	1	3	7	17*	15	2	2	0	229	221	2	9	3	217	216	3	7	3	296	302	4	7	3	200	213					
0	6	3	94	94	1	4	1	130	137	2	2	1	500	490	3	0	1	231	230	3	7	4	19*	30	4	0	0	329	327					
0	6	4	504	499	1	4	2	16*	6	2	2	2	323	317	3	0	3	627	642	3	0	2	79	01	4	0	1	106	102					
0	6	5	46	50	1	4	3	546	537	2	2	3	200	199	3	0	5	670	690						5	0	1	66	63					

Table III-3. Positional and thermal parameters for $(SF_3)_2GeF_6$.

Atom	x	y	z	B_{11}	B_{22}	B_{33}	B_{12}	B_{13}	B_{23}
Ge	.5	.5	0	.0083(1)	.00307(5)	.00541(8)	0	0	-.0007(1)
S	0	.25615(8)	.0651(1)	.0112(2)	.00345(8)	.0077 (2)	0	0	.0012(2)
F1	.1842(2)	.1547 (1)	.0267(2)	.0189(4)	.0057 (2)	.0132 (3)	.0074(5)	.0060(6)	.0002(3)
F2	0	.1437 (2)	.3475(3)	.0178(5)	.0055 (2)	.0090 (3)	0	0	.0056(5)
F3	.5	.1757 (2)	.3819(3)	.0193(5)	.0071 (2)	.0074 (3)	0	0	-.0039(5)
F4	.2946(2)	.4160 (1)	.1298(2)	.0133(3)	.0066 (2)	.0088 (2)	-.0045(4)	.0035(5)	.0019(3)

Table III-4. ℓnK_p vs. 1/T data for ClO_2GeF_5 and $(SF_3)_2GeF_6$.

$ClO_2^+GeF_5^-$: $\Delta H^o_{298} = 29.1(4)$ kcal mole^{-1}
$\Delta S^o_{298} = 90(1)$ cal mole^{-1} K^{-1}

$1/T \times 10^3 (K^{-1})$	$-\ell nK_p$ (obs.)	$-\ell nK_p$ (calc.)
3.562	7.09	7.05
3.512	6.29	6.32
3.464	5.57	5.61
3.412	4.92	4.85
3.355	3.93	4.02
3.304	3.29	3.27
3.262	2.68	2.65

$(SF_3)_2GeF_6$: $\Delta H^o_{298} = 42.9(6)$ kcal mole^{-1}
$\Delta S^o_{298} = 125(2)$ cal mole^{-1} K^{-1}

$1/T \times 10^3 (K^{-1})$	$-\ell nK_p$ (obs.)	$-\ell nK_p$ (calc.)
3.661	15.97	16.01
3.593	14.62	14.55
3.529	13.19	13.17
3.473	11.98	11.96
3.416	10.60	10.73
3.288	8.02	7.97

Table III-5. Lattice energy calculations for SiF_4, UF_6, and OsO_4.

	ρ = .333 Å			ρ = .345		ρ = .360	
	SiF_4	UF_6	OsO_4	SiF_4	UF_6	SiF_4	UF_6
$U_{dd}+U_{dq}$(kcal)	16.62	29.37	27.64	17.94	31.59	19.60	34.69
U_z(kcal)	0.5	0.2	0.5	0.5	0.2	0.5	0.2
U_r(kcal)	11.40	19.91	18.63	12.62	22.13	14.38	25.23
ε_F(eV)	46.90	52.24	-	51.00	56.63	56.98	63.32
ε_O(eV)	-	-	58.53	-	-	-	-
$\bar{r}_F$(Å)	1.053	1.079	-	1.053	1.077	1.055	1.079
$\bar{r}_O$(Å)	-	-	1.144	-	-	-	-

SiF_4: $q_F = -.171$, $q_{Si} = +.684$ $\quad$ UF_6: $q_F = -.221$, $q_U = +1.326$

OsO_4: $q_O = -.2915$, $q_{Os} = +1.166$

	F	Os	Si	U	O
α(Å^3)	0.80	2.00	1.20	2.50	0.90
ε(eV)	-	15.3	14.7	15.0	-

Table III-6. Lattice Enthalpies and Basic Radii.

	SF_3BF_4	$NOUF_6$	ClO_2BF_4	KBF_4	$(SF_3)_2GeF_6$	IF_6AsF_6
U_{elec} (kcal)	147.8	137.8	154.2	160.6	413.3	123.15
U_{dd} (kcal)	37.14	26.21	35.13	22.37	72.73	45.13
U_{dq} (kcal)	4.46	3.15	4.22	2.68	8.73	5.42
U_r (kcal)	46.27	36.24	45.01	35.54	113.58	48.26
U_z (kcal)	0.2	0.2	0.3	0.5	0.2	0.2
U_L (0 K, kcal)	142.9	130.7	148.2	149.7	381.0	125.2
ΔH_L^o (298K, kcal)	144.1	131.6	149.4	149.9	382.8	126.4
$\bar{r}$ (Å)	$\bar{r}_S = 1.147$	$\bar{r}_{NO} = 1.262$	$\bar{r}_{Cl} = 1.150$	$\bar{r}_K = 1.193$	$\bar{r}_S = 1.193$	$\bar{r}_F = 1.100$

For all calculations, $\rho = .333$ Å, and for all except IF_6AsF_6, $\bar{r}_F = 1.066$ Å.

Table III-6 (continued).

charge distributions:

SF_3^+: $q_S = +.9442$, $q_F = +.0186$

BF_4^-: $q_B = +.1420$, $q_F = -.2855$

UF_6^-: $q_U = +.5846$, $q_F = -.2641$

ClO_2^+: $q_{Cl} = +1.083$, $q_O = -.0415$

GeF_6^{2-}: $q_{Ge} = +.3148$, $q_F = -.3858$

IF_6^+: $q_I = +2.2834$, $q_F = -.2139$

AsF_6^-: $q_{As} = +.9638$, $q_F = -.3273$

	F	O	S	Cl	B	U
α ($\mathring{A}^3$)	0.80	0.90	1.20	1.20	0.05	2.50
ε (eV)	49.57	58.53	21.06	21.42	22.63	15.00

	Ge	K	NO	As	I
α ($\mathring{A}^3$)	0.75	1.03	1.00	0.70	1.00
ε (eV)	14.34	28.63	28.60	16.80	17.20

Table III-7. Selected internuclear distances and angles for $(SF_3)_2GeF_6$

Distances:

Ge	F2	1.787(1)	S	F2	2.367(2)
Ge	F4	1.783(1)	S	F3	1.515(2)
S	F1	1.519(1)	S	F4	2.420(1)

Angles:

F2-Ge-F4	89.83(5)	F2-S-F3	178.47(8)
F1-S-F1	96.23(10)	F2-S-F4	96.38(4)
F1-S-F2	82.86(6)	F3-S-F4	84.63(5)
F1-S-F3	96.12(8)	F4-S-F4	96.75(6)
F1-S-F4	179.22(7), 83.51(5)		

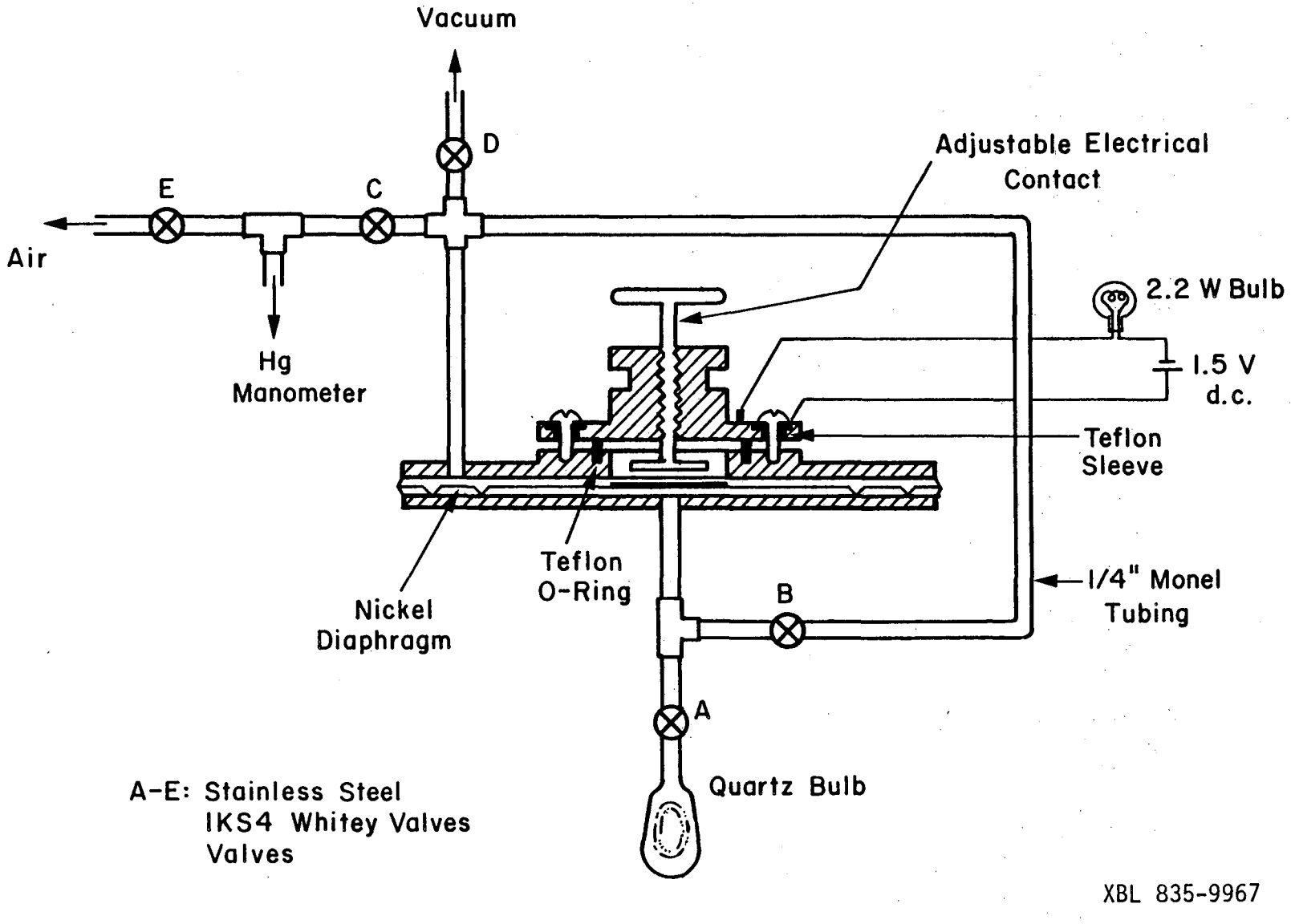

Figure III-1. The pressure transmitter gauge.

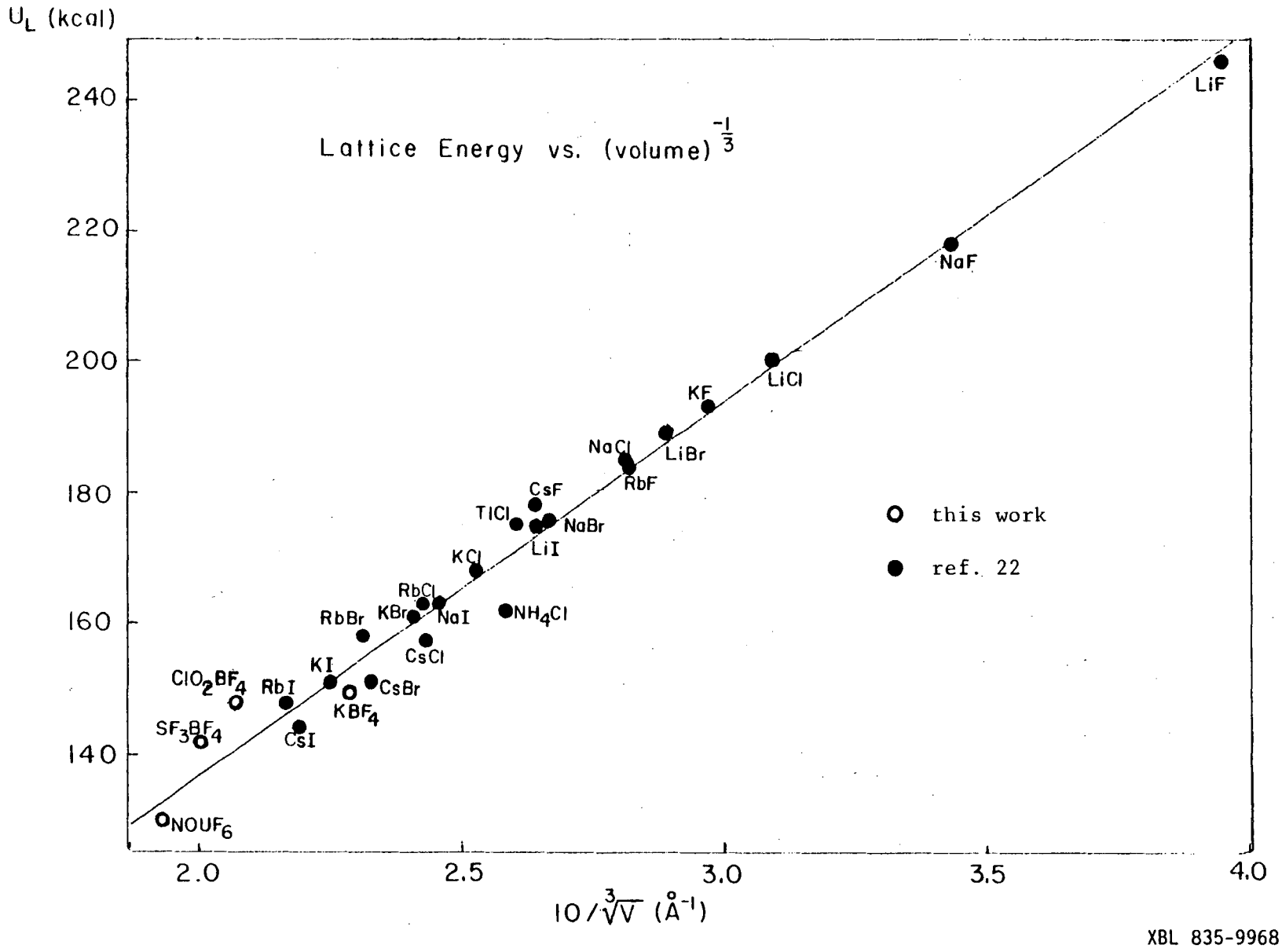

Figure III-2. Correlation of lattice energies with molecular volumes.

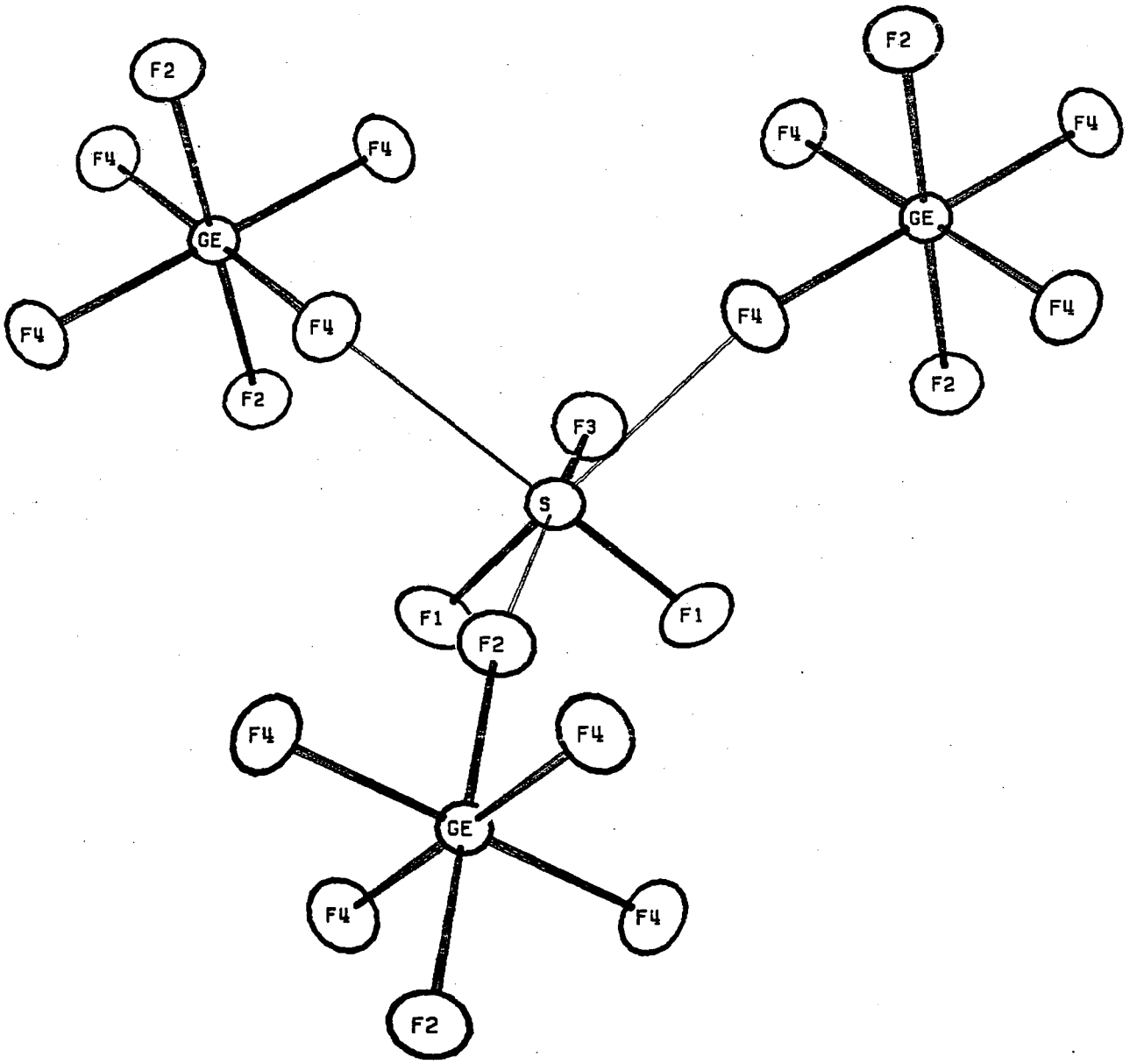

XBL 837-10663

Figure III-3a. Sulfur coordination environment in the $(SF_3^+)_2GeF_6^{2-}$ structure.

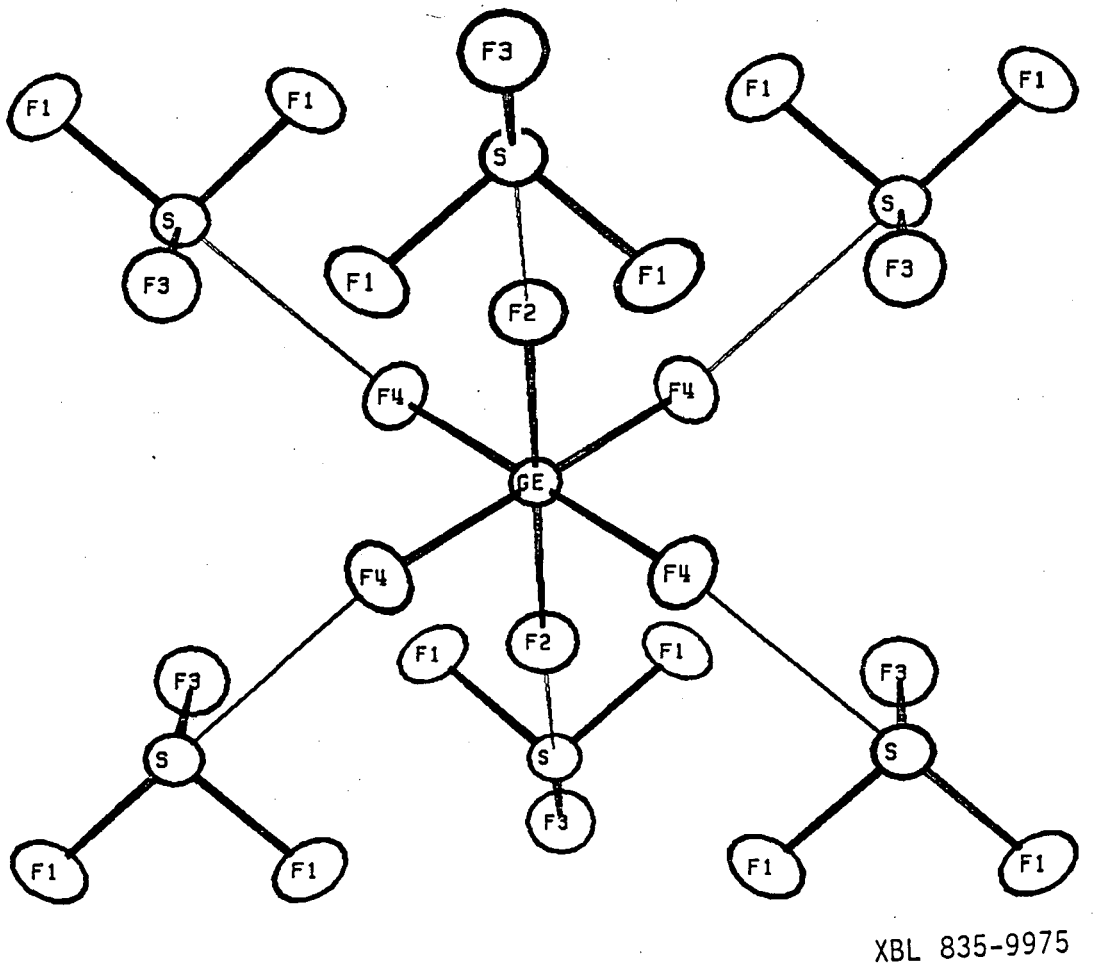

Figure III-3b. Germanium coordination environment in the $(SF_3^+)_2GeF_6^{2-}$ structure.

CHAPTER IV

CALCULATION OF THE THERMODYNAMIC STABILITY OF SOME FLUORO-CATIONS AND ANIONS

A. Introduction

In this chapter the thermochemical approach outlined in Chapter III is applied to the problem of the fluoride ion donor or acceptor power (or electron affinity) of a number of molecular fluorides. Many of these have been assessed before[1]; it is hoped however that the present results are a little more accurate, as they derive from more careful evaluations of the necessary reaction entropies and lattice enthalpies.

The derived quantities may be useful in a number of ways. For instance, the following graphite intercalation reactions are known[2,3]:

$$8C + OsF_6 \rightarrow C_8^{+}OsF_6^{-} \qquad (1)$$

$$8C + AsF_5 \rightarrow C_8AsF_5 \qquad (2)$$

It is postulated[4] that $3/2\ C_8AsF_5 \equiv C_{12}^{+}AsF_6^{-}\cdot AsF_3$. This ionic formulation will seem most reasonable if one can establish that the free energy change for the half-cell reaction:

$$3/2\ AsF_5(g) + e^{-} \rightarrow AsF_6^{-}(g) + \tfrac{1}{2}\,AsF_3(g) \qquad (3)$$

is about as exothermic as that of

$$OsF_6(g) + e^{-} \rightarrow OsF_6^{-}(g) \qquad (4)$$

This problem can be reduced to the determination of (4) and the free energy change for

$$AsF_5(g) + F^{-}(g) \rightarrow AsF_6^{-}(g) \qquad (5)$$

since the free energies of formation of AsF_3, AsF_5, and F^{-} are known and together with (5) provide the value of (3). The value of (5) may be obtained from a Born-Haber cycle representing the formation of a suitable ionic salt, $A^{+}AsF_6^{-}$, where the other terms in the cycle are

known.

B. Estimation of entropy changes

It is often the case that the enthalpy change of a reaction, $\Delta H°$, is not known. The sign of the free energy change is known from the reaction's occurrence or non-occurrence; therefore, an estimate of the entropy change will provide an upper or lower limit for $\Delta H°$. The entropies of gases or liquids involved in the reaction are often known and tabulated, and if not, they may generally be calculated by standard methods. Solids, however, are more problematic. One may measure their specific heats, but this approach is not always viable, particularly for hypothetical compounds. Two attempts were made to correlate the entropies of ionic solids with more easily calculable quantities -- the first method is entirely empirical and the second derives from the Debye approximation for a solid.

1. Correlation of $\Delta S°_{298}$ with molecular volume

It is reasonable to expect that the entropy of a solid will increase monotonically with the number of atoms per mole. This should in turn increase monotonically with the molar mass, volume, heat capacity, etc. Empirically, it is found that the molar volume and entropy are linearly related for a large number of crystalline solids; a plot of this relation is shown in figure IV-1. No mass dependence is evident in the plot, and the correlation is equally good for ionic salts and covalently bound compounds, to within 5 - 10 e.u. (this represents a TS error of 1.5 - 3 kcal mole^{-1} at 298 K). It is likewise observed that $S°_{298}$ vanishes as the molar volume goes to zero.

2. The Debye model for $S°_{298}$

Lewis and Gibson[5] found in 1917 that the specific heats of many

ionic solids obey the Debye relation[6],

$$C_v = 3Nk(T/T_D)^3 \int_0^{T_D} [e^x x^4/(e^x - 1)^2]dx,$$

where N is the number or ions per mole and T_D ($\equiv h\nu_D/k$) is the Debye temperature. The entropy is found by integrating the specific heat, $S°_T = \int_0^T (C_p/T)dT$, and substituting one finds[6]:

$$S°_T = 9Nk(\frac{T}{T_D})^3 \int_0^{T_D/T} \{-\ell n(1 - e^{-x}) + \frac{x}{e^x - 1}\}x^2 dx + \int_0^T \frac{C_p - C_v}{T} dT$$

The last term is often neglected[5], since it typically comprises about 2% of $S°_T$. Then for $T >> T_D$, the expression simplifies to

$$S°_T \approx 3Nk(4/3 - \ln(T_D/T) + \ldots) \qquad (8)$$

The Debye treatment assumes a linear dispersion relation ($\omega = cK$) for phonons in an isotropic solid, and so one obtains $T_D = hc/(2\pi k)\cdot(6\pi^2 N/V)^{1/3}$, where c is the speed of sound. For a crystal containing two kinds of ions the phonon dispersion relation for the acoustic branch near $K = 0$ is[7]:

$$\omega^2 = [2\gamma/(m_1 + m_2)]a_o^2 K^2 \qquad (9)$$

where a_o is the length of the unit cell edge, γ is the Hooke's law force constant which restores the ions to their equilibrium positions, and m_1 and m_2 are the masses of the ions. Recognizing that $d\omega/dK\ (K \to 0) = c$, we have

$$T_D = h/2\pi k[2\gamma/(m_1 + m_2)]^{1/2}(12\pi^2)^{1/3} \qquad (10)$$

The problem is then one of finding γ and combining (8) and (10) to get the entropy. The forces acting in a crystal are the gradients of the potentials, discussed in Chapter III, which comprise the lattice energy. The coulombic and dispersion forces, which tend to collapse the crystal, are balanced by the closed-shell repulsive force. These potentials, from Chapter III, are:

$$U_c = Mz^2/r_o \tag{11}$$

$$U_{dd} = C/r_o^6, \quad U_{dq} = D/r_o^8 \tag{12}$$

$$U_r = b\sum \exp[(r_i + r_j)/\rho]\exp(-r_{ij}/\rho) \tag{13}$$

For highly symmetric crystals with only one kind of nearest neighbor interaction (e.g., NaCl, CsCl, ZnS structures) the repulsive potential may be further simplified. Counting only nearest neighbor interactions,

$$U_r = B \exp(-r_o/\rho) \tag{14}$$

At the equilibrium interionic distance, r_o, the forces add up to zero:

$$0 = -B/\rho \exp(-r_o/\rho) + Mz^2/r_o^2 + 6C/r_o^7 + 8D/r_o^9 \tag{15}$$

If we consider a single ion displaced slightly from its equilibrium position in the direction of one of its nearest neighbors, and ignore the contribution of the slowly varying coulombic forces, we obtain:

$$\gamma = -2dF/dr = -2d/dr[b/\rho \exp(-r/\rho) - c/r^7 - d/r^9]_{r=r_o} \tag{16}$$

$$\gamma = 2b/\rho^2 \exp(-r_o/\rho) - 14c/r_o^8 - 18d/r_o^{10} \tag{17}$$

The restoring force arises from the closed shell repulsions; this force is damped by the dispersion forces, which tend to flatten the potential well of the ion. If we make the final approximation that the repulsive force varies much faster than the dispersion forces, then

$$\gamma \simeq 2b/\rho^2 \exp(-r_o/\rho) = \text{const. x } U_r \tag{18}$$

and substituting into (8) and (10), for a particular temperature (e.g. 298 K),

$$S°_{298} = 6R [1/2 \ln(m_1 + m_2) - 1/2 \ln(U_r)] + \text{constant} \tag{19}$$

For complex ions one must take into account the entropy arising from their symmetry numbers, so

$$S°_{298} = 3R[\ln(m_1 + m_2) - \ln(U_r) + \ln(\sigma_A\sigma_C)^{1/3}] + \text{const.} \tag{20}$$

A plot of this relation[8a] is shown in figure IV-2 for a number of

simple salts. The observed slope is 5.8 e.u., in good agreement with the expected 3R (= 5.96 e.u.). For more complex salts (such as SF_3BF_4 and ClO_2BF_4), $S°_{298}$ deviates positively from the curve, ostensibly because (14) does not hold and because the stronger dispersion forces diminish γ significantly.

The utility of equation (20) is thus limited to simple salts, for which U_r is known, with weak dispersion forces; the $S°_{298}$ vs. molecular volume correlation of figure IV-1 is more generally applicable, and was therefore used to estimate $\Delta S°_{298}$ for a number of pertinent reactions[8b], listed in Table IV-1.

Listed in Table IV-2 are estimates for lattice enthalpies, which are based on the U_L vs. volume cube root relation of figure III-2. The linear relation is:

$$U_L(\text{kcal}) = 556.3V^{-1/3}(\text{Å}^{-1}) + 26.3$$

For salts with strongly coordinating cations (e.g., SF_3^+, ClF_2^+, XeF_5^+) or very large formula unit volumes (e.g., $MF_6^+M'F_6^-$), the London energy is expected to be high and so a positive correction of 6 kcal mole^{-1} in $\Delta H°_L$ was applied; for NO^+ or O_2^+ salts, a negative correction of 4 kcal mole^{-1} (as was found for $NO^+UF_6^-$) was used.

C. Estimation of electron and fluoride ion affinities

1. Transition metal hexafluorides

The electron affinities of WF_6 and PtF_6 have been measured by a number of techniques. For WF_6 values of 104[9] and 81[10] kcal mole^{-1} have been reported; the latter derives from an I.C.R. experiment in which WF_6 is observed to capture an electron from F^- but not from Cl^- in the gas phase. Assuming that the $WF_6 + Cl^-$ reaction is genuinely endothermic, the electron affinity of WF_6 must lie between those of F and Cl (80 and

83 kcal $mole^{-1}$, respectively). The electron affinity of PtF_6 has been measured using an effusion mass spectrometer to observe ion-molecule equilibria in the gas phase[11]; this method is less precise, and a value of $EA(PtF_6)$ = 184(7) kcal is given. It is thought that the electron affinities of the third row transition metal hexafluorides increase smoothly from WF_6 to PtF_6, since they are nearly isomorphous and have a smoothly increasing nuclear charge, poorly screened by the 5d electrons, across the series. This contention[12] is borne out by the increasing ability of the later members of the series to oxidize NO, ONF, or O_2.

i) $\underline{PtF_6}$: The salt $O_2^+PtF_6^-$ sublimes in vacuo[13] between 90° and 130°C, the gas phase species being PtF_6 and molecular oxygen[14]. If we assume a vapor pressure of 2 - 5 torr at 373 K, then we have $\Delta G°_{373}$ = 9-10 kcal $mole^{-1}$ for the reaction $O_2PtF_6(s) \rightarrow O_2(g) + PtF_6(g)$. From the calculated $T\Delta S°$ (28 kcal), $\Delta H°_{L,O_2PtF_6}$ (-134 kcal), and the ionization potential of O_2 (278 kcal) we have $EA(PtF_6)$ = 181-182 kcal $mole^{-1}$.

ii) $\underline{RuF_6}$,$\underline{RhF_6}$: These compounds form dioxygenyl salts[15] which sublime readily near room temperature. By analogy to the PtF_6 case (except here $T\Delta S°$ = 22 kcal $mole^{-1}$), these are assigned an electron affinity of 175 - 176 kcal $mole^{-1}$. It is perplexing that the experimental results[15] seem to indicate that the electron affinities of RuF_6 and RhF_6 are very close. Since the screening power of the 4d electrons is quite poor, it is reasonable to expect that RhF_6 should have the higher electron affinity, by ca. 1 eV; a difference of approximately that magnitude is found (see below) for OsF_6 and IrF_6.

iii) $\underline{IrF_6}$: No dioxygenyl salt is observed[16] under several atmospheres O_2 at 298 K. This implies that $\Delta H°_{298}$ for $O_2(g) + IrF_6(g) = O_2IrF_6(s) \geq -20$ kcal $mole^{-1}$ and $EA(IrF_6) \leq 160$ kcal $mole^{-1}$.

iv) $\underline{OsF_6}$: Unlike IrF_6, OsF_6 does not react with ONF to liberate F_2 by the reaction[17]:

$$ONF + MF_6 \rightarrow NO^+MF_6^- + \tfrac{1}{2}F_2 \qquad (21)$$

For this reaction, $T\Delta S° = -18$ kcal mole^{-1} is calculated at T = 298 K. Since $\Delta H°(ONF(g) = NO^+(g) + F^-(g)) = 187$ kcal and $\Delta H°(F^-(g) = \tfrac{1}{2}F_2(g) + e^-) = 62$ kcal, using the $NO^+MF_6^-$ lattice enthalpy (-133 kcal) in a Born Haber cycle, one finds that $EA(MF_6)$ must exceed 134 kcal mole^{-1} to give $\Delta G°_{298} \leq 0$. Whether or not this is the case for OsF_6 is not resolved, since ONF and OsF_6 do react[17], not according to (21), but to give $NOOsF_7$.

v) $\underline{ReF_6}$: NO and ReF_6 combine to give the salt $NO^+ReF_6^-$, which is involatile at 298K. Assuming that the dissociation enthalpy of NO^+ReF_6 is about the same as that of $O_2^+PtF_6^-$, from the ionization potential of NO (213 kcal) and the lattice enthalpy of $NOReF_6$ (-133 kcal), we obtain $EA(ReF_6) \geq 117 - 118$ kcal mole^{-1}.

If we take the electron affinities to increase linearly from ReF_6 to PtF_6, then from $EA(ReF_6) = 117$ and $EA(PtF_6) = 182$, we obtain $EA(OsF_6) = 139$ and $EA(IrF_6) = 160$ kcal mole^{-1}. Extrapolation to WF_6 gives $EA(WF_6) = 95$ kcal mole^{-1}.

2. Fluoride ion donors

i) $\underline{XeF_6}$: The standard enthalpy of the reaction $XeF_6(g) = XeF_5^+(g) + F^-(g)$ has been measured by photoelectron spectroscopy[18] and found to be 210 kcal mole^{-1}. From the observed ease of sublimation of $XeF_5^+GeF_5^-$ at ca. 40°C, the enthalpy of the reaction:

$$XeF_6(g) + GeF_4(g) = XeF_5^+GeF_5^-(s) \qquad (22)$$

may be estimated. If the vapor pressure is 25 - 50 torr at 313 K, then $\Delta G°_{313}$ is -4 to -5 kcal mole^{-1}, and from the $T\Delta S°$ estimate in Table IV-1

(-26 kcal mole^{-1}), we calculate $\Delta H°$ = -30 kcal mole^{-1}. The calculated lattice enthalpy is -133 kcal, and the fluoride ion affinity of GeF_4 is 100 kcal (from Chapter III), and so we find $\Delta H°(XeF_6(g) = XeF_5^+(g) + F^-(g))$ =202 kcal mole^{-1}.

ii) $\underline{ClF_3}$: The enthalpy of dissociation of two salts of the ClF_2^+ ion has been measured from dissociation vapor pressure data. For

$$ClF_3(g) + BF_3(g) = ClF_2^+BF_4^-(s) \qquad (23)$$

$\Delta H°_{298}$ = -24 kcal mole^{-1} was found[19], while for the PF_6^- salt:

$$ClF_3(g) + PF_5(g) = ClF_2^+PF_6^-(s) \qquad (24)$$

$\Delta H°_{298}$ = -16 kcal has been reported[20]. The lattice enthalpies of $ClF_2^+BF_4^-$ and $ClF_2^+PF_6^-$ are estimated to be -150 and -139 kcal mole^{-1}, respectively. Since the fluoride ion affinity of BF_3 is 92 kcal (see Chapter III), and that of PF_5 is 101 kcal[21], we calculate $\Delta H°(ClF_3(g) = ClF_2^+ + F^-(g))$ = 218 kcal from the BF_3 cycle and 224 kcal from the PF_5 cycle. Since the salt $ClF_2^+GeF_5^-$ does not form when ClF_3 and GeF_4 are combined at 273 K, the enthalpy of the reaction:

$$ClF_3(g) + GeF_4(g) = ClF_2^+GeF_5^-(s) \qquad (25)$$

cannot be more exothermic than about -21 kcal mole^{-1} ($T\Delta S°$ is estimated at -23 kcal). If the lattice enthalpy of ClF_2GeF_5 is -144 kcal, then $\Delta H°(ClF_3(g) = ClF_2^+(g) + F^-(g))$ is $\geq$ 223 kcal mole^{-1}. It seems likely that the value of 218 kcal mole^{-1} derived from the BF_3 cycle is too low, since the corresponding enthalpy for $ClO_2F(g) = ClO_2^+(g) + F^-(g)$ is 217 kcal, and since ClO_2F and GeF_4 combine to form the stable salt $ClO_2^+GeF_5^-$. The lattice enthalpies of $ClO_2^+GeF_5^-$ and $ClF_2^+GeF_5^-$ cannot be very different, and their sublimation entropies must be quite close.

iii) $\underline{IF_7}$: The reaction:

$$IF_7(g) + XeF_5^+AsF_6^-(s) = IF_6^+AsF_6^-(s) + XeF_6(g) \qquad (26)$$

does not proceed spontaneously[22] at 298 K. We calculate in this case $T\Delta S° = 4$ kcal mole^{-1} and expect a lattice energy difference of 3 kcal mole^{-1} (endothermic), and so the standard enthalpy change for

$$IF_7(g) = IF_6^+(g) + F^-(g) \qquad (27)$$

must be at least 1 to 2 kcal greater than the corresponding XeF_6 dissociation enthalpy. Thus for (27), $\Delta H° \geq 204$ kcal mole^{-1}.

Since the reaction

$$IF_7(g) + GeF_4(g) = IF_6^+GeF_5^-(s) \qquad (28)$$

appears to proceed only near 0°C and under several atmospheres of GeF_4, we expect $\Delta G°_{273} \simeq +2$ kcal mole^{-1} and from $T\Delta S° = -20$ kcal we obtain $\Delta H° \simeq -18$ kcal mole^{-1}. The lattice enthalpy of $IF_6^+GeF_5^-$ is expected to be −129 kcal, and so the calculated value for $\Delta H°(27)$ is ca. +211 kcal mole^{-1}.

3. Arsenic pentafluoride

The fluoride ion affinity of AsF_5 may be evaluated by completing Born-Haber cycles for $SF_3^+AsF_6^-$ and $IF_6^+AsF_6^-$. The dissociation pressures of both of these compounds have been measured as a function of temperature; unfortunately, the accuracy of these measurements is in question, because in both experiments the compound was found to attack its container to give volatile products. For the reaction:

$$IF_7(g) + AsF_5(g) = IF_6^+AsF_6^-(s) \qquad (29)$$

$\Delta H° = -44$ kcal and $\Delta S° = 121$ e.u. were reported[23]. Such a large enthalpy change implies a fluoride ion affinity of 129 for AsF_5, using $\Delta H°_L(IF_6^+AsF_6^-) = -126$ kcal and $\Delta H°(27) = +211$ kcal. This fluoride ion affinity is undoubtedly too high, since no $ReF_7 - AsF_5$ adduct is observed at low temperature, and since the enthalpy change for the process:

$$ReF_7(g) = ReF_6^+(g) + F^-(g) \qquad (30)$$

has been reliably estimated[24] at ≤ 223(5) kcal mole^{-1}. The entropy change for (29) is expected from the $S°_{298}$ - volume correlation to be 72 e.u.; the reported value of 121 e.u. lies quite far from this expectation, as is probably in error.

When $IF_6^+AsF_6^-$ was heated to 50°C, no vapor pressure was detectable, using the pressure transmitter gauge described in Chapter III. If we take P_{323} ≤ 5 torr, then $\Delta G°_{323}$ ≤ -7.3 kcal and, from $T\Delta S°$ = -23 kcal, we calculate $\Delta H°$ ≤ -30 kcal mole^{-1} for (29). This indicates that the fluoride ion affinity of AsF_5 is ≥ 115 kcal mole^{-1}.

The enthalpy change for:

$$SF_4(g) + AsF_5(g) = SF_3^+AsF_6^-(s) \qquad (31)$$

has been reported[25] to be -31 kcal mole^{-1}, with $\Delta S°$ = 65 e.u. Since the estimated lattice enthalpy of $SF_3^+AsF_6^-$ is -134 kcal, and $\Delta H°(SF_4(g) = SF_3^+(g) + F^-(g))$ = +211 kcal (from Chapter III), we obtain a value of 108 kcal mole^{-1} for the AsF_5 fluoride ion affinity. The ca. 115 kcal value is preferred because of the problems associated with the measurement of $\Delta H°(31)$.

We are now in a position to evaluate the free energy change for:

$$3/2\ MF_5(g) + e^- = MF_6^- + \tfrac{1}{2}\,MF_3 \qquad M = P, As \qquad (32)$$

The heats of formation[26] of AsF_5, AsF_3, PF_5, and PF_3 are 295.7, 197.9, 377.2, and 228.7 kcal mole^{-1}, respectively. From the fluoride ion affinities of AsF_5 (115 kcal) and PF_5 (101 kcal), the heat of formation of F^- (-62 kcal), and the heats of formation above we calculate $\Delta H°(32)$ = -89, -128 kcal for M = P, As. Combining this $\Delta H°$ with the expected $T\Delta S°$ value (-2 kcal) we obtain $\Delta G°_{298}(32)$ = -87, -126 kcal for M = P, As. One can see that the oxidizing power of AsF_5 by this reaction is

inferior to that of OsF_6 and UF_6, which intercalate graphite spontaneously; it is significantly greater than that of ReF_6, which does not intercalate. The ready reduction[27] of graphite/AsF_6^- salts with AsF_3 (to produce AsF_5), demonstrates that the free energy change of (32) for M = As (-126 kcal $mole^{-1}$) lies very near the thermodynamic threshold for intercalation of graphite by electron oxidizers.

Summary

From existing thermodynamic data and from estimates of the appropriate reaction entropies and lattice energies, the electron and fluoride ion affinities of a number of molecular and ionic fluorides have been re-evaluated using a Born-Haber cycle approach. Estimates of the electron affinities were as follows: PtF_6, 182; RuF_6, 176; RhF_6, 176; IrF_6, $\leq$160; OsF_6, 139; ReF_6, 117 kcal $mole^{-1}$. Estimates of fluoride ion affinities gave: AsF_5, 115; XeF_5^+, 202; ClF_2^+, 223; IF_6^+, 211 kcal $mole^{-1}$.

References

1. D.D. Gibler, Ph.D. thesis, U.C. Berkeley (1973).

2. The ionic formulation is supported by measurements of the magnetic susceptibility of $C_8^+OsF_6^-$. N. Bartlett, E.M. McCarron, and B.W. McQuillan, Synth. Metals, 1, 221 (1979/80).

3. E.R. Falardeau, L.R. Hanlon, and T.E. Thompson, Inorg. Chem., 17, 301 (1978).

4. N. Bartlett, R.N. Biagioni, B.W. McQuillan, A.S. Robertson, and A.C. Thompson, J. Chem. Soc. Chem. Comm., 200 (1978).

5. G.N. Lewis and G.E. Gibson, J. Amer. Chem. Soc., 39, 2554 (1917).

6. J.E. Mayer and M.G. Mayer, "Statistical Mechanics", 2nd Ed., Wiley, N.Y. and London, 254 (1965).

7. C. Kittel, "Introduction to Solid State Physics", 3rd Ed., Wiley, N.Y. and London, 112 (1976).

8. (a) The U_r values were taken from H.D.B. Jenkins and K.F. Pratt, Proc. Roy. Soc. Lond. A, 356, 115 (1977) except for KBF_4, which was taken from Chapter III. (b) Values of $S°_{298}$ for gases were taken from the JANAF Termochemical Tables, 2nd Ed. (1971). Where data were not available, they were estimated from the entropies of isoelectronic compounds: e.g., ClO_2F ($S°_{298}$ = 68 e.u.) estimated from PF_3 (65.2 e.u.) and SOF_2 (66.6 e.u.).

9. C.D. Cooper and R.N. Compton, Bull. Am. Phys. Soc., 19, 1106 (1974).

10. P.M. George and J.L. Beauchamp, Chem. Phys., 36, 345 (1979).

11. M.I. Nikitin, L.N. Sodorov, and M.V. Korobov, Int. J. Mass. Spec. Ion Phys., 37, 13 (1981).

12. N. Bartlett, Angew. Chem. Int. Ed., 7, 433 (1968) and references

contained therein.

13. N. Bartlett and D.H. Lohmann, J. Chem. Soc., 5253 (1962).

14 M.J. Vasile and W.E. Falconer, J. Chem. Soc. Dalton, 316 (1978).

15. A.J. Edwards, W.E. Falconer, J.E. Griffiths, W.A. Sunder, and M.J. Vasile, J. Chem. Soc. Dalton, 1129 (1974).

16. N.K. Jha, Ph.D. Thesis, Univ. of British Columbia (1965).

17. S.P. Beaton, Ph.D. Thesis, Univ of British Columbia (1966).

18. J. Berkowitz, W.A. Chupka, P.M. Guyon, J.H. Holloway, and R. Sporr, J. Phys. Chem., 75,1461 (1971).

19. H. Selig and J. Shamir, Inorg. Chem., 3, 294 (1964)

20. K.O. Christe and A.E. Pavlath, Z. Anorg. Allgem. Chem., 335, 210 (1965).

21. G.L. Rosenthal, unpublished results, from measurements of the dissociation enthalpies of $ClO_2^+PF_6^-$ and $SF_3^+PF_6^-$.

22. N. Bartlett and F.O. Sladky, J. Amer. Chem. Soc., 90, 5316 (1968).

23. K.O. Christe and W. Sawodny, Inorg. Chem, 6, 1783 (1967).

24. S. Yeh and N. Bartlett, unpublished results.

25. N. Bartlett and P.L. Robinson, J. Chem. Soc., 3417 (1961).

26. A.A. Woolf, J. Fluorine Chem., 15, 533 (1980).

27. E.M. McCarron, Ph.D. thesis, U.C. Berkeley (1980) and T.E. Thompson, E.M. McCarron, and N. Bartlett, Synth. Metals, 3, 255 (1981).

Table IV-1. Calculated reaction entropies.

Reaction (S^o_{298} in parentheses)	T(K)	$-T\Delta S^o_{298}$(kcal)
$O_2(g) + MF_6(g) = O_2^+MF_6^-(s)$ (M = Ir,Pt,Ru,Rh)	298	22
	373	28
(49) (82) (57)		
$NO(g) + ReF_6(g) = NO^+ReF_6^-(s)$	298	23
(50) (82) (56)		
$XeF_6(g) + GeF_4(g) = XeF_5^+GeF_5^-(s)$	313	26
(85) (72) (75)		
$ClF_3(g) + BF_3(g) = ClF_2^+BF_4^-(s)$	298	25
(68) (61) (46)		
$ClF_3(g) + PF_5(g) = ClF_2^+PF_6^-(s)$	298	23
(68) (72) (62)		
$ClF_3(g) + GeF_4(g) = ClF_2^+GeF_5^-(s)$	273	23
(68) (72) (54)		
$IF_7(g) + XeF_5^+AsF_6^-(s) = IF_6^+AsF_6^-(s) + XeF_6(g)$	298	-4
(88) (76) (94) (85)		
$IF_7(g) + GeF_4(g) = IF_6^+GeF_5^-(s)$	273	20
(88) (72) (85)		
$IF_7(g) + AsF_5(g) = IF_6^+AsF_6^-(s)$	323	23
(88) (78) (94)		
$SF_4(g) + AsF_5(g) = SF_3^+AsF_6^-(s)$	323	26
(72) (78) (71)		
$3/2AsF_5(g) + e^- = AsF_6^-(g) + \frac{1}{2}AsF_3(g)$	298	2
(117) (5) (82) (34)		
$3/2PF_5(g) + e^- = PF_6^-(g) + \frac{1}{2}PF_3(g)$	298	2
(108) (5) (76) (31)		

Table IV-2. Calculated lattice enthalpies.

compound	formula unit volume($\AA^3$)	$-\Delta H_L^o$ (kcal/mole)
$O_2^+MF_6^-$ (M = Pt,Ir,Ru,Rh)	123	134
$NO^+ReF_6^-$	127	133
$XeF_5^+GeF_5^-$	171	133
$ClF_2^+BF_4^-$	105	150
$ClF_2^+PF_6^-$	140	139
$ClF_2^+GeF_5^-$	122	144
$XeF_5^+AsF_6^-$	193	129
$IF_6^+AsF_6^-$	214	126
$IF_6^+GeF_5^-$	193	129
$SF_3^+AsF_6^-$	162	134

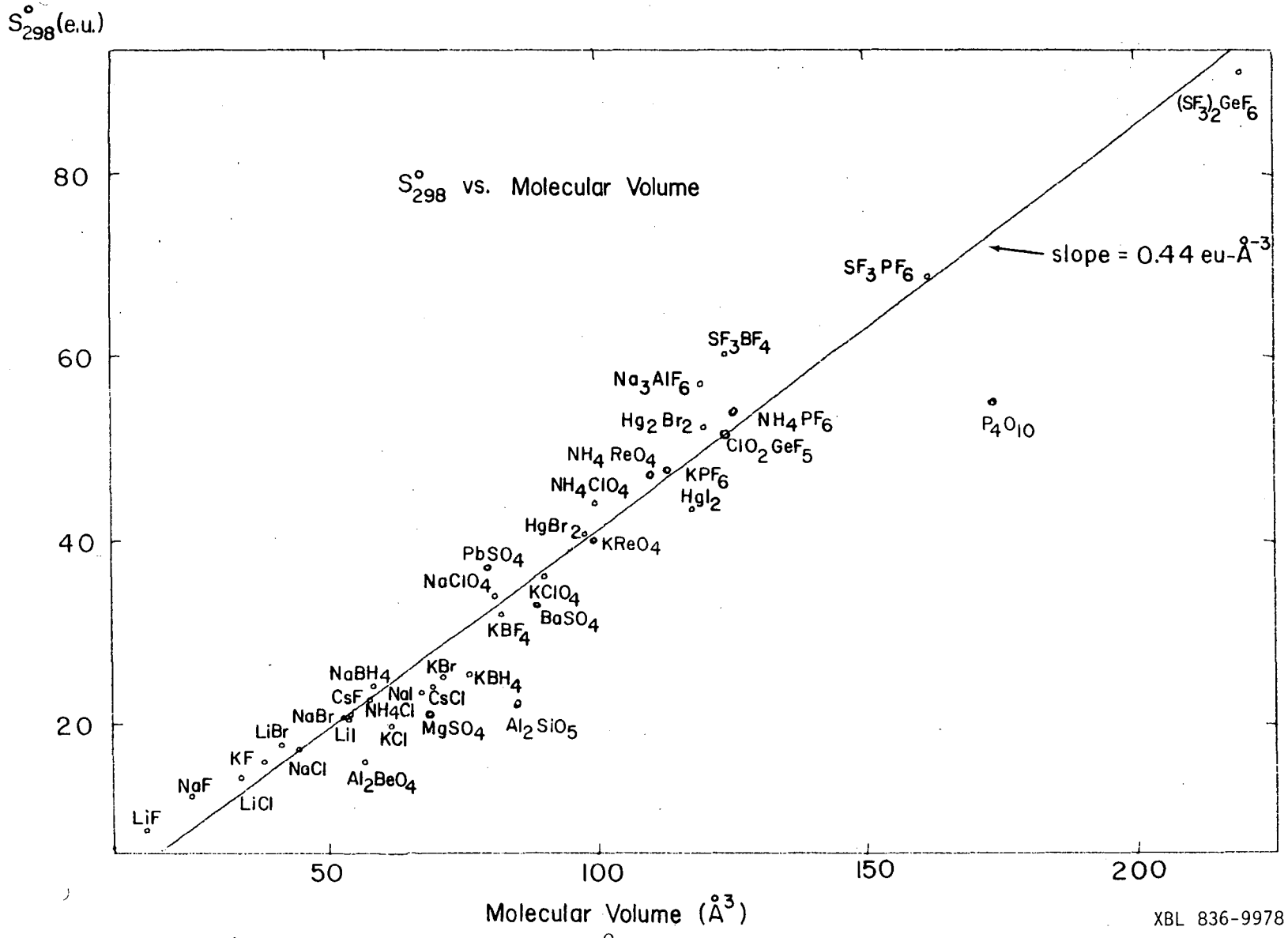

Figure IV-1. Correlation of S°_{298} with the molecular volumes of solids.

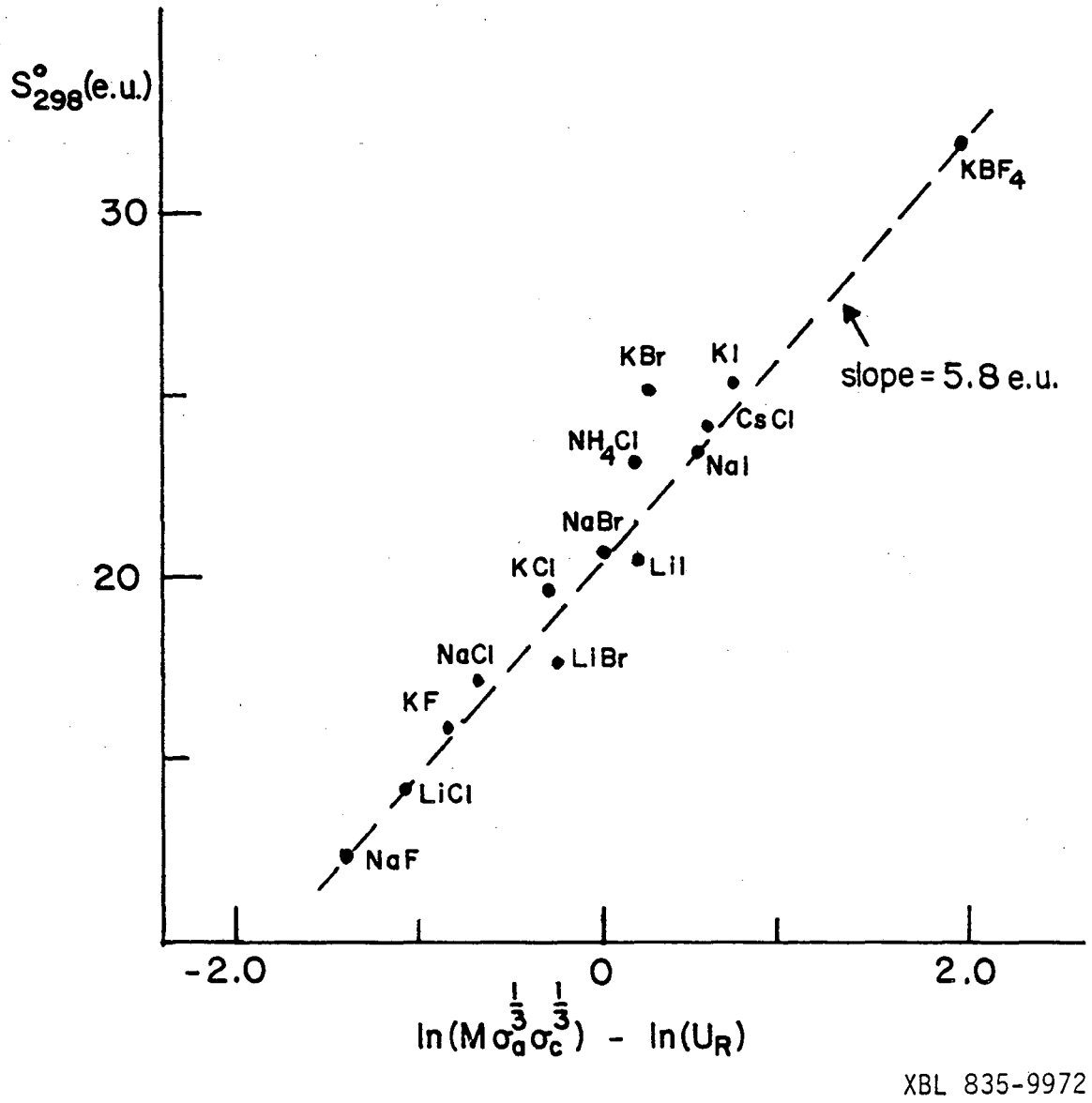

Figure IV-2. Correlation of S°_{298} with repulsion energy.

CHAPTER V

SOME NEW METAL FLUORIDE AND HYDROFLUORIDE INTERCALATION COMPOUNDS OF GRAPHITE

A. Introduction

Highly oxidized intercalation compounds of graphite have been known for quite some time[1]. These compounds were formulated as graphite salts nearly half a century ago[2]; while the controversy still rages as to its extent[3], it is clear that in most cases of oxidative intercalation, electron transfer from the graphite host to the intercalant occurs. In some cases there is as much as one electron transferred for every six or eight carbon atoms[4], and yet in this process the structural integrity of the carbon sheets is remarkably preserved; the change in the intralayer C - C distance with intercalation is seldom more that about .003 Å.

In this chapter the synthesis and properties of some new intercalation compounds are described: some metal fluoride and hydrofluoride graphite salts, and a series of graphite hydrofluorides which treads the line between a salt and a covalent compound. The latter series of compounds represents the highest degree of oxidation yet observed for carbon sheets which retain their planarity, electrical conductivity, and near constancy of the intralayer C - C distance. The bonding of fluorine to carbon in these compounds is weak and may, for most of the series, be reversed chemically (to form graphite salts) or electrochemically (to form graphite).

The graphite used in these experiments was obtained from two sources: highly ordered pyrolytic graphite (HOPG) was graciously supplied by Dr. Arthur Moore of Union Carbide, Carbon Products Division,

Parma, Ohio. This was used either in monolithic pieces (1 cm. x 1 cm. x 0.1 cm.), or in powdered form (particle size 0.1 - 0.7 mm.). Union Carbide SP-1 graphite powder (particle size ~ 0.3 mm.) was also used. Both SP-1 and HOPG powders show a high degree of order in their x-ray diffraction patterns and have hexagonal unit cell dimensions: a = 2.461(2), c = 6.706(5) Å. In all cases the graphite was heated in vacuo to a red glow and then subjected to mild fluorination (ca. 200 torr for one hour) at room temperature before intercalation. Similar experimental results were generally obtained from either HOPG powder or SP-1; however the large variation in particle size of the HOPG powder sometimes led to an inhomogeneous product.

B. Reactions of graphite with MF_x Lewis acids and fluorine

1. Graphite/SiF_4/F_2

Since the free energy change for the half-cell reaction:

$$SiF_4(g) + \tfrac{1}{2} F_2(g) + e^- = SiF_5^-(g)$$

has been estimated[5] to be about -123 kcal mole^{-1}, while that of

$$3/2\ AsF_5(g) + e^- = AsF_6^- + \tfrac{1}{2} AsF_3(g)$$

is comparable (-126 kcal, from Chapter IV), it seemed reasonable that a graphite salt of SiF_5^- or SiF_6^{2-} could be prepared. Previous attempts to prepare such salts were not successful[6].

HOPG powder (9.0 mmol) was reacted for one day at 60°C in a small (~ 10 cc volume) Monel bomb, with excess SiF_4 (4.1 mmol) and F_2(4.1 mmol); the pressure inside the bomb was estimated at 10-15 atm. The product of this reaction was a black, vacuum stable powder which contained approximately 80% carbon by elemental analysis. The x-ray powder pattern of this material established (see Table V-1) that it was a third-stage graphite salt with unit cell dimensions a = 2.463(5), c =

14.70(3) Å. SiF_4 was displaced from this powder when it was reacted with either PF_5, AsF_5, or HF.

Subsequent experiments[7] (conducted by Mr. Guy Rosenthal) established that a second stage salt could be prepared and that its composition was $C_{24}^{+}SiF_5^{-}$.

2. Graphite/AlF_3/F_2

Since AlF_3 is involatile and does not dissolve in HF or other suitable solvents, its intercalation into graphite would be expected to be hampered kinetically. However, the fluoride ion affinity of gaseous AlF_3 has been reported to be in excess of 100 kcal $mole^{-1}$. Also, intercalated fluoroaluminates might be of interest electrochemically since the $(AlF_4)_n^{n-}$, $(AlF_5)_n^{2n-}$, and AlF_6^{3-} ions all exist in salts.

Graphite is known to react with $AlCl_3$ in the presence of chlorine. Following the literature method[8], freshly sublimed $AlCl_3$ (excess) was reacted with HOPG powder (8.5 mmol), at 250°C, in a quartz reactor under 500 torr Cl_2. The excess $AlCl_3$, which sublimed to the cool end of the tube, was periodically shaken back onto the graphite. After 24 hours, the excess $AlCl_3$ was removed by sublimation. The product of the reaction was a pure second stage salt, $\underline{a}$ = 2.457(3), $\underline{c}$ = 12.79(2) Å, of composition $C_{20}AlCl_{3+\delta}$, with $\delta \sim 0.5$.

When $C_{20}AlCl_{3+\delta}$ was reacted with gaseous fluorine (2 atm.) at -78°C or at ambient temperature, fluorine uptake by the sample was slight and no change was observed in the x-ray powder pattern. At higher fluorine pressures (10-20 atm.) the reaction produced chlorine fluorides and oxyfluorides and carbon tetrafluoride as gaseous products, and graphite and AlF_3 as the solid products. The loss of aluminum halide from the graphite galleries is apparently driven by the stability of solid AlF_3;

that is, the fluoride ion affinity of solid AlF_3 is significantly inferior to that of gaseous AlF_3, the difference being the enthalpy of sublimation. This poor fluoride ion affinity thus renders $C_x^{\delta+}AlF_{3+\delta}^{\delta-}$ thermodynamically unstable relative to graphite, AlF_3, and F_2.

3. Graphite/SnF_4/F_2

The discovery[9] that both GeF_5^- and GeF_6^{2-} salts of graphite may be prepared, and the fact that $(SnF_5)_n^{n-}$ and SnF_6^{2-} ions occur in the solid state, stimulated an investigation of the graphite-SnF_4 system.

When HOPG powder is reacted with SnF_4 (dissolved in anhydrous HF, under two atmospheres F_2 pressure) or with $(NO_2^+)_2SnF_6^{2-}$ (in HF solution, with no added F_2), a blue-black material of approximate composition $C_{34}SnF_x$ is obtained. The x-ray powder pattern of this compound (Table V-2) indicates a second stage compound, $\underline{a}$ = 2.454(4), $\underline{c}$ = 11.62(5) Å. Gravimetric determinations gave x = 9-10, and so "extra" fluorine or HF is taken up by the graphite in these preparations. In accord with this observation is the presence of a non-indexable line in the x-ray powder pattern at d = 6.38 Å. This was later found to be the strongest line in the pattern of the graphite hydrofluoride $C_{2.0}F_{0.83}(HF)_{0.17}$.

The tin to fluorine atomic ratio in the graphite - SnF_x phase is uncertain. For doubly charged anions the coulombic force is greater and so a small $\underline{c}$-axis spacing is expected; thus, $C_{24}^{2+}PtF_6^{2-}$ has[4] $\underline{c}$ = 10.9 Å, and $C_{24}^{2+}GeF_6^{2-}$ has[9] $\underline{c}$ = 11.2 Å, while for $C_{24}^{+}GeF_5^{-}$, $\underline{c}$ = 11.5 Å was reported[9]. The relatively large $\underline{c}$-axis spacing of the second stage SnF_x phase may indicate $x < 6$.

No fluorine uptake is observed, nor is there any change in the x-ray powder pattern, when $C_{34}SnF_x$ is subjected to two atmospheres

pressure of fluorine for one day.

C. Intercalation compounds of graphite with HF and F_2

It is well known that graphite and fluorine do not interact at room temperature and ordinary pressures. At higher temperatures (380 - 600°C) a reaction does occur to produce the fluorides $(CF)_n$ and $(C_2F)_n$. In these lamellar compounds, fluorine atoms are known to bind covalently to the carbon atoms, which are arranged in puckered sheets[10,11]. As a consequence of the tetrahedral geometry of the carbon atoms in these sheets, $(CF)_n$ and $(C_2F)_n$ are electrical insulators.

When the reaction is catalyzed by gaseous HF, graphite does intercalate fluorine spontaneously at room temperature. The first accounts[12] of such a reaction describe the first stage compounds $C_xF_{1-\delta}(HF)_\delta$, where $3.57 < x < 4.03$ and δ was assumed to be small. Later studies[13,14] have shown that δ is appreciable (0.27 - 0.34); elemental analysis is not always performed, however, and numerous reports have appeared in the literature[15,16,17,18] of experiments involving "C_4F", and indeed "C_4F" is available commercially. The prejudice towards this stoichiometric formulation is perhaps motivated by the C_4F structure originally proposed[12] from x-ray powder diffraction; in it the fluorines are covalently bound to the carbon atoms of an apparently planar sheet, and the fluorine to carbon distance, which cannot be unequivocally determined, is assumed to be 1.4-1.5 Å. The present study has established that the composition range for first stage $C_xF_{1-\delta}(HF)_\delta$ is in fact much larger than previously described, with x varying between 1.95 and about 5 or 6.

The interaction of graphite and fluorine in liquid HF (in a quartz vessel) has been reported to result in the formation of hydrofluoride

salts[19] $C_{24n}^{+}HF_2^{-}\cdot 4HF$, where n is the stage. In the present study not these, but new hydrofluoride salts of graphite, were observed.

1. Graphite bifluorides

i) Preparation: When graphite (HOPG chips or powder, or SP-1 powder) is shaken together with fluorine (2 atm.) in the presence of excess anhydrous, liquid HF, immediate fluorine uptake and a slight warming of the HF occurs. The reaction may be followed tensimetrically: when one atom of fluorine has been taken up for every 18-20 carbon atoms, a pure third-stage compound, $C_{\sim 18}HF_2$, is obtained after pumping. Allowing more fluorine uptake, one obtains a mixture of the third and second stages, and with still more fluorine the pure second stage compound of composition $C_{11-14}HF_2$. Hydrogen analysis consistently gave H/F ratios in the range 0.46 - 0.60 for these samples.

ii) Crystal structure: The 00ℓ diffraction patterns of $C_{18}HF_2$ and $C_{12}HF_2$ prepared from HOPG chips are shown in figure V-1. Diffraction lines persist to high angle, and so it is clear that these compounds possess a high degree of ordering in the c-axis direction. From the 00ℓ intensity data the relative positions of the carbon and fluorine atoms along the z-axis were determined[20]; the observed and calculated intensities, and atomic z-parameters, are listed in Table V-3, and the structure of $C_{12}HF_2$ is depicted in figure V-2. In both structures the fluorine atoms lie nearly midway between the enclosing carbon sheets, the elevation of the fluorine atoms above the nearest carbon atom plane being about 2.8 Å. Since the sum of the van der Waals' radii of carbon and fluorine is about 3.0 Å, the structures establish that the ionic formulations $C_{12}^{+}HF_2^{-}$ and $C_{18}^{+}HF_2^{-}$ are appropriate.

X-ray powder (Debye-Scherrer) diffraction data for $C_{11.2}^{+}HF_2^{-}$ are

given in table V-4. The observed d-spacings require that the c-axis of the cell be 19.47 Å, twice that of the primitive cell required by the 00ℓ data. The ordering of the hk0 intensities is the same as in hexagonal graphite, which suggests that the superlattice is a consequence of the carbon layer stacking AB/BA/AB... (the stacking sequence is ABAB... in hexagonal graphite and ABCABC... in rhombohedral graphite). This sequence provides an equal number of A and B layers in the hk0 projection, and also accounts for the doubled unit cell with systematically absent 00ℓ, ℓ ≠ 2n and hhℓ, ℓ ≠ 2n. The fluorine atom array is likely (see section iii) to be highly disordered in the ab plane. In order to locate the fluorine atoms crystallographically, the visually estimated powder intensities must be corrected for absorption effects (which diminish the intensity of low angle lines) and for preferred orientation of the powder grains (which greatly enhances hk0 intensity relative to hkℓ and 00ℓ). In Table V-4 the visually estimated intensities for hkℓ lines are compared with those calculated assuming that only the carbon atoms contribute to the scattering (calculated hk0 intensities were arbitrarily multiplied by 4 to correct for preferred orientation). One sees that the gross features of the diffraction pattern are accounted for by this model; however, the fluorine atoms must contribute in a small way to the hkℓ scattering, perhaps because they prefer certain sites in the ab plane. The intensity data are unfortunately not of sufficient quality to distinguish these sites.

iii) ^{19}F - nmr of graphite bifluoride: The ^{19}F - nmr spectrum of a powder sample containing a mixture of the two phases, $C_{2.15}F_{0.83}(HF)_{0.17}$ and C_xHF_2 ($x \sim 12$) was run by Dr. H. Resing and coworkers[21] at a fluorine resonance frequency of 56.45 MHz. The spectrum showed both

broad and narrow-line components; the latter may be ascribed exclusively to the bifluoride phase, since ^1H spectra[22] of $C_{2.15}F_{1-\delta}(HF)_\delta$ show that the HF species contained in it undergo hindered rotation or exchange (i.e., a broadened line) at 300 K on a 360 MHz instrument; the fluorine lines of $C_{2.15}F_{1-\delta}(HF)_\delta$ are therefore expected to be broadened at room temperature and below by dipolar couplings. The narrow line component attributed to $C_{\sim 12}HF_2$ shows no broadening, even at the lowest temperature accessible in the experiment (150 K). Figure V-3a shows the narrow line; it is situated at δ = -188(1) ppm (upfield from $CFCl_3$) and has a full width at half maximum of 21 ppm. There is a marked assymetry, the low field side of the line being most intense. Since the chemical shift tensors, like the graphite lattice, must possess uniaxial symmetry, it is most reasonable to ascribe the assymetry of the peak to the two components of the chemical shift, $\delta_\parallel$ and $\delta_\perp$, of the fluorine nuclei. For a randomly oriented powder grain, the B $\perp$ $\underline{c}$ -axis orientation is twice as likely as B $\parallel$ $\underline{c}$, so the low field extremum of the peak must represent $\delta_\perp$. Similar results have been obtained[21] for first stage graphite/AsF_5, where $\delta_\parallel - \delta_\perp$ = -15 ppm, and for graphite/HSO_3F, where $\delta_\parallel - \delta_\perp$ = -80 ppm.

For the chemical shift anisotropy to be manifested in the spectrum, dipolar interactions of the fluorine nuclei and protons must by averaged away by some motional process. Complete dipolar averaging for molecular species such as bifluoride (HF_2^-) or other hydrofluoride ions (e.g., $H_2F_3^-$, $H_3F_4^-$) requires either isotropic rotation of the ions (which would average away the chemical shift anisotropy as well), or exchange of fluorine nuclei between ions; the latter preserves the shift anisotropy, provided all of the ions have a preferred orientation in the

graphite gallery. This seems to be the most plausible explanation, particularly in light of the x-ray structural data. The activation enthalpy for the exchange process must be less that about 5-6 kcal $mole^{-1}$ for the line to be narrowed by this rapid chemical exchange at 150 K. In contrast, the activation enthalpy for proton exchange in $C_{2.15}F_{0.83}(HF)_{0.17}$, which shows incipient line narrowing at 300 K, is about 11-12 kcal $mole^{-1}$.

iv) Electrical conductivity of C_xHF_2: The ab plane electrical conductivities of several graphite bifluoride samples were measured in collaboration with Dr. T.E. Thompson of SRI International, Menlo Park, Ca., using the contactless rf method[23]; the exact experimental procedure has been discussed elsewhere[4,6]. Results are presented in Table V-5 for various compositions of C_xHF_2. The per-plane conductivity is 1.4 - 2.0 times that of graphite for second-stage and roughly 5 times that of graphite for third-stage compositions. Loss of conductivity, with high concentration of (charged) guest species, has been observed in other graphite intercalation compounds[4,6].

Graphite itself is a semimetal, with a small density of electronic states at the Fermi energy (E_F) and a much higher density of states above and below E_F. The enhanced ab-plane conductivity of oxidatively intercalated graphites is generally explained in terms of the equation $\sigma = ne\mu$, where n is the number of carriers. Intercalation greatly increases the number of carriers, as E_F sinks to a region of high density of states (the sheet is doped with holes). The more the Fermi energy is displaced into the valence band, the higher the density of states, since the dispersion curve is roughly parabolic. The carrier mobility decreases, however, when the charge on the graphite sheets

becomes very high, because holes are localized in the vicinity of intercalated anions. In addition, structural distortions[4] of the sheet may arise from Fermi surface instabilities akin to the Peierls distortion in a one dimensional metal; hence the density of states again is decreased near E_F, and the number of carriers diminishes. Such distortions are known for two dimensional metals such as the group VB dichalcogenides[24]. Another explanation for the loss of conductivity at high concentrations of intercalant proposes a charging limit of $C_{\sim 20}^{+}$ which cannot be exceeded for acceptor intercalants. Past this point covalent bonds are thought to be formed between the graphite sheets and the intercalating species; concomitant out-of-plane puckering of carbon atoms is then thought to cause loss of hole mobility. This limit seems unlikely, however, in light of the $C_{12}^{+}HF_2^{-}$ and $C_{14}^{+}AsF_6^{-}$ crystal structures[26]. In neither structure does the anion approach to within bonding distance of the carbon atoms.

2. First stage graphite hydrofluorides

i) Preparation: All efforts to produce a first stage bifluoride akin to $C_{12}^{+}HF_2^{-}$ were unsuccessful. Instead, it was found that treatment of graphite powder with F_2 and liquid or gaseous HF produced, after one day of pumping, first stage hydrofluorides of the general formula $C_xF_{1-\delta}(HF)_\delta$, where $x/\delta \sim 12$ and $2 \leq x \leq 5 - 6$.

ii) Powder patterns and structure of $C_xF_{1-\delta}(HF)_\delta$: These compounds are hexagonal with nearly constant a-axis and smoothly varying c-axis dimensions; no superlattice lines are apparent in the rather simple diffraction patterns. X-ray powder data for x = 2.8 and x = 2.5, which are typical of the entire series, are presented in Table V-6. The breadth of the 00ℓ lines, and the fact that their intensity rapidly

decreases with increasing Bragg angle, suggest that the degree of ordering in the c-axis direction is poor. The c-spacing thus represents only an average interlayer distance. The relative intensities of 001 and 002 also indicate that the fluorine atoms do not lie midway between the carbon sheets.

The ordering of the hk0 intensities (these lines are sharp and persist to high Bragg angle) suggests that the layering sequence of the sheets is AAA...; however a perfect alignment of the carbon atoms, with eclipsing fluorines, does not reproduce the observed intensities, but gives I(200) > I(210). The correct ordering of the intensities (Table V-6) is obtained by displacing the fluorine atoms away for the eclipsed position by .08 Å, along the direction of the C - C bond. Equivalently, a slight displacement of some of the carbon atom density away from x,y = ±(1/3, 2/3) will give the correct ordering. This may be a consequence of small distortions away from hexagonal symmetry of the individual carbon sheets; threefold disordering of orthorhombically distorted sheets will result in the observed hexagonal diffraction symmetry.

From this structural data, it appears that the fluorine atoms are bound to carbon; unfortunately, like Rudorff[12], we cannot determine the C - F bond distance. The constancy of the a-spacing (Table V-7) and sharpness of the hk0 lines argues strongly for planar carbon sheets in the series (the case for planarity is borne out by the vibrational spectra of $C_xF_{1-\delta}(HF)_\delta$, which are discussed in section vii).

iii) Physical properties: Compounds in the series $C_xF_{1-\delta}(HF)_\delta$ are black in color and are insensitive to air and moisture, at least over a period of several days. If not thoroughly pumped, they will lose small amounts of HF on standing and so can attack glass. Preparations in the

series which were analyzed for hydrogen generally showed C/H atomic ratios of 11-12. Examples are $C_{2.05}FH_{0.18}$ (C/H = 11.6), $C_{2.70}FH_{0.22}$ (C/H = 12.3) and $C_{3.75}FH_{0.33}$ (C/H = 11.4). Warming $C_{2.05}FH_{0.18}$ at 140°C in vacuo for two days brings about the loss of some HF to give a composition $C_{2.25}FH_{0.09}$. The c-axis spacing of this heated material shrinks from 6.25 to 5.92 Å, but the a spacing remains constant at 2.464 Å. Heating to 350°C causes further c-axis contraction (to 5.65 Å) with no significant change in a.

The lattice parameters and electrical resistivities of the members of this series are shown in Table V-7. The resistivity shows a dramatic increase (by ten orders of magnitude) between C/F = 5.2 and C/F = 2, the marked upturn in ρ occurring near C/F ~ 2.7. Near the high ρ end of the series, the a-spacing expands by ~ 0.01 Å, indicating a slight weakening of the C - C bond at these compositions. For conducting members of the series, C/F $\geq$ 2.3, the logarithm of the resistivity was found to decrease slightly with increasing temperature, the activation energy for carrier generation being on the order of .005 eV for C/F = 3.7 and .02 eV for C/F = 2.4. Such behavior is characteristic of a semimetal or a doped semiconductor. The most likely doping mechanism is through creation of holes by forming HF_2^- ions; unfortunately, Hall effect measurements, which could distinguish between the two conduction mechanisms, were not performed.

iv) XPS spectrum of $C_{2.5}F_{1-\delta}(HF)_\delta$: X-ray photoelectron spectra were recorded by Dr. K.D. Bomben and Prof. W.L. Jolly, using a freshly cleaved sample of $C_{2.5}F_{1-\delta}(HF)_\delta$, which had been prepared by exhaustive fluorination (2 weeks) of an HOPG chip in the presence of liquid HF. The binding energies obtained (reported here relative to the C 1s level

of a graphite standard, 284.2 eV) are compared in Table V-8 to those of other compounds. The binding energy of fluorine in this sample is intermediate between that of fluorine in LiF and fluorine in teflon or $(C_2F)_n$. This suggests that the fluorine bears a partial negative charge and that the C - F bond herefore has semi-ionic character. The carbon binding energy indicates that the bulk of the carbon resembles carbon in graphite, and not in $(C_2F)_n$ or teflon where the carbon coordination geometry is tetrahedral.

v) <u>^{19}F and ^{1}H nmr spectra of $C_{2.15}F_{0.83}(HF)_{0.17}$</u>: The ^{19}F nmr spectrum, recorded by Resing and coworkers[21], is shown in figure V-3b. It consists of a single broad resonance line, centered at -188 ppm relative to $CFCl_3$, upon which is superimposed the narrow line resonance of some $C_{12}^{+}HF_2^{-}$ in the sample. The broad line shows no sign of motional narrowing at 300 K; a gaussian fit to the temperature independent lineshape of the broad line indicates a fluorine second moment of 4.4 gauss^2. The magnitude of the second moment may be derived from the structure by the van Vleck formula[28], which is a summation in r^{-6} of the interactions between dipolar nuclei in the solid. The presence of both fluorine and hydrogen in the $C_{2.15}F_{0.83}(HF)_{0.17}$ phase unfortunately limits the utility of the measurement, since many possible structures will give rise to the observed second moment. It is clear, nevertheless, that the fluorine nuclei do not undergo motional averaging at 300 K.

The proton spectrum of a sample of $C_{2.15}F_{1-\delta}(HF)_{\delta}$ which was free of $C_{12}^{+}HF_2^{-}$ was recorded by Dr. K. Zilm, and is shown in figure V-4. The width of the proton line (37 ppm) may be ascribed to dipolar interactions which are, at 300 K, beginning to be averaged away by

hindered rotation or exchange of the proton-containing species. The activation enthalpy for this process is about 11-12 kcal $mole^{-1}$.

It is clear that the HF in $C_xF_{1-\delta}(HF)_\delta$ interacts strongly with the host lattice. The most likely HF binding mechanism is through hydrogen bonds to the C - F fluorines which appear, from the XPS, to bear a partial negative charge. Two other models for HF interaction also seem plausible: binding of the HF fluorine to carbon or formation of ionic species, such as HF_2^-, in the galleries. In the case of the former model, we expect the ratio of aromatic to C - F carbon atoms in $C_{2.05}F_{0.82}(HF)_{0.18}$ to be 1.05:1 (1.6(2):1 was found -- see section vi). For the latter model, formation of a large concentration of anions in the galleries, and equivalent hole concentrations in the carbon sheets, should give rise to electronic conduction in $C_{2.05}F_{0.82}(HF)_{0.18}$. The observed resistivity of this compound is however in excess of 10^7 Ω - cm.

vi) <u>^{13}C nmr of $C_xF_{1-\delta}(HF)_\delta$</u>: ^{13}C nmr spectra of powders for which C/F = 3.70 and C/F = 2.05 were run by Drs. B.L. Hawkins and G.E. Maciel of the Regional NMR Facility, Colorado State University, Fort Collins, Colorado. The technique used was that of $^{19}F \rightarrow {}^{13}C$ cross-polarization (which greatly enhances the ^{13}C signal and at the same time removes the ^{19}F scalar and dipolar couplings) and magic angle spinning (which averages out chemical shift anisotropy). The pulse sequences used were standard[29]: a 90° pulse, followed by a ^{19}F spin-locking (and decoupling) pulse causes the ^{19}F magnetization to decay with a characteristic time $T_{1\rho}$. The ^{13}C spins are brought into contact with the ^{19}F spins, and so magnetized, by supplying a pulse which satisfies the Hartmann-Hahn double resonance condition[30] for a time t (the cross-polarization

interval). Since the characteristic cross-relaxation time of the ith carbon spin, T_{CF}^{i}, depends on the strength of the dipolar coupling with its ^{19}F nearest neighbors, the observed spectral intensity, which depends on $T_{1\rho}$, t, and T_{CF}^{i}, will be sensitive to the distance between C_i and the nearest fluorine atoms.

A representative spectrum is shown in figure V-5. For both C/F ratios (3.70 and 2.05), two peaks, separated by 47 ppm, are observed; the similarity of the spectra suggests that the same bonding environments are found in both compounds. The low field peak (δ = +135 ppm relative to TMS) shows spinning sidebands, displaced ± 97 ppm from the central peak, which indicates a large chemical shift anisotropy for these carbons. This chemical shift and shift anisotropy are characteristic of aromatic (i.e., graphite-like) carbons. The high field peak is attributed to carbon atoms which are attached directly to fluorines. In addition to these, a small peak at 112 ppm may be resolved in some of the spectra. This peak is attributed to a small concentration of $>CF_2$ carbon atoms, which are probably located at the surface of the powder grains. The infrared spectrum (section vii) also shows evidence of these $>CF_2$ groups.

The ratio of the two kinds of carbon, their T_{CF}'s, and the fluorine $T_{1\rho}$, may be determined by varying the contact time t. Figure V-6 shows the spectrum of $C_{2.05}F_{0.82}(HF)_{0.18}$ as a function of contact time. Note that the high field peak is magnetized more quickly than the graphitic peak, indicating direct attachment of fluorine. The magnetization of the ith carbons is given by[31]:

$$M_i = kN_i[1 - T_{CF}^{i}/T_{1\rho}]^{-1}[\exp(-t/T_{1\rho}) - \exp(-t/T_{CF}^{i})]$$

where N_i is the relative concentration of the i spins and k is an

instrumental constant. A six-parameter fit gives the cross-relaxation times and the ratio of the two kinds of carbon from the integrated intensities (Table V-9). The fit is quite good for the high field peak; for the graphitic peak, a satisfactory fit can only be obtained from the superposition of approximately equal concentrations of spins with short (0.40(5) msec) and long (2.49(8) msec) values of T_{CF}. The ratio of graphitic to non-graphitic carbons in $C_{2.05}F_{0.82}(HF)_{0.18}$ is 1.6(2):1, close to the expected 1.50, assuming that the HF is not bound to carbon or present as HF_2^-. This indicates that the carbon atoms which are bonded to fluorine do not do so via three-center, four electron F-C-F bonds (a model which would account for the semi-ionic character of the F - C bond), but instead attach to a single fluorine atom.

The ^{13}C nmr spectra are consistent with a structure like that proposed by Rudorff for tetracarbon monofluoride[12]. The persistence of graphitic carbon, even at C/F ratios as low as two, suggests that delocalized π-bonding is maintained in the carbon sheets.

vii) Vibrational spectra of $C_xF_{1-\delta}(HF)_\delta$: Transmission infrared spectra of $C_{2.5}F_{1-\delta}(HF)_\delta$ were recorded by Mr. Morgan P. Conrad. The sample was prepared by grinding a chip of Nasa graphite in such a way that the c-axis lay in the plane of the resulting thin flake. This arrangement exploits the high conductivity anisotropy of graphite and its compounds; electromagnetic radiation may be transmitted through the graphite provided its electric vector is aligned parallel to the c-axis. The flake was intercalated by reaction with fluorine and HF vapor, and the resulting i.r. spectrum is shown in figure V-7. An enormous absorption, centered at about 1090 cm^{-1}, is attributed to C - F stretching. Comparison with the C - F stretching frequencies in $(CF)_n$

and $(C_2F)_n$, which are 1219 and 1221 cm^{-1}, respectively, indicates a C - F bond order of slightly less than unity. Bands situated at 1587 and 850 cm^{-1} are assigned to C - C stretching and carbon out-of-plane motions; these vibrations, also found in the Raman spectra (below), are known for graphite itself and occur at practically the same frequency[32]. The 1270 band, which lies in the C - F stretching region, may arise from a small concentration of $>CF_2$ groups at the surface of the chip.

Raman spectra (figure V-8) were recorded from powdered samples for several compositions. The spectra are all virtually identical to the spectrum of graphite powder[32], except that the Raman relative of the 850 cm^{-1} i.r. band is seen (at 839 cm^{-1}), and a broad band at 1355 cm^{-1} is also observed. Such a band is seen in graphite powder which is poorly ordered or which has been disordered by grinding, and has been attributed to a Brillouin zone boundary mode which is Raman inactive in crystallites of large extent[33]; it is essentially an in-plane ring-breathing vibration. The intensity of this band relative to the graphite E_{2g}-like band at ~ 1600 cm^{-1} indicates the extent of the ordered domains in the ab plane, which is in the range of 50 to 100 Å. The intensity of the C - F stretching band is expected to be weak, and it is in fact only barely discernable in the spectra. A slight shifting (~ 30 cm^{-1}) towards lower frequency of the ~ 1600 cm^{-1} band is found for the highest fluorine concentrations, indicating a very slight weakening of the C - C bond, in accord with the increased bond distance (by .006 Å) inferred form the crystallographic a-spacings. The Raman spectra establish, by the presence of only graphite-like modes, even at a C/F ratio of two, that the planarity of the carbon sheets in

$C_xF_{1-\delta}(HF)_\delta$ is maintained.

viii) Bonding and electronic structure in $C_xF_{1-\delta}(HF)_\delta$:

The vibrational spectra of $C_xF_{1-\delta}(HF)_\delta$, together with structural information gleaned from x-ray and nmr data, indicate that the carbon atoms which are bound to fluorine lie in virtually undistorted, planar carbon sheets. These carbon atoms must still make nearly full use of their p_z orbitals in π-bonding within the sheet; still, the p_z orbital must be used to bind the fluorine atom. The bonding molecular orbital composed of fluorine sp hybrid and carbon p_z atomic orbitals is still of appropriate symmetry to overlap with the neighboring carbon p_z orbitals, and so the π-bonding persists; the wavefunctions of the π-electrons are nevertheless strongly perturbed by the deep potential well at the C - F carbon. Detailed band structure calculations[34] for C_4F, which assume a C - F bond distance of 1.4 Å, show that this perturbation gives rise to an energy gap of ~ 2 eV between the valence and conduction bands. For higher concentrations of fluorine the energy gap must increase, and so the metal to insulator transition may be rationalized. The persistence of a black color in $C_2F_{1-\delta}(HF)_\delta$ is probably a consequence of the fact that a structural defect occurs every 50 - 100 Å in the basal plane, disrupting the band structure. These defects are however separated by relatively large areas of insulator, and so do not give rise to conduction.

Since some of the electron density of the C - F bond is required to maintain the nearly constant C - C π-bond order, the effective C - F bond order is reduced from unity; this effect is manifested in the low C - F stretching frequency and the chemical lability of the C - F bond (see part 4). Since the van der Waals' diameter of fluorine is about

2.7 Å, it is likely that the occurrence of two C - F linkages on the same side of the sheet in meta positions would be sterically disfavored; the closest F - F contacts in such an arrangement would be only 2.46 Å. A possible structure for the ideal limiting stoichiometry C_2F is shown in figure V-9a. In this structure each carbon sheet has orthorhombic symmetry. Such a sheet may distort, with alternating single and double bonds (figure V-9b), to produce a puckered sheet. An alternative C_2F structure (figure V-10) cannot distort in this way, but in it each fluorine atom has two fluorine nearest neighbors at 2.46 Å. The details of the fluorine atom placement in C_2F are thus still uncertain.

3. HF - deficient second-stage compounds

When gaseous HF and fluorine are reacted with graphite for a short time a material of approximate composition $C_{8.8}F_{0.60}(HF)_{0.40}$ is produced. X-ray powder data for this compound (Table V-10) show that it consists of more than one phase, the dominant phase being characterized by a broad 00ℓ line at d = 4.3 Å and a series of sharp hk0 lines, indexed to a 2 × a hexagonal superlattice. The tentative interpretation of this data is that this is a second stage compound, c = 8.6 Å, akin to first stage $C_xF_{1-\delta}(HF)_\delta$, in which fluorine is attached to only one side of the carbon sheet.

Figure V-11 shows a possible structure for the ideal composition C_8F in the hk0 projection. The cell has the correct superlattice, and the fluorines will all scatter in phase for the 110 reflection, which is observed as a line of medium intensity in the powder pattern (the intensity of this superlattice line probably has no carbon component). AA stacking of carbon sheets across a gallery and AB stacking of

contiguous carbon sheets (as in the $C_{12}^{+}HF_2^{-}$ structure) gives the observed ordering I(220) > I(200).

When $C_{8.8}F_{0.60}(HF)_{0.40}$ is reacted with liquid HF and is subsequently pumped out, the x-ray diffraction pattern shows a mixture of second and third stage graphite bifluorides.

4. Chemical and electrochemical reactions of graphite hydrofluorides

i) Intercalation reactions: Both first and second stage graphite hydrofluorides undergo intercalation reactions with strong Lewis acids such as AsF_5, GeF_4, and PF_5. The reaction of graphite bifluoride ($C_{12}^{+}HF_2^{-}$) with GeF_4 (1 atm.) is sluggish, and a mixture of second and third stage compounds is formed. If the pressure is increased to about 10 atm., a pure first stage compound, a = 2.455(3), c = 7.83(2) Å is obtained, in which the C/Ge ratio is about 8. Reaction with PF_5 under similar conditions gives only compounds of high stage ($\geq$ 3). AsF_5 intercalates in stoichiometric quantities[26] to give $C_{12}AsF_6 \cdot HF$, a first stage salt, with c = 8.0 Å. Apparently quite a strong Lewis acid is required in order to expand the graphite galleries and at the same time abstract a fluoride ion from HF_2^{-}.

First stage $C_xF_{1-\delta}(HF)_\delta$ reacts with GeF_4 and AsF_5 under 10 atm pressure to produce first stage compounds, c ~ 8.0 Å. The amount of Lewis acid taken up is limited by the value of x, and for x $\simeq$ 2 no reaction, even with AsF_5, is observed. No reaction with AsF_3 was observed, for 2 $\leq$ x $\leq$ 3, and the reaction with water to produce HF, graphite, and (presumably) O_2 is extremely slow. Compounds in this series swell in anhydrous, liquid HF; the c-axis spacing increases by 0.5 to 0.6 Å, even at $C_{2.0}F_{1-\delta}(HF)_\delta$. This increase represents an

additional volume of 1.3-1.4 $Å^3$ per carbon atom, or about one HF molecule for every 11-14 carbons. The diffraction patterns show no discernable change in the presence of HF, except for this increase in c.

ii) Electrochemical reversibility: The enthalpy of formation of tetracarbon monofluoride has been estimated to be about -44 kcal per mole of fluorine atoms[35]; thermodynamically, it should be a potent oxidizer, readily reduced by even the most electronegative metals. For example, $\Delta H°_f$ for PbF_2 is -160 kcal $mole^{-1}$. Assuming the entropy changes are small, the C,C_4F couple is then expected to be 2.1 V below the Pb,PbF_2 couple in the electrochemical series. Previous work has established[17,36] that the potential of this couple is near the thermodynamically expected value for compounds with C/F ratios ≥ 4.

In the present study it was found that for C/F ratios > 2.3, graphite hydrofluorides and bifluorides may be reduced electrochemically. The open circuit potential (using HF/NaF as the electrolyte), against Pb,PbF_2, for $C_xF_{1-\delta}(HF)_\delta$ were determined as follows (x in parentheses): (3.7), 2.03; (2.7), 2.2; (2.5), 2.38 V. The cell used for these measurements consisted of a teflon "T" union connected via compression fittings to two glassy carbon electrodes approximately 1 mm. in diameter (Atomergic Chemetals Corp., Plainview, N.Y.), and to the electrolyte reservoir. The two electrode compartments were separated by a wad of porous teflon filter membrane (Chemplast, Inc., Wayne, N.J.).

With a resistive load in series, it was possible to assess the internal resistance of the cell using a variety of electrolytes and counterelectrodes (Table V-11). Note that the internal resistance is by far the lowest when the electrolyte is HF. This is undoubtedly a

consequence of the fact that HF enters the graphite galleries readily and may assist strongly in the removal of fluoride as HF_2^-, $H_2F_3^-$, etc. It is superior in this respect to H_2O, which is a weaker Lewis acid, and which cannot attach a fluoride ion to make a planar anion.

The intercalation of fluorine was found to be completely reversible for C/F ratios in excess of 2.3. Compounds in the series $C_xF_{1-\delta}(HF)_\delta$ could be prepared electrochemically from graphite, using PbF_2 as a source of fluoride ion, and a driving potential of 3.0 V (for $x < 2.6$, the electrochemical synthesis is impracticable, possibly because an insulating surface layer (i.e., $x \simeq 2.2$) is formed on the powder grains). Compounds so synthesized have diffraction patterns identical to those prepared from graphite, HF, and F_2. Chips of $C_{2.5}F_{1-\delta}(HF)_\delta$ and $C_{12}^+HF_2^-$, when placed in a large excess of powdered graphite and HF, were reduced completely to graphite (this arrangement is essentially a shorted electrochemical cell). In figure V-12 the powder diffraction patterns of these chips before and after reduction are compared with that of SP-1 graphite. While the reduction is quite complete in both cases, the second stage bifluoride is reduced to a graphite which is well ordered; the product of the $C_{2.5}F_{1-\delta}(HF)_\delta$ reduction shows disorder (probably in the stacking sequence of the sheets).

Carefully carried out electrochemical experiments on the graphite hydrofluorides may lead to thermodynamic information as yet not revealed. In the present work, well ordered graphites with large particle grains were always used, in order that x-ray studies would provide structural information. Poorly ordered graphites of sub-micron particle size, however, hold the most promise for dynamical studies which require proximity to electrochemical equilibrium, and for workable

electrochemical cells.

Summary

Both SiF_4 and SnF_4 have been found to intercalate graphite in the presence of fluorine. HF and fluorine are intercalated together into graphite to produce the bifluorides $C_{12}^{+}HF_2^{-}$ and $C_{18}^{+}HF_2^{-}$; the structures of these compounds indicate that they are ionic salts. The ^{19}F n.m.r. spectrum reveals that rapid exchange of fluorine between anions occurs in $C_{12}^{+}HF_2^{-}$.

For compounds in the series $C_xF_{1-\delta}(HF)_\delta$, the c-axis dimension and resistivity vary smoothly, the latter by ten orders of magnitude, between x = 5-6 and x = 2. Vibrational and n.m.r. spectra, together with x-ray structural data, establish that the carbon atom sheets are planar and nearly isodimensional with those of graphite. Fluorine atoms are found to eclipse carbon atoms in the structure making weak, two center C - F bonds. HF is present in the structure and binds to these fluorine atoms via weak hydrogen bonds.

The fluorination of graphite, to produce the bifluorides or $C_xF_{1-\delta}(HF)_\delta$, is chemically and electrochemically reversible for $x \geq 2.3$.

References

1. P. Schauffautl, J. Prakt. Chem., 21, 155 (1841).

2. A Frenzel and U. Hoffmann, Z. Elektrochem., 40, 511 (1934).

3. J.E. Fischer, J. Chem. Soc. Chem. Comm., 545 (1978).

4. N. Bartlett, E.M. McCarron, B.W. McQuillan, and T.E. Thompson, Synth. Metals, 1, 221 (1979/80).

5. M.K. Murphy and J.L. Beauchamp, J. Amer. Chem. Soc., 99, 4992 (1977) estimate the enthalpy change to be -130 kcal $mole^{-1}$; $-T\Delta S°$ at 298 K is about 7 kcal $mole^{-1}$.

6. E.M. McCarron, Ph.D. Thesis, U.C. Berkeley (1980).

7. G.L. Rosenthal and N. Bartlett, to be submitted for publication.

8. W. Rudorff and R. Zeller, Z. Anorg. Allgem. Chem., 279, 182 (1955).

9. E.M. McCarron, Y.J. Grannec, and N. Bartlett, J. Chem. Soc. Chem. Comm., 890 (1980).

10. W. Rudorff and G. Rudorff, Z. Anorg. Allgem. Chem., 253, 281 (1947).

11. Y. Kita, N. Watanabe, and Y. Fujii, J. Amer. Chem. Soc., 101, 3832 (1979).

12. W. Rudorff and G. Rudorff, Chem. Ber., 80, 417 (1947).

13. R.J. Lagow, R.B. Badachhape, P. Ficalora, J.L. Wood, and J.L. Margrave, Synth. Inorg. Met. Org. Chem., 2, 145 (1972).

14. R.J. Lagow, R.B. Badachhape, J.L. Wood, and J.L. Margrave, J. Chem. Soc. Dalton, 1268 (1974).

15. C.A. Wilkie, G.Y. Lin, and D.T. Haworth, J. Sol. St. Chem., 30, 197 (1979).

16. D.T. Clark and J. Peeling, J. Polymer Sci., 14, 2941 (1976).

17. M.S. Wittingham, J. Electrochem. Soc., 122, 1288 (1975).

18. K. Brauer and K.R. Moyes, U.S. Pat. 3,514,337 (1970).

19. W. Rudorff, Z. Anorg. Allgem. Chem, 254, 319 (1947).

20. The diffraction geometry and the computer program used to solve the structure are described by R.N. Biagioni, Ph.D. thesis, U.C. Berkeley (1980).

21. L.G. Banks, H.A. Resing, M.J. Moran, P. Brant, and G.R. Miller, unpublished results.

22. K. Zilm, private communication.

23. C. Zeller, A Denenstein, and G.M.T. Foley, Rev. Sci. Instr., 50, 602 (1979).

24. J.A. Wilson, F.J. DiSalvo, and S. Mahajan, Phys. Rev. Lett., 32, 882 (1974), and Adv. Phys., 24, 117 (1975).

25. J.E. Fischer, A. Metrot, P.J. Flanders, W.R. Salaneck, and C.F. Brucker, Phys. Rev. B, 23, 5576 (1981).

26. F. Okino and N. Bartlett, to be submitted for publication.

27 "Handbook of Photoelectron Spectroscopy", G.E. Muilenberg, Ed., Perkin-Elmer Corp., Eden Prairie, Minn. (1978).

28. J.H. van Vleck, Phys. Rev., 74, 1168 (1948).

29. For a simple description of the CP-MAS experiment, see C.A. Yannoni, Acc. Chem. Res., 15, 201 (1982).

30. S.R. Hartmann and E.L. Hahn, Phys. Rev., 128, 2042 (1962).

31. M. Mehring, "High Resolution NMR in Solids", Springer-Verlag, Berlin (1976).

32. S.A. Solin, Physica, 99B, 443 (1980).

33. F. Tuinstra and J.L. Koenig, J. Chem. Phys., 53, 1126 (1970).

34. N.A.W. Holzwarth, S. Rabii, and S.G. Louie, Phys. Rev. Lett., in press.

35. J.L. Wood, R.B. Badachhape, R.J. Lagow, and J.L. Margrave, J. Phys. Chem., 73, 3139 (1969).

36. F. Beck, W. Kaiser, and H. Krohn, Angew. Chem. Suppl., 57 (1982).

Table V-1. X-ray powder data for third stage graphite fluorosilicate.

intensity	$1/d^2$(obs.)	$1/d^2$(calc.)	hkl
vs	.0743	.0740	004
w	.0902	--	---
m, broad	.1170	.1156	005
w, broad	.1646	.1666	006
s	.2202	.2197	100
ms, broad	.2383	.2382	102
w, broad	.2973	.2961	008
w, broad	.3854	.3863	106
s	.6595	.6593	110

s = strong, m = medium, w = weak, v = very

hexagonal, $\underline{a}$ = 2.463(5), $\underline{c}$ = 14.70(3) Å

Table V-2. X-ray powder data for second stage graphite fluorostannate.

intensity	$1/d^2$(obs.)	$1/d^2$(calc.)	hkl
mw	.0245	---	---*
vw	.0308	.0296	002
vs, broad	.0691	.0666	003
mw	.0891	.0889	graphite 002
m, broad	.1169	.1185	004
m	.2218	.2214	100
m	.6642	.6643	110

*d = 6.38 Å

hexagonal, $\underline{a}$ = 2.454(5), $\underline{c}$ = 11.62(5) Å

Table V-3. Observed and calculated 00ℓ diffraction intensities for graphite bifluorides.

second stage, $\underline{c}$ = 2 x 9.44Å			third stage, $\underline{c}$ = 12.78Å		
ℓ	I(obs.)	I(calc.)	ℓ	I(obs.)	I(calc.)
2	63	84	1	50	63
4	245	196	2	40	60
6	1000	1000	3	122	178
8	-	3	4	1000	1000
10	89	51	5	3	13
12	197	100	6	-	<1
			7	46	56
			8	85	98

Atomic parameters:

second stage			third stage		
atom	multiplicity	z	atom	multiplicity	z
C	6.00	±.0905 ±.4095	C	3.00	0
F	1.08	±.2375 ±.2625	C	6.00	±.266
			F	1.00	±.485

Isotropic temperature factors ($\beta_C = \beta_F = 1$) were used. No absorption correction was applied to the data.

Table V-4. Powder diffraction data for $C_{11.2}HF_2$.

$1/d^2$(obs.)	$1/d^2$(calc.)	hkl	I(obs.)	I(calc.)
.0954	.0950	006	vvs	1000
.2218	.2204	100	ms	92
.2309	.2310	102	w	8
.2438	.2441	103	s	115
.3170	.3154	106	vw	21
.3809	.3800	0012	w	66
.4352	.4342	109	vw	31
.6626	.6613	110	s	156
.7020	.7035	114	vw	24
.7554	.7563	116	m	61
.8868	.8844	201	w	2
.9043	.9055	203	vw	9
1.0299	1.0413	1112	w	42
1.5430	1.5431	210	w	20
1.5657	1.5668	213	mw	37

The hk0 intensities were multiplied by 4 to correct for preferred orientation. The carbon atom parameters used in the calculation were: $\pm(0,0,z)$; $\pm(1/3,2/3,z)$; $\pm(0,0,\frac{1}{2}-z)$; $\pm(1/3,2/3,\frac{1}{2}-z)$, where z = .0878. The fluorine atoms were located at $z = \pm \frac{1}{4}$ and were given large anisotropic temperature factors so that they would contribute only to the 00ℓ reflections.

Table V-5. a-b plane electrical conductivity of graphite bifluorides.

composition	stages present	$k/k_{graphite}$*
$C_{15.9}HF_2$	2nd, 3rd	1.4
$C_{13.5}HF_2$	2nd	1.4
$C_{12.5}HF_2$	2nd	2.0
$C_{14.5}HF_2$	2nd	1.8
$C_{18.1}HF_2$	3rd	4.8

*Conductivity per plane of carbon atoms, relative to the basal plane conductivity of HOPG. These values are obtained by multiplying the specific conductivity ratio ($\sigma/\sigma_{graphite}$) by t_o/t, the ratio of the sample thickness before intercalation to that after intercalation.

Table V-6. X-ray powder diffraction patterns for first stage $C_x F_{1-\delta}(HF)_\delta$.

C/F = 2.84				C/F = 2.49				
int	$1/d^2$(obs)	$1/d^2$(calc)	hkl	int	$1/d^2$(obs)	$1/d^2$(calc)	hkl	I(calc)*
vs	.0316	.0322	001	vvs	.0277	.0277	001	-
vvw	.1292	.1287	002	vvs	.2204	.2209	100	1000
s	.2212	.2210	100	vs	.6618	.6626	110	340
ms	.6624	.6631	110	w	.8855	.8835	200	22
vvw	.6893	.6953	111	mw	1.5553	1.5461	210	41
vw	.8851	.8842	200	mw	1.9944	1.9878	300	36
				w	2.6525	2.6504	220	24
				vw	2.8603	2.8713	310	5
$\underline{a}$ = 2.456(3), $\underline{c}$ = 5.57(3) Å				$\underline{a}$ = 2.457(3), $\underline{c}$ = 6.01(5) Å				

*The radiation source was MoK_α. hk0 intensities were calculated using for carbon, x,y = ±(1/3,2/3) and for fluorine, x,y = ±(.365,.635). No corrections were made for absorption or thermal motion.

Table V-7. Some physical properties of $C_xF_{1-\delta}(HF)_\delta$.

C/F ratio	$\underline{a}$ (Å)	$\underline{c}$ (Å)	resistivity (Ω-cm)
5.2*	2.456(3)	5.22(2)	$> 8 \times 10^{-3}$
3.67	2.459	5.36	8×10^{-1}
3.20	2.456	5.45	3×10^{0}
2.70	2.460	5.71	2×10^{1}
2.49	2.457	5.90	1×10^{3}
2.42	2.459	6.02	1×10^{3}
2.15	2.468	6.22	1×10^{7}
1.94	2.466	6.45	2×10^{7}

*Contains some $C_{12}^{+}HF_2^{-}$, which is highly conductive.

Table V-8. XPS binding energies of $C_{2.5}F_{1-\delta}(HF)_{\delta}$ and comparison materials.

compound	C 1s, eV	F 1s, eV	reference
$C_{2.5}F_{1-\delta}(HF)_{\delta}$	284.6	686.6	present work
$(C_2F)_n$	288.5 290.4	689.3	11
$(CF_2)_n$	291.8	689.1	27
LiF	--	684.9	27
Graphite	284.2	--	27

Table V-9. Observed and calculated ^{13}C n.m.r. intensities for $C_{2.05}F_{0.82}(HF)_{0.18}$.

	low field peak		high field peak	
contact time (ms)	I(obs)	I(calc)	I(obs)	I(calc)
0.10	285	189	867	674
0.20	351	338	902	910
0.50	627	623	1000	1000
1.00	788	818	915	926
2.00	906	890	754	784
5.00	729	715	432	475
10.00	348	361	181	206
20.00	166	72	76	39

low field carbons: $T_{CF}^{1} = 0.40(5)$ ms, $N_1 = .78(10)$

$T_{CF}^{2} = 2.49(8)$ ms, $N_2 = .79(10)$

high field carbons: $T_{CF} = 0.10(2)$ ms, $N = 1.00$

fluorine $T_{1\rho} = 6.0(5)$ ms

Table V-10. X-ray powder diffraction data for $C_{8.8}F_{0.60}(HF)_{0.40}$.

intensity	$1/d^2$(obs.)	$1/d^2$(calc.)	hkl
s, broad	.0550	.0540	002
m	.0971	.0980	$C_{12}HF_2$, 006
w, broad	.1189	--	?
m	.1659	.1654	110
s	.2207	.2205	200
m, broad	.2417	.2450	$C_{12}HF_2$, 103
w, broad	.3931	.3920	$C_{12}HF_2$, 0012
vs	.6607	.6615	220
w, broad	.7142	.7155	222
mw, broad	.7579	.7595	$C_{12}HF_2$, 116
w	.8837	.8820	400

$\underline{a}$ = 2 x 2.459, $\underline{c}$ = 8.6 Å

Table V-11. Characteristics of some electrochemical cells with $C_{2.7}F_{1-\delta}(HF)_{\delta}$ cathodes.

anode	electrolyte	voltage(OCV)	internal res.(kΩ)*
Li wire	$PC/LiClO_4$	4.4 V	25
Li wire	PC/KPF_6	4.3	15
Al foil	HF/NaF	1.7	4
Al foil	H_2O/NaF	1.5	100
Al foil	$PC/LiClO_4$	1.7	25
Pb/PbF_2	HF/NaF	2.2	2
Hg	HF/NaF	1.9	5
Ag	HF/NaF	1.0	2

*The cell configuration is described in the text.

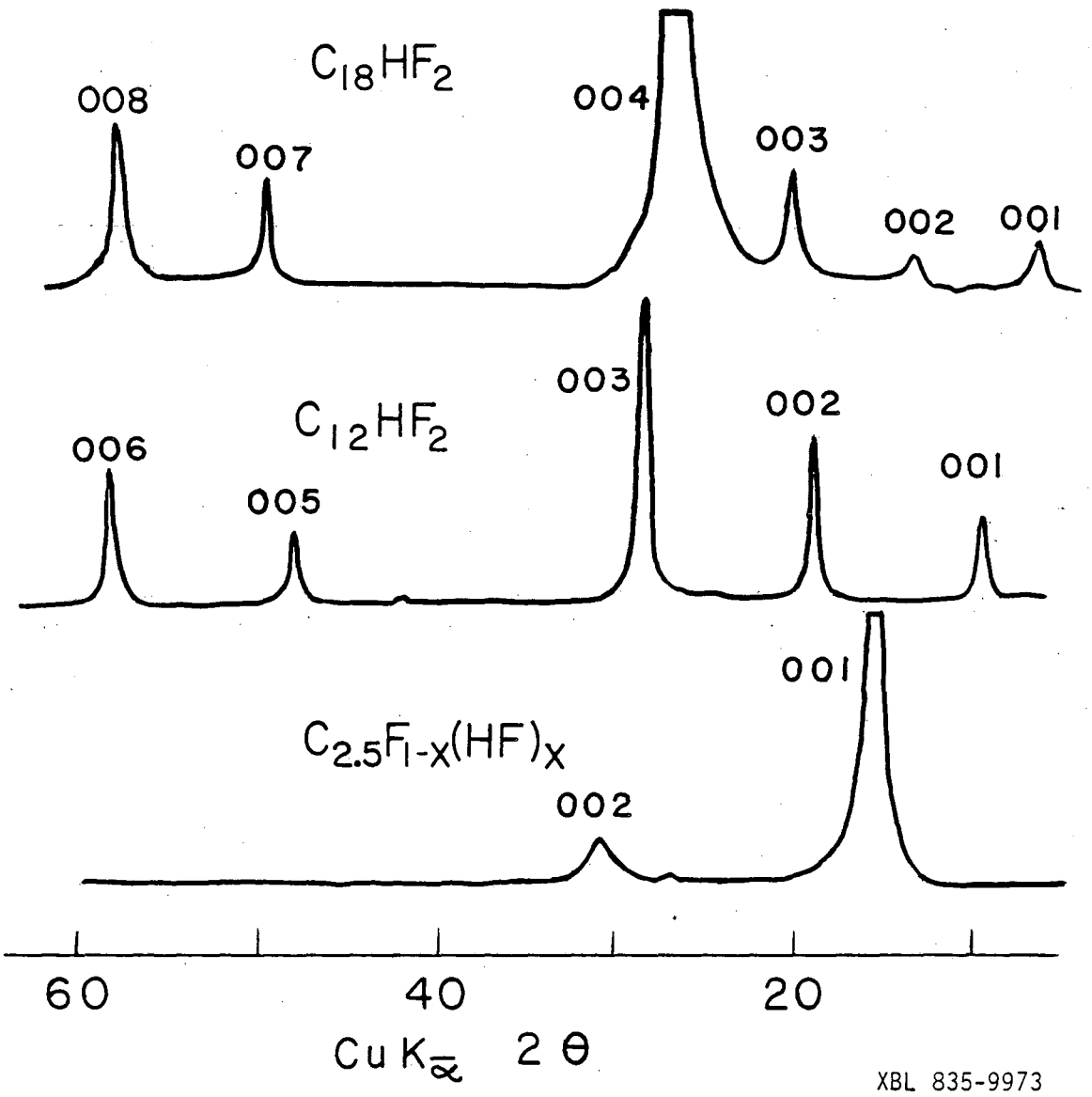

Figure V-1. X-ray diffractometer tracings for graphite hydrofluorides.

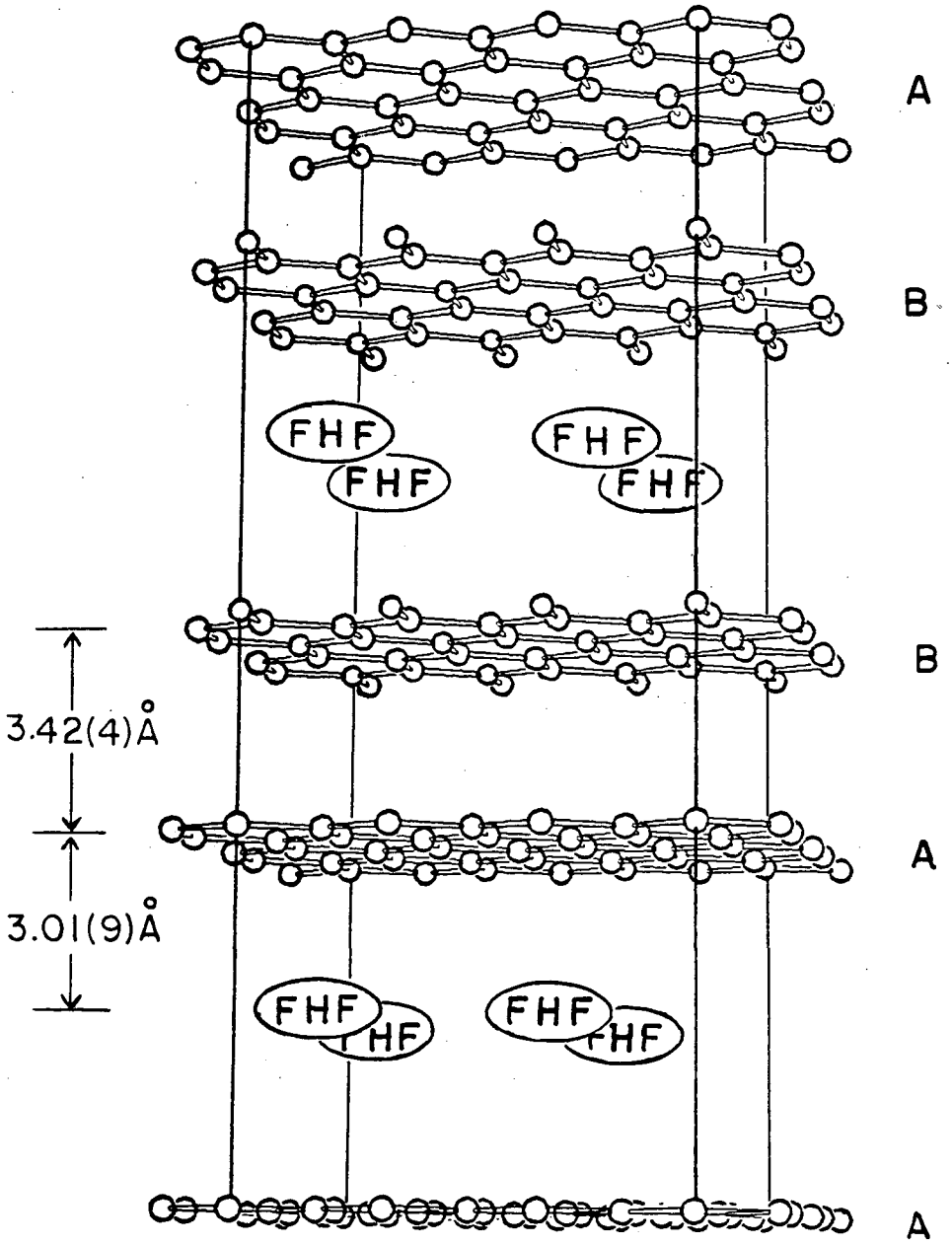

Figure V-2. The crystal structure of $C_{12}^{+}HF_2^{-}$.

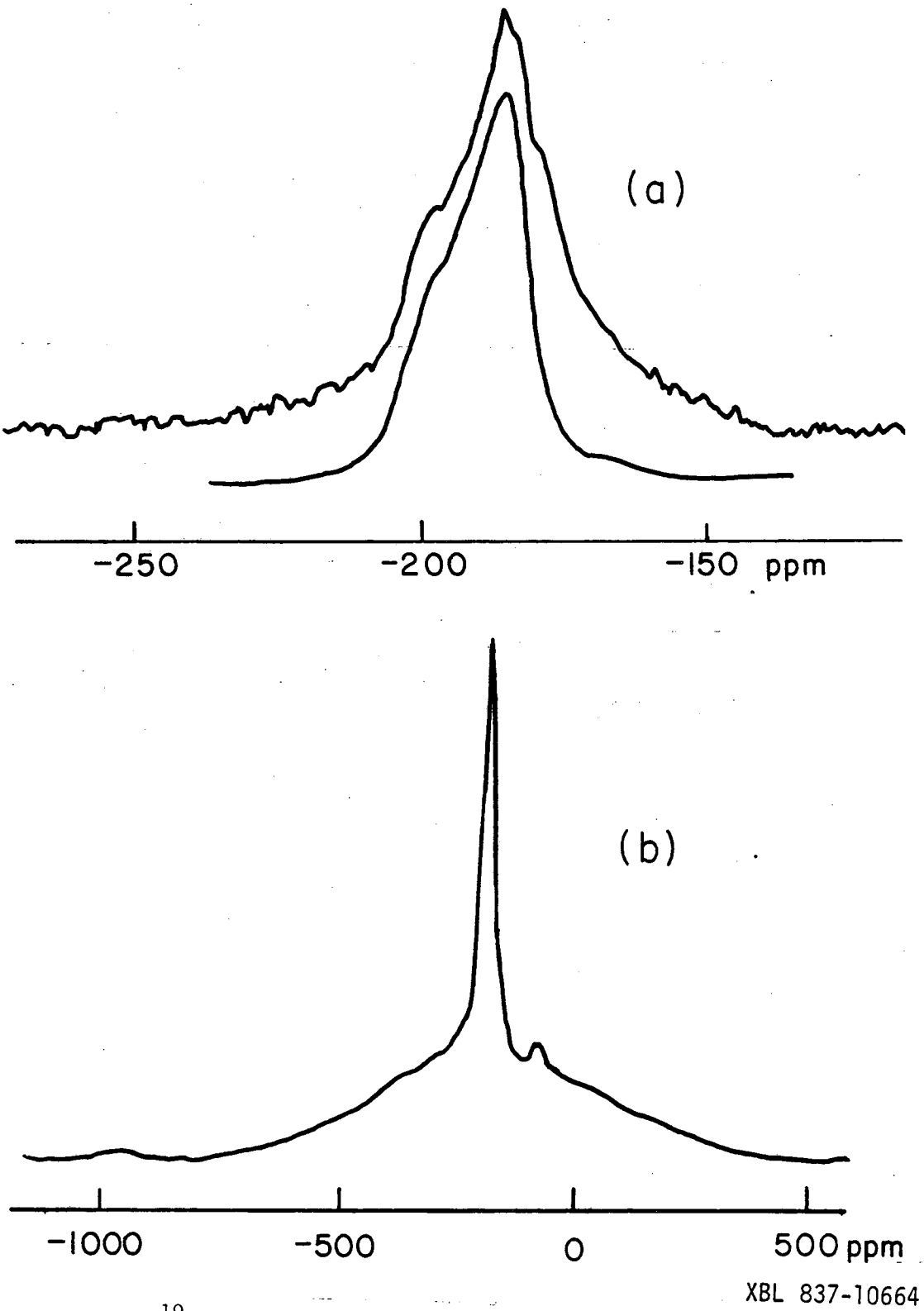

Figure V-3. ^{19}F nmr spectra of graphite hydrofluorides: (a) narrow line attributed to $C_{12}HF_2$, (b) full spectrum showing the $C_{2.15}F_{0.83}(HF)_{0.17}$ broad line.

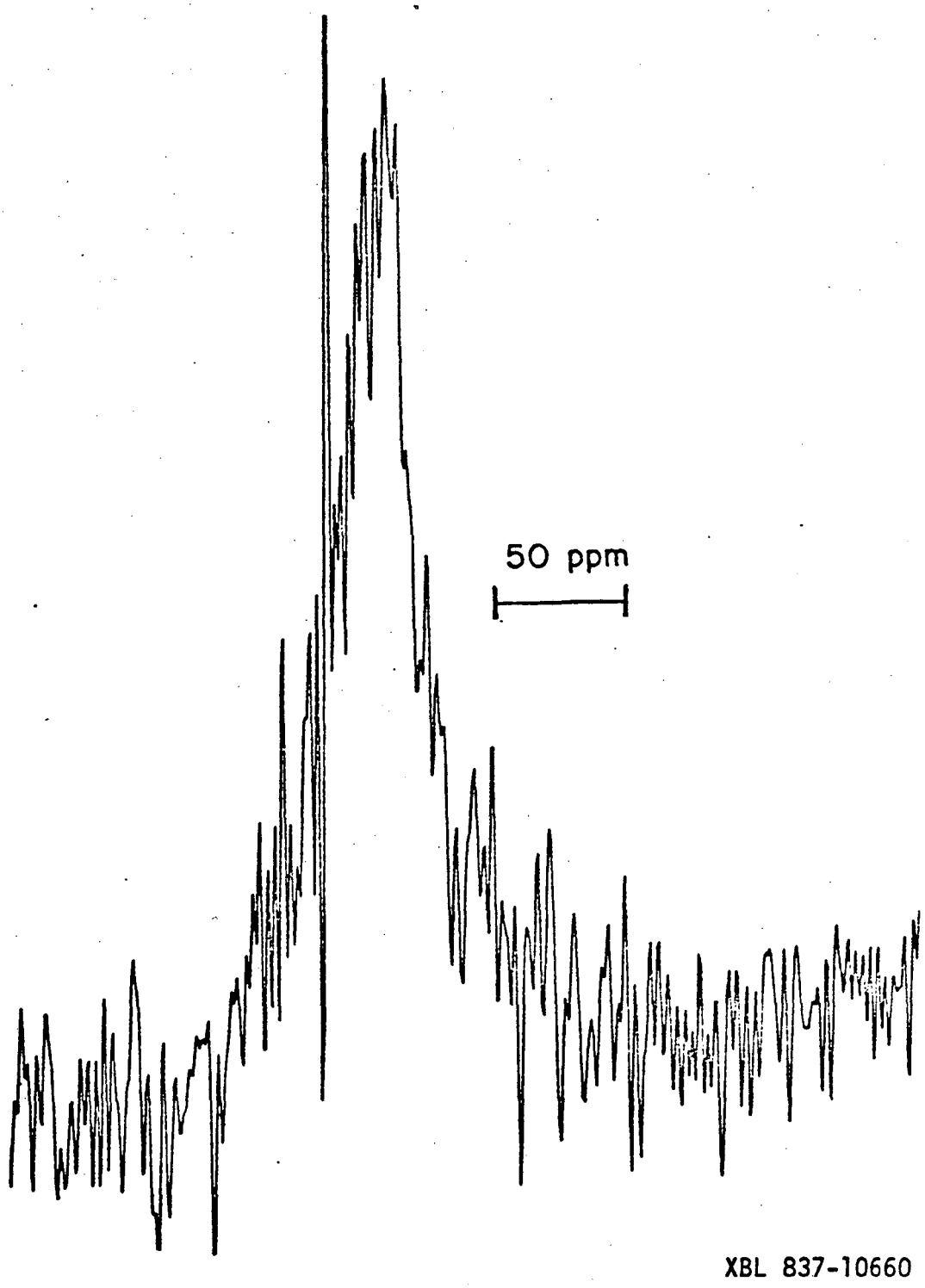

Figure V-4. Proton nmr spectrum of $C_{2.15}F_{0.83}(HF)_{0.17}$.

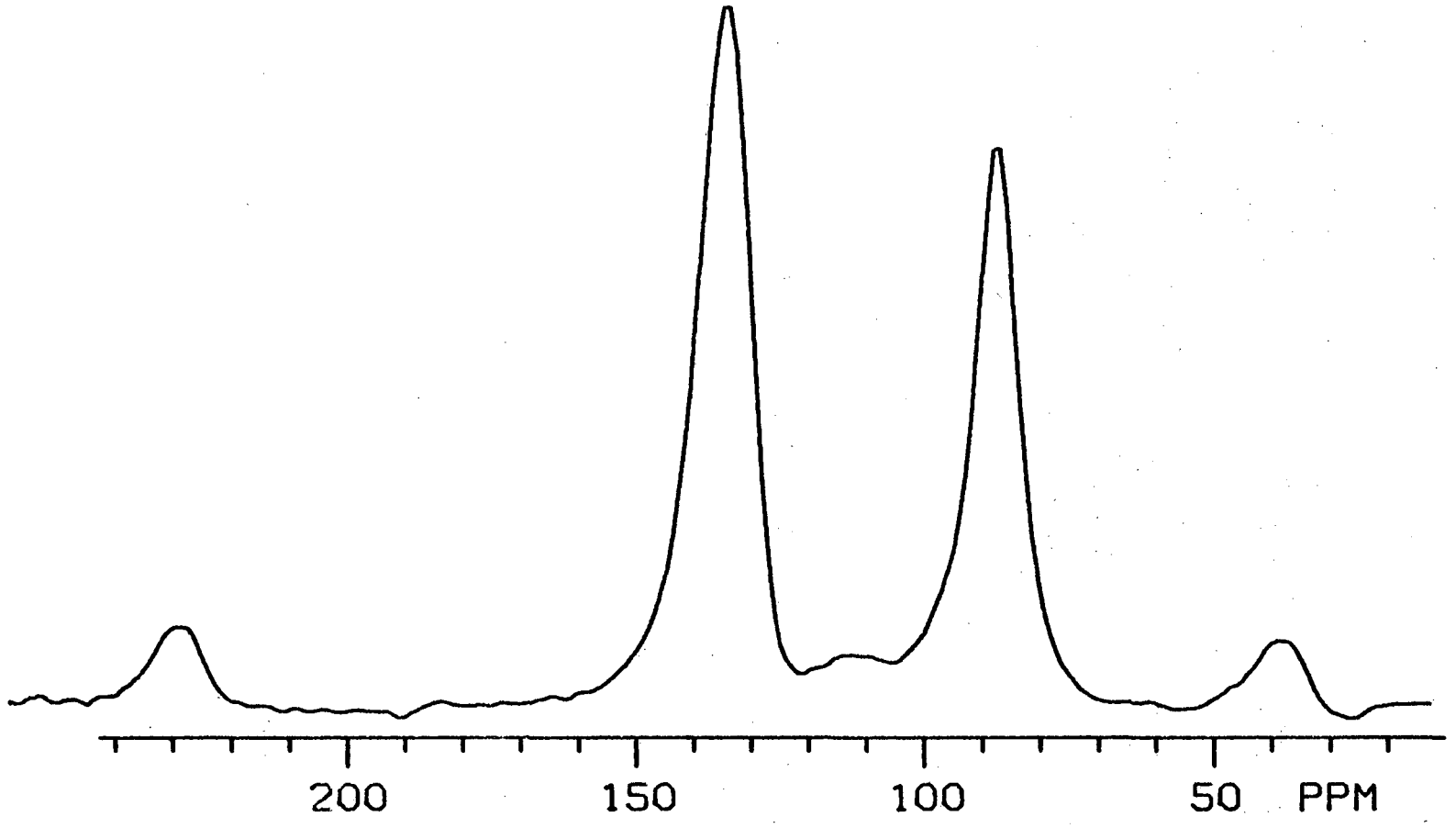

XBL 837-10659

Figure V-5. ^{13}C nmr spectrum of $C_{2.05}F_{1-\delta}(HF)_{\delta}$.

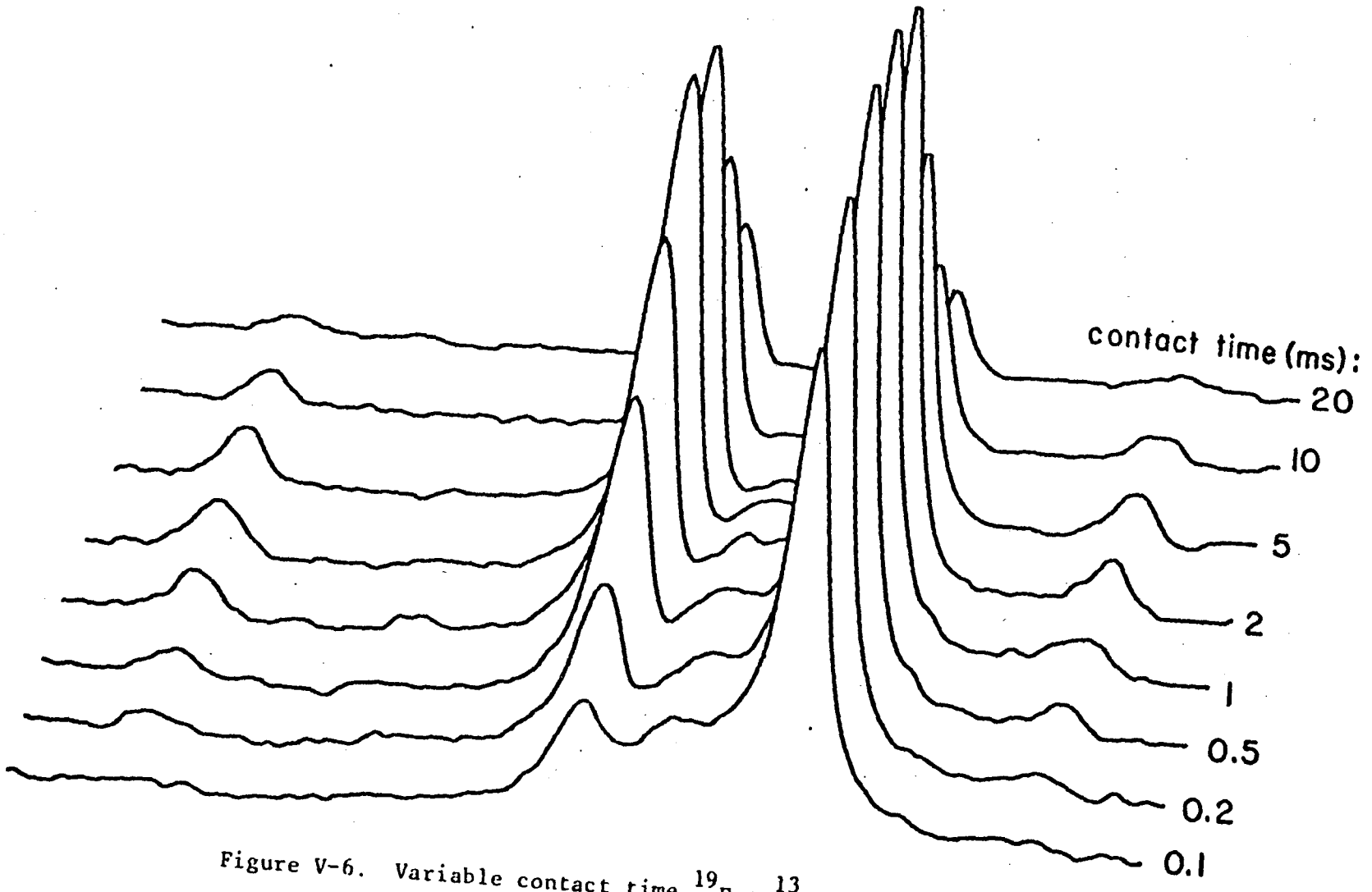

Figure V-6. Variable contact time $^{19}F \rightarrow {}^{13}C$ cross-polarization nmr spectra of $C_{2.05}F_{1-\delta}(HF)_{\delta}$.

XBL 837-10661

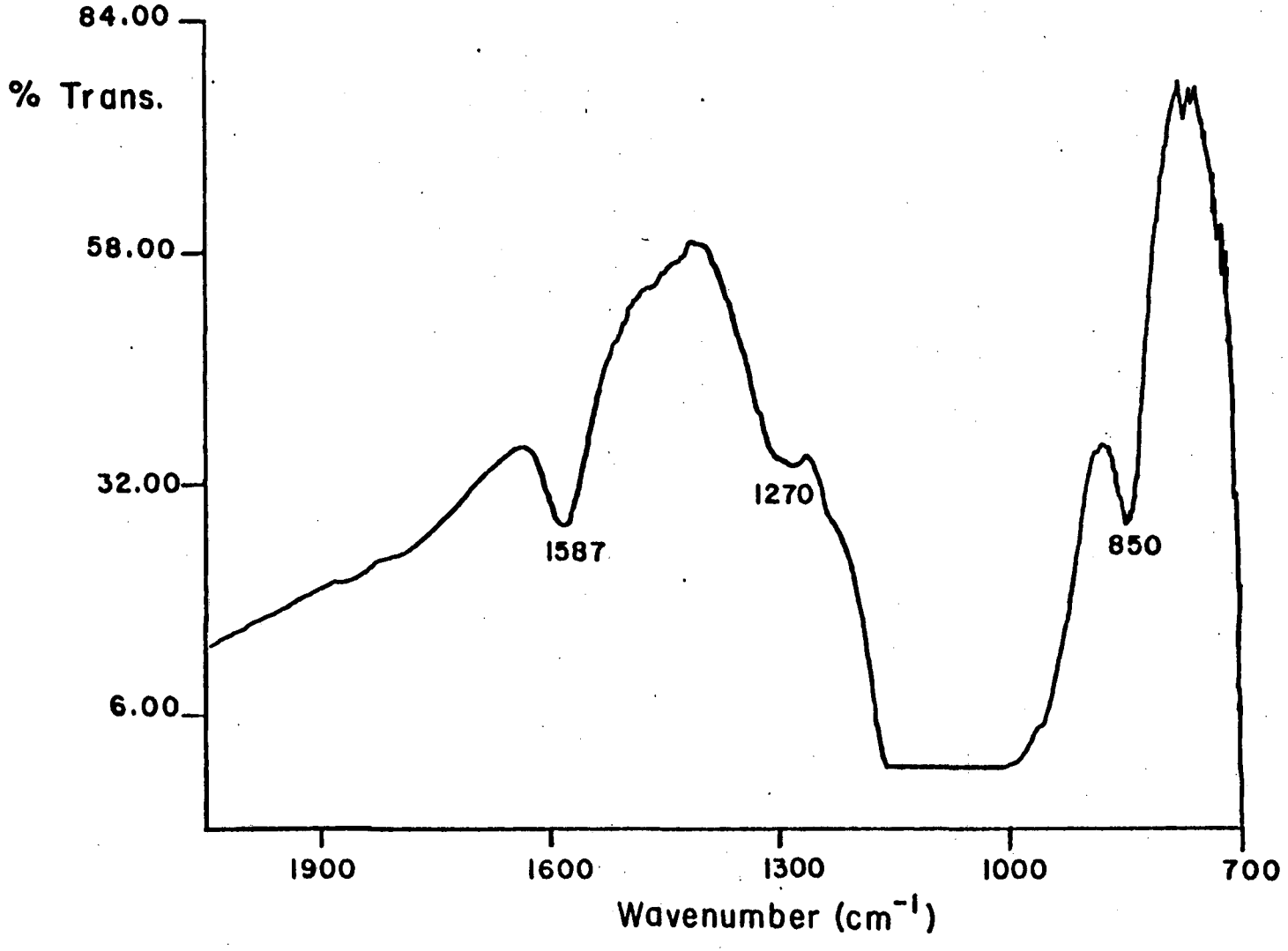

XBL 837-10662

Figure V-7. Infrared spectrum of $C_{2.5}F_{1-\delta}(HF)_{\delta}$.

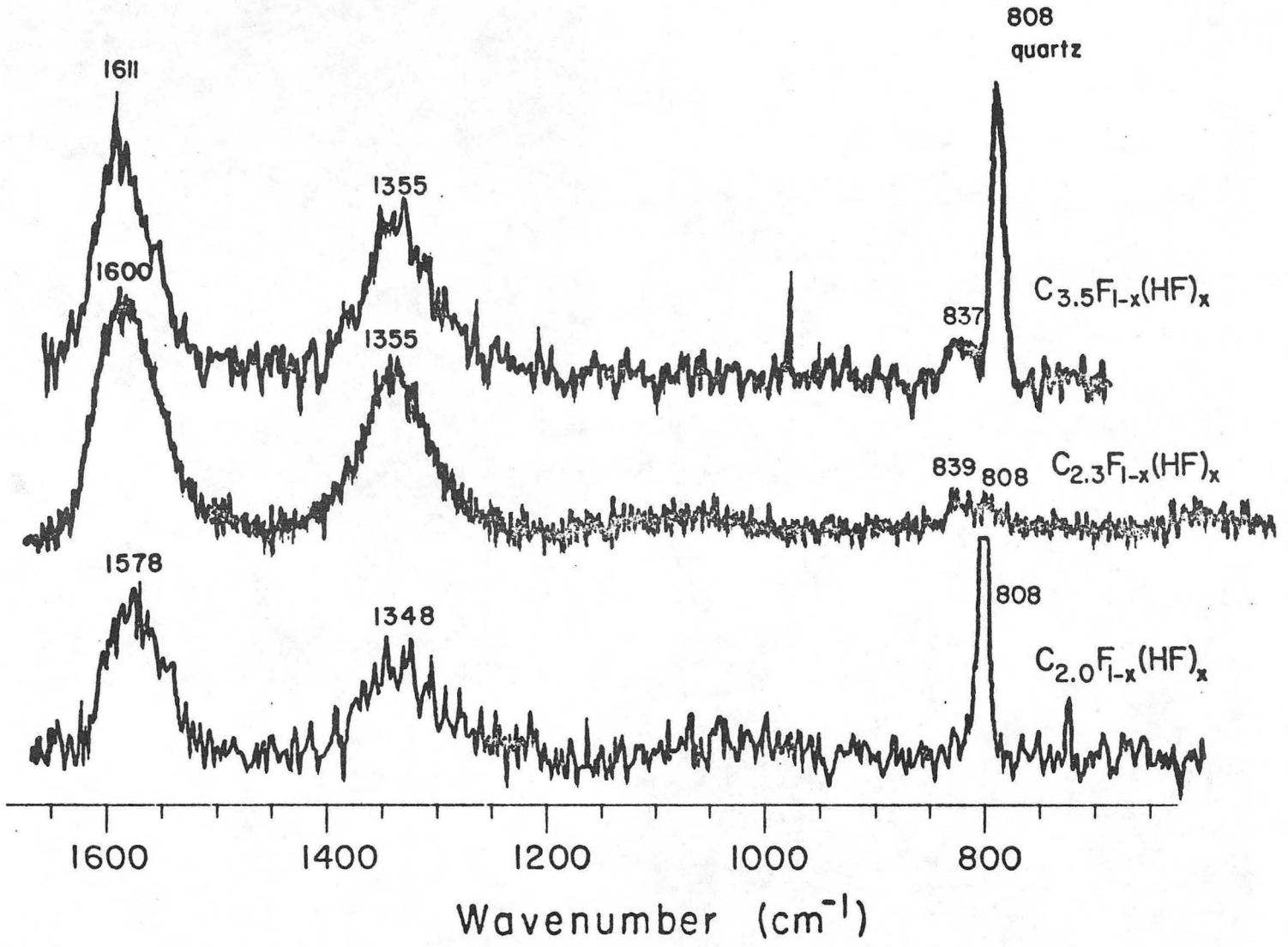

XBL 835-9969

Figure V-8. Raman spectra of first stage graphite hydrofluorides.

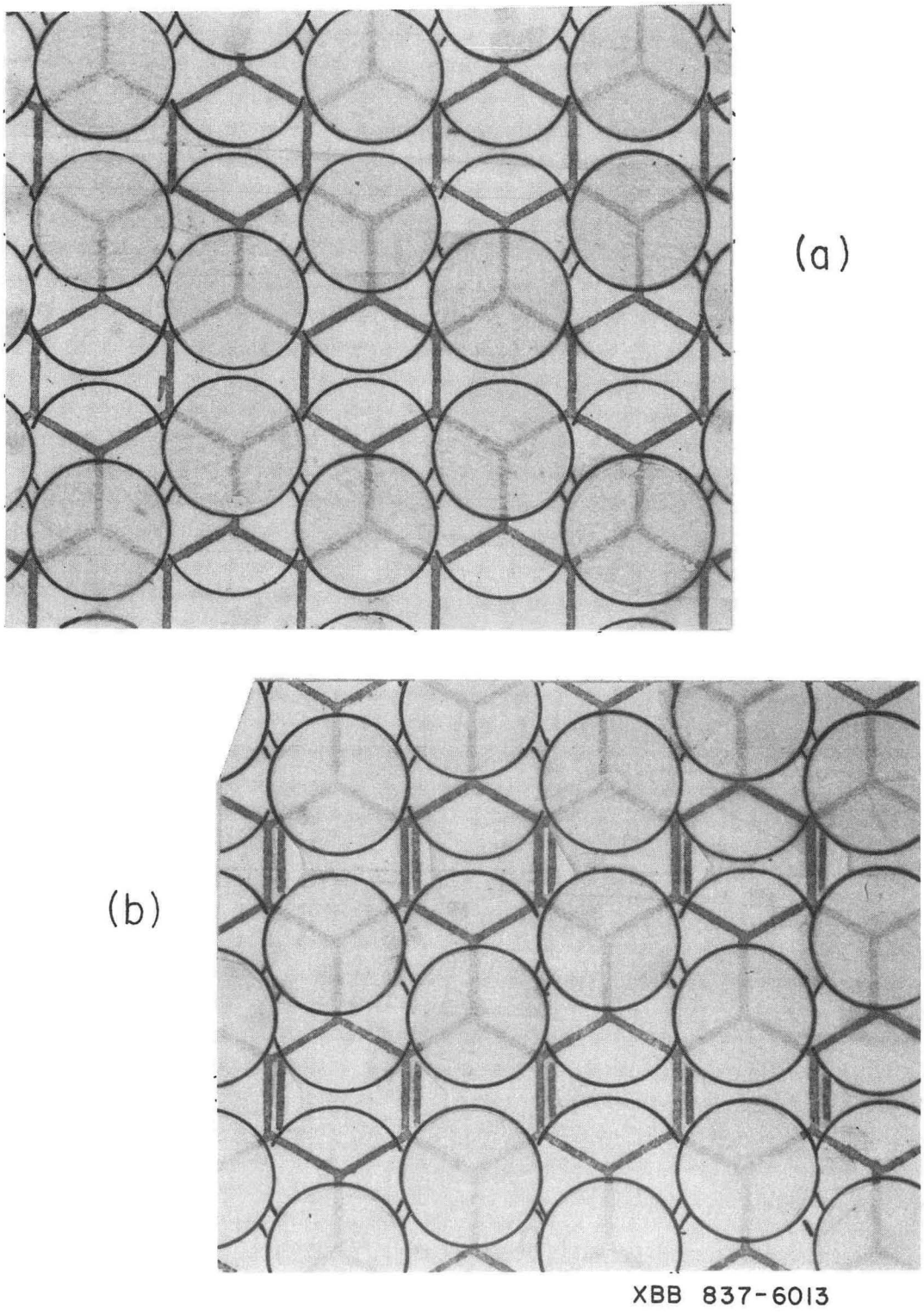

Figure V-9. (a) A possible structure for a single sheet of C_2F, and (b) the same structure showing localized double bonds.

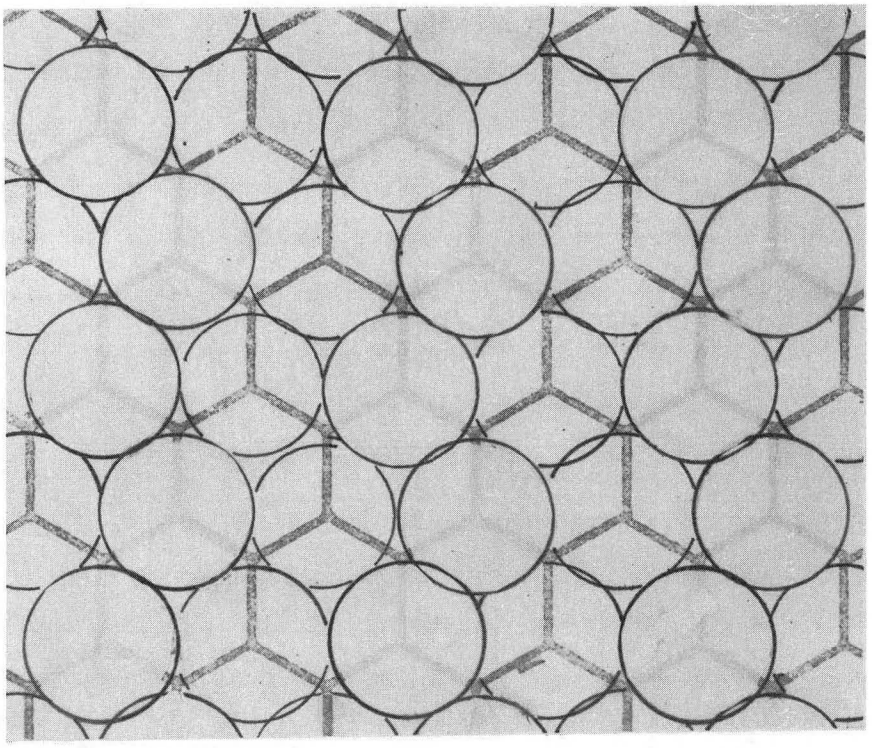

XBB 837-6012

Figure V-10. Another possible structure for C_2F.

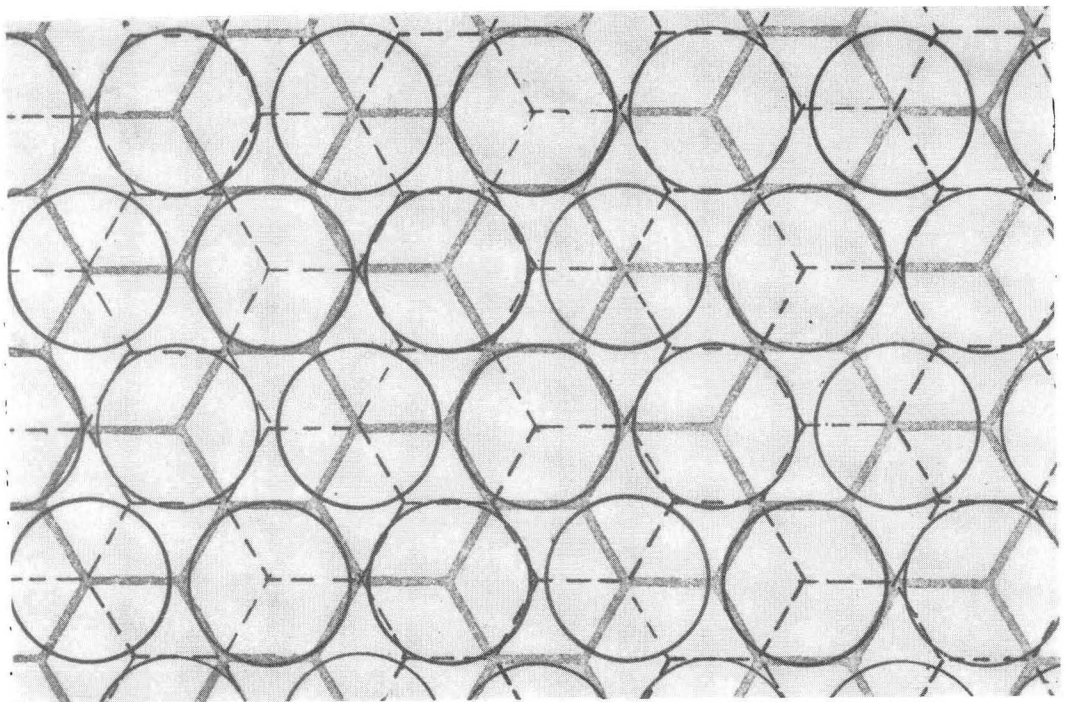

Figure V-11. A possible structure for C_8F in the hk0 projection. The fluorine atoms over the staggered carbons have $\frac{1}{2}$ multiplicity.

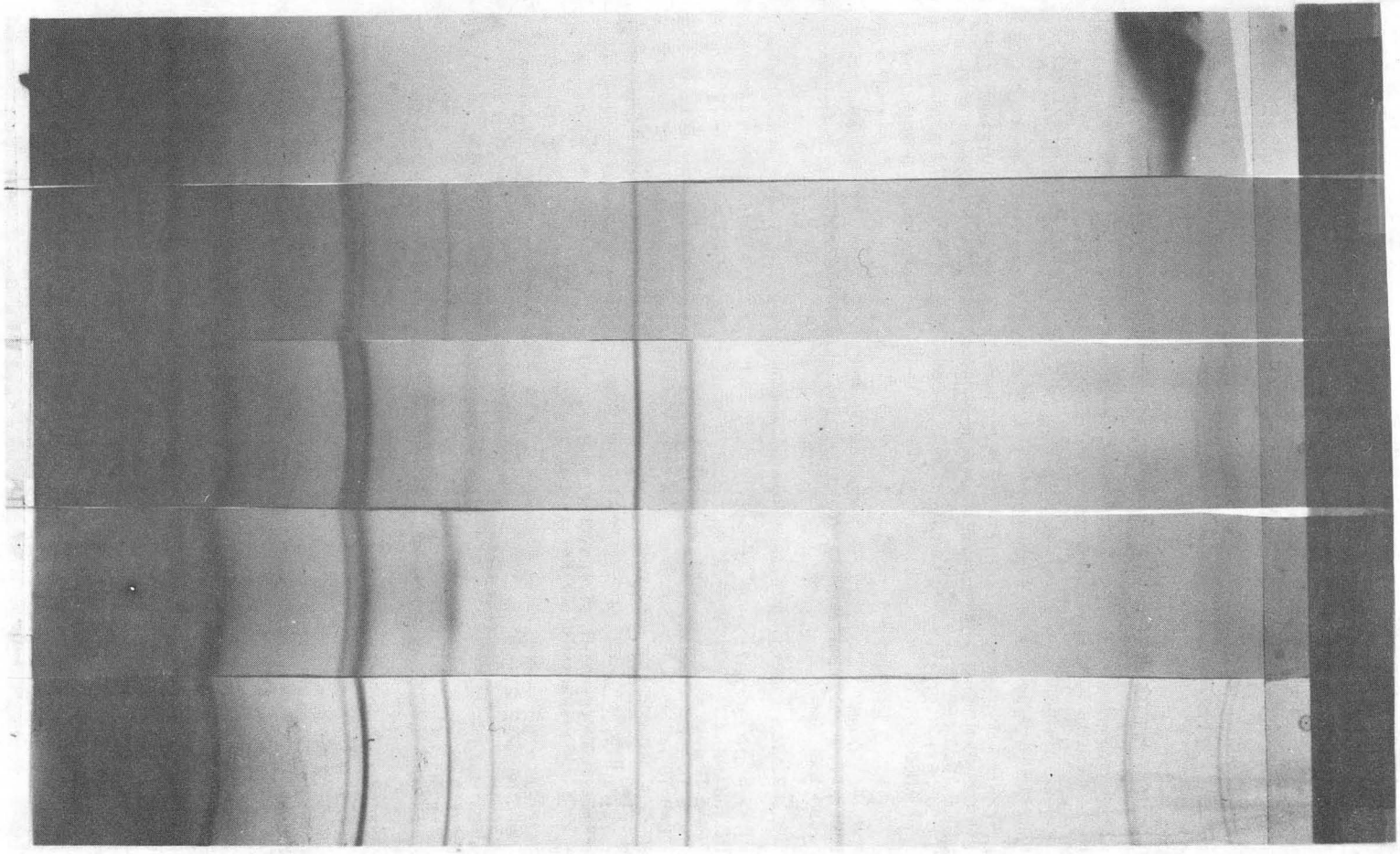

XBB 836-5186

Figure V-12. X-ray powder patterns of graphite hydrofluorides and their reduction products: (a) $C_{2.5}F_{1-x}(HF)_x$, (b) $C_{2.5}F_{1-x}(HF)_x$ reduced with graphite, (c) $C_{12}HF_2$, (d) $C_{12}HF_2$ reduced with graphite, (e) SP-1 graphite.

APPENDIX

The following computer programs, written in Commodore BASIC, were used in the lattice energy computations:

BERTAUT - A PROGRAM TO CALCULATE THE ELECTROSTATIC ENERGY OF A CRYSTALLINE SOLID

```
 1 INPUT"TITLE";T$
 5 INPUT"# OF ATOMS IN THE FORMULA UNIT";N
 6 INPUT"# OF SYMMETRY OPERATIONS IN THE ACENTRICGROUP (EXCLUDING IDENTITY)";NS
 10 INPUT"CELL DIMENSIONS";A,B,C
 20 NA=N*(NS+1)*2+1
 30 PRINT"FOR EACH ATOM, ENTER THE NAME,CHARGE,ANDCOORDINATES"
 40 DIMA$(NA),Q(NA),X(NA),Y(NA),Z(NA),XT(NS),XF(NS),YT(NS),YF(NS),ZT(NS),ZF(NS)
 50 FOR I=1 TO N
 60 PRINTI;:INPUTA$(I),Q(I),X(I),Y(I),Z(I)
 65 NEXT
 68 PRINT"FOR EACH SYMMETRY OPERATION, ENTER      XTRANS, XFACTOR, YTRANS, ETC."
 70 FORI=1TONS:PRINTI;:INPUTXT(I),XF(I),YT(I),YF(I),ZT(I),ZF(I):NEXT
 72 INPUT"CENTRIC SPACE GROUP";C$
 75 INPUT"SUMMATION LIMIT FOR HKL";MA
 78 IFFL=0THENGOSUB400
 80 DM=10
 101 FOR I=1 TO NA-1
 102 FOR J=I+1 TO NA
 103 D=SQR((X(I)-X(J))↑2*A↑2+(Y(I)-Y(J))↑2*B↑2+(Z(I)-Z(J))↑2*C↑2)
 104 IF D<DM THEN DM=D
 105 NEXT:NEXT
 106 R=DM/2:PRINTDM
 107 M=0
 108 PRINT"":PRINT"SUMMATION PROGRESS:"
 109 PRINT" H  K  L"
 110 FOR H=0 TO MA
 120 FOR K=0 TO MA
 130 FOR L=0 TO MA
 132 D=SQR(H↑2/A↑2+K↑2/B↑2+L↑2/C↑2)
 135 FR=0:FI=0
 140 FOR I=1 TO NA
 150 FR=FR+Q(I)*COS(2*π*(H*X(I)+K*Y(I)+L*Z(I)))
 160 FI=FI+Q(I)*SIN(2*π*(H*X(I)+K*Y(I)+L*Z(I)))
 170 NEXT I
 180 F=FR↑2+FI↑2
 181 IF H=0 THEN F=F/2
 182 IF K=0 THEN F=F/2
 183 IF L=0 THEN F=F/2
 190 AL=2*π*R*D
 195 IF AL=0 THEN PH=0:GOTO210
 200 PH=(SIN(AL)-AL*COS(AL))↑2/AL↑8
 210 M=M+F*PH
 215 GOSUB 360
 220 NEXT:NEXT:NEXT
 230 M=-18*M*π*R↑2/(A*B*C)*8
 240 FOR I=1 TO NA
 250 M=M+3*Q(I)↑2/(5*R)
 260 NEXT
 261 OPEN1,4:OPEN2,4,1:OPEN3,4,2
 262 PRINT#1
 265 PRINT#1,CHR$(1);T$
 266 CL=M*N/NA*10↑4*1.602↑2*6.0225*181/(4*π*8.854*757)
 267 PRINT#1,"COULOMB ENERGY(KCAL/MOLE)=";CL
 270 PRINT#1,"MADELUNG CONSTANT=";M*N/NA*DM
 271 PRINT#1,"SUMMATION LIMIT WAS ";MA
 272 PRINT#1,"ION      CHARGE       X         Y         Z"
 273 PRINT#3,"AAA      S9.999    S9.9999  S9.9999  S9.9999"
 274 FOR I=1 TO NA
 275 IF FL=0 THEN 277
 276 IF A$(I)=A$(I-1)THEN 278
 277 PRINT#2,A$(I);CHR$(29);Q(I),X(I),Y(I),Z(I)
```

```
278 NEXT
279 CLOSE1:CLOSE2:CLOSE3
280 INPUT"CHANGE THE CHARGES";K$
289 FL=1
290 IF LEFT$(K$,1)="Y"THEN 310
300 END
310 FOR I=1 TO NA
320 IF A$(I)=A$(I-1)THEN Q(I)=Q(I-1):GOTO340
330 PRINTA$(I);:INPUTQ(I)
340 NEXT
350 GOTO75
360 PRINT"            ":PRINT"□";:PRINTH;:PRINTK;:PRINTL:PRINT"□";:RETURN
400 T=N:FORI=1TON:FORJ=1TONS
405 T=T+1:X(T)=XF(J)*X(I)+XT(J):Y(T)=YF(J)*Y(I)+YT(J):Z(T)=ZF(J)*Z(I)+ZT(J)
410 A$(T)=A$(I):Q(T)=Q(I)
415 FORQ=1TOT-1
420 IFABS(SIN(π*(X(Q)-X(T))))>10↑-5THEN440
425 IFABS(SIN(π*(Y(Q)-Y(T))))>10↑-5THEN440
430 IFABS(SIN(π*(Z(Q)-Z(T))))>10↑-5THEN440
435 T=T-1:Q=T:IFT<NTHENT=N
440 NEXT:NEXT:NEXT:NA=T:T=0
445 IFLEFT$(C$,1)<>"Y"THENRETURN
500 T=NA:FORI=1TONA
510 T=T+1:A$(T)=A$(I):X(T)=-X(I):Y(T)=-Y(I):Z(T)=-Z(I):Q(T)=Q(I)
515 FORQ=1TOT-1
520 IFABS(SIN(π*(X(Q)-X(T))))>10↑-5THEN540
525 IFABS(SIN(π*(Y(Q)-Y(T))))>10↑-5THEN540
530 IFABS(SIN(π*(Z(Q)-Z(T))))>10↑-5THEN540
535 T=T-1:Q=T:IFT<NATHENT=NA
540 NEXT:NEXT:NA=T:T=0
550 RETURN
```

COMPLEX ION - CALCULATES THE INTERNAL ELECTROSTATIC ENERGY OF A COMPLEX ION IN A CRYSTALLINE SOLID

```
10 INPUT"TITLE";T$
20 INPUT"A,B,C";A,B,C
30 INPUT"TOTAL NUMBER OF POINT CHARGES IN THE COMPLEX ION";NC
40 DIMA$(NC),Q(NC),X(NC),Y(NC),Z(NC)
50 INPUT"IS THE ION POLYMERIC";P$
60 IF LEFT$(P$,1)="Y"THEN 120
70 PRINT"FOR EACH POINT CHARGE,ENTER THE NAME,CHARGE,AND COORDINATES"
80 FOR I=1 TO NC
90 PRINTI;:INPUTA$(I),Q(I),X(I),Y(I),Z(I)
100 NEXT
110 GOTO 350
120 INPUT"HOW MANY POINT CHARGES IN THE REPEATING UNIT";NA
130 PRINT"FOR EACH POINT CHARGE,ENTER THE NAME,CHARGE,AND COORDINATES"
140 FOR I=1 TO NA
150 PRINTI;:INPUTA$(I),Q(I),X(I),Y(I),Z(I)
160 NEXT
170 INPUT"HOW MANY UNITS ARE RELATED BY SYMMETRY";NS
180 PRINT"FOR EACH SYMMETRY OPERATION,ENTER XTRANS,XFACTOR,YTRANS,ETC"
185 DIMXT(NS),YT(NS),ZT(NS),XF(NS),YF(NS),ZF(NS),TX(NS),TY(NS),TZ(NS)
190 FOR I=1 TO NS
200 INPUT XT(I),XF(I),YT(I),YF(I),ZT(I),ZF(I)
210 NEXT I
230 FOR I=1 TO NA
240 FOR J=1 TO NS
250 TX(J)=XT(J)+XF(J)*X(I):TY(J)=YT(J)+YF(J)*Y(I):TZ(J)=ZT(J)+ZF(J)*Z(I)
260 FOR K=0 TO J-1
270 IF TX(J)<>TX(K)THEN310
280 IF TY(J)<>TY(K)THEN310
290 IF TZ(J)<>TZ(K)THEN310
300 GOTO340
310 NEXTK
320 T=T+1
330 A$(NA+T)=A$(I):Q(NA+T)=Q(I):X(NA+T)=TX(J):Y(NA+T)=TY(J):Z(NA+T)=TZ(J)
340 NEXTJ:NEXTI
350 U=0
360 FOR I=1 TO NC-1
370 FOR J=I+1 TO NC
```

```
375 RX=X(I)-X(J):RY=Y(I)-Y(J):RZ=Z(I)-Z(J)
380 D=SQR(A↑2*RX↑2+B↑2*RY↑2+C↑2*RZ↑2)
385 PRINTA$(I);" ";A$(J);D
390 U=U-Q(I)*Q(J)/D
400 NEXTJ
410 NEXTI
415 U=U*10↑4*1.602↑2*6.0225*181/(4*π*8.854*757)
420 OPEN1,4:OPEN2,4,1:OPEN3,4,2
421 PRINT#1:PRINT#1,CHR$(1);T$:PRINT#1
422 PRINT#1,"    A         B         C"
423 PRINT#3,"99.9999  99.9999  99.9999"
425 PRINT#2,A,B,C
440 PRINT#1,"ELECTROSTATIC ENERGY(KCAL)=";U
450 PRINT#1,"ATOM      CHARGE         X         Y         Z"
460 PRINT#3,"AAAA     $9.9999   $9.9999  $9.9999  $9.9999"
470 FOR I=1 TO NC
490 IF FL=0 THEN 500
495 IF A$(I)=A$(I-1)THEN510
500 PRINT#2,A$(I);CHR$(29);Q(I),X(I),Y(I),Z(I)
510 NEXTI
570 CLOSE1:CLOSE2:CLOSE3
580 INPUT"WOULD YOU LIKE TO CHANGE THE CHARGES";Q$
590 IF LEFT$(Q$,1)="Y"THEN 605
600 END
605 PRINT"FOR EACH ION,ENTER THE CHARGE"
610 FOR I=1 TO NC
620 IF A$(I)=A$(I-1)THENQ(I)=Q(I-1):GOTO640
630 PRINTA$(I);:INPUTQ(I)
640 NEXTI
645 FL=1
650 GOTO 350
```

```
BASIC RADIUS - CALCULATES THE REPULSION RADIUS OF THE LIGAND ATOMS IN A
               MOLECULAR CRYSTAL

 10 INPUT"TITLE";T$
 20 INPUT"CELL DIMENSIONS";A,B,C:A=A↑2:B=B↑2:C=C↑2
 40 INPUT"# OF ATOMS IN THE FORMULA UNIT";N
 45 INPUT"# OF SYMMETRY OPERATIONS IN THE ACENTRICGROUP (EXCLUDING IDENTITY)";NS
 47 NA=N*(NS+1)*2+1
 50 DIMA$(NA),X(NA),Y(NA),Z(NA),AL(NA),E(NA),Q(NA),R(NA)
 51 DIMXT(NS),YT(NS),ZT(NS),XF(NS),YF(NS),ZF(NS)
 60 PRINT"FOR EACH ATOM, ENTER THE NAME, CHARGE,  AND COORDINATES"
 75 FORI=1TON
 80 PRINTI;:INPUTA$(I),Q(I),X(I),Y(I),Z(I)
 90 NEXT
100 PRINT"ENTER POLARIZABILITY(A↑3)
102 FORI=1TON
104 IFA$(I)=A$(I-1)THENAL(I)=AL(I-1):GOTO108
106 PRINTA$(I);:INPUTAL(I)
108 NEXT
110 PRINT"ENTER CHARACTERISTIC ENERGY(EV)"
112 FORI=1TON
114 IFA$(I)<>A$(1)THEN118
116 PRINTA$(I);:INPUTE(I)
118 NEXT
145 PRINT" FOR EACH SYMMETRY OPERATION, ENTER     XTRANS, XFACTOR, YTRANS, ETC.
150 FORI=1TONS:PRINTI;:INPUTXT(I),XF(I),YT(I),YF(I),ZT(I),ZF(I):NEXT
151 INPUT"SUBLIMATION TEMPERATURE(K)";TS:TS=TS*.001987
152 INPUT"CENTRIC SPACE GROUP";C$
153 INPUT"COULOMB ENERGY, SUBLIMATON ENTHALPY      (KCAL/MOLE)";UC,HS
154 INPUT"ZERO POINT ENERGY(KCAL), REPULSION       PARAMETER(A)";UZ,RH
155 T=N:FORI=1TON:FORJ=1TONS
160 T=T+1:X(T)=XF(J)*X(I)+XT(J):Y(T)=YF(J)*Y(I)+YT(J):Z(T)=ZF(J)*Z(I)+ZT(J)
165 A$(T)=A$(I):Q(T)=Q(I):AL(T)=AL(I):E(T)=E(I)
170 FORQ=1TOT-1
175 IFABS(SIN(π*(X(Q)-X(T))))>10↑-5THEN195
180 IFABS(SIN(π*(Y(Q)-Y(T))))>10↑-5THEN195
185 IFABS(SIN(π*(Z(Q)-Z(T))))>10↑-5THEN195
190 T=T-1:IFT<NTHENT=N
195 NEXT:NEXT:NEXT:NA=T:T=0
210 IF LEFT$(C$,1)="Y"THENGOSUB500
220 GOSUB600
225 PRINTNA
```

```
230 FORI=1TON
240 FORJ=1TONA
250 FORQ=-1TO1:FORT=-1TO1:FORS=-1TO1
252 IFJ>N+.5THEN260
254 IFABS(Q)>.5THEN260
255 IFABS(S)>.5THEN260
256 IFABS(T)>.5THEN260
258 GOTO300
260 R=SQR(A*(X(I)-X(J)+Q)↑2+B*(Y(I)-Y(J)+S)↑2+C*(Z(I)-Z(J)+T)↑2)
265 IFR=0THEN300
266 IFA$(I)=A$(1)ORA$(J)=A$(1)THENRR=0:GOTO290
285 RR=(R/6.21428572/RH-1)*EXP(-1*R/RH)*(1+Q(I)/8+Q(J)/8)
286 RE=RE+EXP(-1*R/RH)
290 UR=UR+RR:S1=3/4*AL(I)*AL(J)/R↑6
291 IFA$(I)=A$(1)ANDA$(J)=A$(1)THENSA=SA+S1
292 IFA$(I)<>A$(1)ANDA$(J)=A$(1)THENSB=SB+S1
293 IFA$(I)=A$(1)ANDA$(J)<>A$(1)THENSB=SB+S1
294 IFA$(I)<>A$(1)ANDA$(J)<>A$(1)THENSC=SC+S1
300 NEXT:NEXT:NEXT:NEXT:NEXT
301 UR=RH/2*LOG((HS-UC*(1-1/6.21428572)-TS+UZ)/(UR*7.1934244))
302 RE=RE*EXP(2*UR/RH)*7.1934244
303 UD=(HS-UC+UZ-TS+RE)/(1.12*23.05)
304 A1=SC/2
305 B1=E(1)*SC/2+E(1)*SB+E(1)*SA/2-UD
306 C1=E(1)↑2*SA/2-UD*E(1)
307 FORI=1TONA:IFA$(I)=A$(1)THEN309
308 E(I)=(-B1+SQR(B1↑2-4*A1*C1))/(2*A1)
309 NEXT
310 OPEN1,4:OPEN2,4,1:OPEN3,4,2
315 PRINT#1:PRINT#1,CHR$(1),T$
318 PRINT#1,"HEAT OF SUBLIMATION(KCAL/MOLE)= ";HS
319 PRINT#1,"COULOMB ENERGY=                 ";UC
320 PRINT#1,"REPULSION PARAMETER RHO=        ";RH
321 PRINT#1,"ZERO POINT ENERGY=              ";UZ
322 PRINT#1,"BASIC RADIUS(A)=                ";UR
323 PRINT#1,"CALCULATED REPULSION ENERGY=    ";RE
324 PRINT#1,"UD + UQ=                       ";HS-UC-TS+RE+UZ
325 PRINT#1,"SUBLIMATION TEMPERATURE(K)=     ";TS/.001987
335 PRINT#1,"CELL DIMENSIONS:"
336 PRINT#1,"     A         B         C"
337 PRINT#3," 99.9999  99.9999  99.9999"
338 PRINT#2,SQR(A),SQR(B),SQR(C)
340 PRINT#1,"ATOM  CHARGE        X       Y       Z    POL.(A↑3)  CHR.EN.(EV)"
350 PRINT#3,"AAAA  $9.9999   $.9999 $.9999 $.9999   9.9999      99.9999"
360 FORI=1TONA
370 PRINT#2,A$(I);CHR$(29);Q(I),X(I),Y(I),Z(I),AL(I),E(I)
380 NEXT
390 END
500 T=NA:FORI=1TONA
510 T=T+1:X(T)=-X(I):Y(T)=-Y(I):Z(T)=-Z(I):A$(T)=A$(I):Q(T)=Q(I)
512 AL(T)=AL(I):E(T)=E(I)
520 FORQ=1TOT-1
530 IFABS(SIN(π*(X(Q)-X(T))))>10↑-5THEN570
540 IFABS(SIN(π*(Y(Q)-Y(T))))>10↑-5THEN570
550 IFABS(SIN(π*(Z(Q)-Z(T))))>10↑-5THEN570
560 T=T-1:IFT<NATHENT=NA
570 NEXT:NEXT:NA=T:T=0
580 RETURN
600 FORI=1TONA
610 IFX(I)<0THENX(I)=X(I)+1
620 IFY(I)<0THENY(I)=Y(I)+1
630 IFZ(I)<0THENZ(I)=Z(I)+1
640 IFX(I)>=1THENX(I)=X(I)-1
650 IFY(I)>=1THENY(I)=Y(I)-1
660 IFZ(I)>=1THENZ(I)=Z(I)-1
670 NEXT:RETURN
```

```
2ND BASIC RADIUS - CALCULATES THE DISPERSION ENERGY, THE REPULSION
                   ENERGY, AND THE REPULSION RADIUS OF THE CENTRAL
                   ATOM IN THE CATION FOR A CRYSTALLINE SALT


 10 INPUT"TITLE";T$
 20 INPUT"CELL DIMENSIONS";A,B,C:A=A↑2:B=B↑2:C=C↑2
 40 INPUT"# OF ATOMS IN THE FORMULA UNIT";N
 45 INPUT"# OF SYMMETRY OPERATIONS IN THE ACENTRICGROUP (EXCLUDING IDENTITY)";NS
 47 NA=N*(NS+1)*2+1
 50 DIMA$(NA),X(NA),Y(NA),Z(NA),AL(NA),E(NA),Q(NA),R(NA)
 51 DIMXT(NS),YT(NS),ZT(NS),XF(NS),YF(NS),ZF(NS)
 54 PRINT
 55 PRINT"BASIC RADIUS WILL BE CALCULATED FOR ATOM #1":PRINT
 60 PRINT"FOR EACH ATOM, ENTER THE NAME, CHARGE,  AND COORDINATES"
 75 FORI=1TON
 80 PRINTI;:INPUTA$(I),Q(I),X(I),Y(I),Z(I)
 90 NEXT
 95 PRINT"ENTER THE POLARIZABILITY(A↑3)AND        CHARACTERISTIC ENERGY(EV)"
100 FOR I=1TON
105 IF A$(I)=A$(I-1)THENE(I)=E(I-1):AL(I)=AL(I-1):GOTO115
110 PRINTA$(I);:INPUT AL(I),E(I)
115 NEXT
116 PRINT"ENTER THE BASIC RADIUS"
117 FORI=2TON
118 IFA$(I)=A$(I-1)THENR(I)=R(I-1):GOTO120
119 PRINTA$(I);:INPUTR(I)
120 NEXT
135 INPUT"# OF ATOMS IN THE ION CONTAINING ATOM 1 ";N1
145 PRINT" FOR EACH SYMMETRY OPERATION, ENTER     XTRANS, XFACTOR, YTRANS, ETC.
150 FORI=1TONS:PRINTI;:INPUTXT(I),XF(I),YT(I),YF(I),ZT(I),ZF(I):NEXT
151 INPUT"CENTRIC SPACE GROUP";C$
152 INPUT"REPULSION PARAMETER(A)";RH
153 INPUT"COULOMB ENERGY";UC
155 T=N:FORI=1TON:FORJ=1TONS
160 T=T+1:X(T)=XF(J)*X(I)+XT(J):Y(T)=YF(J)*Y(I)+YT(J):Z(T)=ZF(J)*Z(I)+ZT(J)
165 A$(T)=A$(I):Q(T)=Q(I):AL(T)=AL(I):E(T)=E(I):R(T)=R(I)
170 FORQ=1TOT-1
175 IFABS(SIN(π*(X(Q)-X(T))))>10↑-5THEN195
180 IFABS(SIN(π*(Y(Q)-Y(T))))>10↑-5THEN195
185 IFABS(SIN(π*(Z(Q)-Z(T))))>10↑-5THEN195
190 T=T-1:Q=T:IFT<NTHENT=N
195 NEXT:NEXT:NEXT:NA=T:T=0
210 IF LEFT$(C$,1)="Y"THENGOSUB500
220 GOSUB600
225 PRINTNA
230 FORI=1TON
240 FORJ=1TONA
250 FORQ=-1TO1:FORT=-1TO1:FORS=-1TO1
251 IFABS(Q)>.5THEN260
252 IFABS(S)>.5THEN260
253 IFABS(T)>.5THEN260
254 IFI<N1+.5ANDJ>N1+.5THEN260
255 IFI>N1+.5ANDJ>N+.5THEN260
256 IFI>N1+.5ANDJ<N1+.5THEN260
258 GOTO300
260 R=SQR(A*(X(I)-X(J)+Q)↑2+B*(Y(I)-Y(J)+S)↑2+C*(Z(I)-Z(J)+T)↑2)
265 IFR=0THEN300
266 R1=R(I)-R:R2=R(J)-R:R3=R(I)+R(J)-R
267 IFA$(I)=A$(1)ANDA$(J)=A$(1)THENSA=SA+(1+(Q(I)+Q(J))/8)*R/RH*EXP(-R/RH)
268 IFA$(I)=A$(1)ANDA$(J)<>A$(1)THENSB=SB+(1+(Q(I)+Q(J))/8)*R/RH*EXP(R2/RH)
269 IFA$(I)<>A$(1)ANDA$(J)=A$(1)THENSB=SB+(1+(Q(I)+Q(J))/8)*R/RH*EXP(R1/RH)
270 IFA$(I)<>A$(1)ANDA$(J)<>A$(1)THENSC=SC+(1+(Q(I)+Q(J))/8)*R/RH*EXP(R3/RH)
276 IFA$(I)=A$(1)ANDA$(J)=A$(1)THENAS=AS+(1+(Q(I)+Q(J))/8)*EXP(-R/RH)
277 IFA$(I)=A$(1)ANDA$(J)<>A$(1)THENBS=BS+(1+(Q(I)+Q(J))/8)*EXP(R2/RH)
278 IFA$(I)<>A$(1)ANDA$(J)=A$(1)THENBS=BS+(1+(Q(I)+Q(J))/8)*EXP(R1/RH)
279 IFA$(I)<>A$(1)ANDA$(J)<>A$(1)THENCS=CS+(1+(Q(I)+Q(J))/8)*EXP(R3/RH)
285 UD=UD+1/R↑6*AL(I)*AL(J)*E(I)*E(J)/(E(I)+E(J))*3/4*23.05
300 NEXT:NEXT:NEXT:NEXT:NEXT:UQ=UD*.12
301 AR=SB↑2+4*SA*(UC+6*UD+8*UQ)/7.1934244-SC)
302 UR=RH*LOG((-SB+SQR(AR))/(2*SA))
303 RE=7.1934244*(EXP(2*UR/RH)*AS+EXP((UR)/RH)*BS+CS)
310 OPEN1,4:OPEN2,4,1:OPEN3,4,2
315 PRINT#1:PRINT#1,CHR$(1),T$
319 PRINT#1,"COULOMB ENERGY(KCAL/MOLE)=       ";UC
320 PRINT#1,"DIPOLE-DIPOLE DISPERSION ENERGY=";UD
321 PRINT#1,"DIPOLE-QUADRUPOLE ENERGY=        ";UQ
322 R(1)=UR:FORI=1TONA:IFA$(I)=A$(1)THENR(I)=UR
323 NEXT
```

```
324 PRINT#1,"REPULSION PARAMETER(A)=          ";RH
325 PRINT#1,"REPULSION ENERGY=               ";RE
335 PRINT#1,"CELL DIMENSIONS:"
336 PRINT#1,"     A         B         C"
337 PRINT#3," 99.9999  99.9999  99.9999"
338 PRINT#2,SQR(A),SQR(B),SQR(C)
340 PRINT#3,".9 S9A   .9 S9A   .9 S9A"
341 PRINT#1,"SYMMETRY OPERATIONS:":FORI=1TONS
345 PRINT#2,XT(I);XF(I);"X";CHR$(29);YT(I);YF(I);"Y";CHR$(29);ZT(I);ZF(I);"Z"
346 NEXT
347 IF LEFT$(C$,1)<>"Y"THENPRINT#1,"ACENTRIC SPACE GROUP"
348 IF LEFT$(C$,1)="Y"THENPRINT#1,"CCENTRIC SPACE GROUP"
349 PRINT#1,"ATOM   CHARGE       X         Y         Z    RADIUS  POL(A↑3) CHR.EN.(EV)
350 PRINT#3,"AAAA  S9.9999   S.9999 S.9999 S.9999  9.9999   9.9999    99.9999"
360 FORI=1TONA
370 PRINT#2,A$(I);CHR$(29);Q(I),X(I),Y(I),Z(I),R(I),AL(I),E(I)
380 NEXT
390 END
500 T=NA:FORI=1TONA
510 T=T+1:X(T)=-X(I):Y(T)=-Y(I):Z(T)=-Z(I):A$(T)=A$(I):Q(T)=Q(I):R(T)=R(I)
515 AL(T)=AL(I):E(T)=E(I)
520 FORQ=1TOT-1
530 IFABS(SIN(π*(X(Q)-X(T))))>10↑-5THEN570
540 IFABS(SIN(π*(Y(Q)-Y(T))))>10↑-5THEN570
550 IFABS(SIN(π*(Z(Q)-Z(T))))>10↑-5THEN570
560 T=T-1:Q=T:IFT<NATHENT=NA
570 NEXT:NEXT:NA=T:T=0
580 RETURN
600 FORI=N+1TONA
610 IFX(I)<0THENX(I)=X(I)+1
620 IFY(I)<0THENY(I)=Y(I)+1
630 IFZ(I)<0THENZ(I)=Z(I)+1
640 IFX(I)>=1THENX(I)=X(I)-1
650 IFY(I)>=1THENY(I)=Y(I)-1
660 IFZ(I)>=1THENZ(I)=Z(I)-1
670 NEXT:RETURN
```

ACKNOWLEDGEMENTS

To Professor Neil Bartlett I offer my most sincere thanks and appreciation; the great enthusiasm and insight he brought to the most intractable problems were equalled only by the patience, warmth, and kindness he showed me during my graduate years.

To the many collaborators in this work, I owe a debt of gratitude: Dr. Bernard Desbat, for the vibrational analysis of the pentafluorogermanate salts; Dr. Frederick J. Hollander, who solved some of the crystal structures; Mr. Morgan P. Conrad, Dr. Kenneth D. Bomben, Dr. Kurt Zilm, and Dr. Bruce L. Hawkins who ran, respectively, the i.r., XPS, ^{1}H n.m.r., and ^{13}C n.m.r. spectra of $C_xF_{1-\delta}(HF)_\delta$; Dr. Thomas E. Thompson who performed conductivity measurements on the graphite bifluorides; Dr. Henry Resing, for the ^{19}F n.m.r. spectrum of $C_xF_{1-\delta}(HF)_\delta$ and C_xHF_2; Professors David Templeton, Herbert Strauss, and Leo Brewer for valuable discussions on the subject of lattice energy calculations. I thank also my coworkers Barry McQuillan, Sam Yeh, Fujio Okino, and Guy Rosenthal, whose work on related projects helped me think through my own.

I would like to thank as well the person who brings the coffee and doughnut holes to seminars, for feeding me three times a week for four years. I bid fond farewell to that zany, happy-go-lucky, rag-tag, wild bunch of barbecuers, beer-drinkers, and ne'er-do-wells who comprise the Bartlett group and the fifth floor of Latimer. Goodbye and good luck.

This work was supported by the U.S. Department of Energy under contract no. DE-AC03-76 SF00098.

This report was done with support from the Department of Energy. Any conclusions or opinions expressed in this report represent solely those of the author(s) and not necessarily those of The Regents of the University of California, the Lawrence Berkeley Laboratory or the Department of Energy.

Reference to a company or product name does not imply approval or recommendation of the product by the University of California or the U.S. Department of Energy to the exclusion of others that may be suitable.

TECHNICAL INFORMATION DEPARTMENT
LAWRENCE BERKELEY LABORATORY
UNIVERSITY OF CALIFORNIA
BERKELEY, CALIFORNIA 94720